

AN ABSTRACT OF THE DISSERTATION OF

Brian M. Dixon for the degree of Doctor of Philosophy in Molecular and Cellular Biology presented on March 20, 2008

Title: The Aging Endoplasmic Reticulum

Abstract approved:

Tory M. Hagen

Hallmarks of aging include the accumulation of aberrant proteins and a lower resistance to stresses. Because the endoplasmic reticulum (ER) functions to fold proteins and possesses unique stress sensing pathways, the central hypothesis of this dissertation is that the ER is a target of cellular aging and significantly underlies these age-related phenotypes. This hypothesis was tested using isolated microsomes from young (3-6 mo) and old (24-26 mo) rats and a novel primary hepatocyte cell culture model that maintains the aging phenotype.

The ER luminal oxidation/reduction (redox) environment, exemplified by the glutathione redox ratio (GSH:GSSG), is vital for both ER stress signaling and the regulation of ER oxidoreductase activity. Therefore, the hepatic microsomal GSH:GSSG

ratio from young and old rats was determined. Our results showed that the GSH:GSSG ratio in young rats was 3.8:1 and that, in contrast to the age-related *loss* of GSH redox in whole liver, microsomal GSH:GSSG *increased* to 6.4:1 in old rats. This increase is sufficient to convert ER oxidoreductases from *folding* proteins to enzymes involved in protein *unfolding*. These results show that the ER is under an increased stress with age, yet no activation of ER stress response pathways was detected. Using the aging cell culture model noted above to examine the loss of ER stress response with age, we show that following induction of an ER stress by tunicamycin, ER-mediated “pro-apoptotic” pathways were intact with age, but induction of “pro-survival” genes were significantly delayed. Taken together, these show that aging leads to: 1) a *reductive* shift in ER thiol redox, and 2) an attenuation of ER stress response.

Lastly, previous work showed that (*R*)-alpha-lipoic acid (R-LA) restores GSH levels and redox status in aged rat livers. To determine whether R-LA also reversed the age-related changes in ER GSH redox status, young and old rats were supplemented with R-LA. Results showed that R-LA reversed both the age-related increase in the ER GSH redox state and induced protective ER stress response pathways in a manner similar to young animals. Thus, R-LA may be an effective therapeutic to maintain ER homeostatic mechanisms with age.

© Copyright by Brian M. Dixon
March 20, 2008
All Rights Reserved

The Aging Endoplasmic Reticulum

by
Brian M. Dixon

A DISSERTATION

submitted to

Oregon State University

in partial fulfillment of
the requirements for the
degree of

Doctor of Philosophy

Presented March 20, 2008
Commencement June 2008

Doctor of Philosophy dissertation of Brian M. Dixon
presented on March 20th, 2008

APPROVED:

Major Professor, representing Molecular and Cellular Biology

Director of the Molecular and Cellular Biology Program

Dean of the Graduate School

I understand that my dissertation will become part of the permanent collection of Oregon State University Libraries. My signature below authorizes release of my dissertation to any reader upon request.

Brian M. Dixon, Author

ACKNOWLEDGEMENTS

The acknowledgements section—the part of my dissertation I can thank those people who have been an inspiration in my life. Please indulge me here as there are a lot of people I would like to thank.

In my tenure working on my degree, I have seen and experienced a lot—maybe more than was just. Academically, the old adage, “education is a journey, not a destination”, couldn’t apply more to my graduate years. I have experienced a lot during this journey. Some of the lowest times in my life were during graduate school as well as some of the highest. I’ve learned a lot about myself—and others—during this time. I don’t know what lies ahead, but I know graduate school has taught me a lot and shaped much of who I am today. I hope that anyone reading this will always remember a couple important things I have learned during this experience – not necessarily the science herein, although I hope you’ll find that sound as well, but rather some bigger, more important things in my humble opinion. That is simply to keep things in perspective. Remember what is important in this life. It is easy to get caught up in our own little worlds. Step back and look at things in the context of the “Big Picture”. Ask yourself what is really important and pick your battles carefully. And most importantly never forget to have fun and laugh as much as possible. I know it is cliché but life really is too short not to enjoy it as much as possible...every second possible. Personally, I like to find motivations in simple quotes; “Bumper Sticker Solutions” as an old, professor of mine, John Orrelle, used to call them. One I find especially poignant:

"What I do today is important because I am exchanging a day of my life for it."

Think about that for a minute...

As I mentioned there have been a handful of people in my life that have been instrumental in shaping who I am today. I would like to thank those people, in case I haven't already done so.

First and foremost are my Parents, Don and Gerri Dixon. Everything you ever did in your lives, from the time my Brother and I were born, was to give us the best life possible. I don't think you thought of yourselves once when we were growing up. The home environment you provided was second-to-none. It was caring, nurturing, and in my case, full of "tough love" when needed. How you balanced running my Brother and I to all of the different activities we were involved in, I'll never know. The fact you both are so selfless has given me gifts I will treasure the rest of my life. I only hope to be half the parents you are. Dad, thank you for teaching me some of life's most important lessons and teaching me so many "life skills". Mom, what can I say to express all the gratitude I have for you? Simply put, you are an angel!!! I love you guys very much. Thank you for everything!!!

Next would be my brother, Kevin. Kevin, despite a few semi-traumatic years you and I had growing up, I can't possibly tell you how fortunate I feel to have a brother like you. I'm thankful we've grown to appreciate our differences and have become so close in our later years. You have been a tremendous positive influence and inspiration in my life in so many ways. You are the reason I even considered going to graduate school. I have told you this before, but even though you are my younger brother, you are someone I look-up to. Thank you. I wish you and Meredith all the happiness in the world.

Next is Rex Watkins, my childhood swimming coach for so many years. Rex, I have had the opportunity to thank you personally; however, I don't think my words did justice to the positive influence you have had, and will always have, on my life. And what I really think is ironic, is that you don't realize the positive impact you have on everyone you mentor just by doing what you do and being who you are. The way you lead your life is a model for the youth who see it and look up to you. I don't think you realize the effect you have because you just do what you do—you just don't realize that by simply doing that in it self, you are a role model. Simply put, you lead by example. This might be the best gift you have given me. The best place to lead is from the front; if you want to lead, lead by example. We need more Rex Watkins in the world. Thank you!

Next is John Orrelle, one of my earliest college professors. John, I haven't had the chance to thank you personally—you simply retired before I could track you down again. And it looks like you have succeeded in your goal of “falling off the face of the Earth” once you did retire. British Columbia if I remember correctly. I hope the fish have been finding your hook. If it wasn't for you, I doubt this small-town kid, who almost never went to college, would have ever made it through his first year. It was your first class on the very first day that proved learning could be fun. You showed me how to learn and succeed academically and that's the gift of a lifetime. Thank you for that! I only wish all of my classes could have been so fun. It's nice to think back and remember what it was like to have a professor who actually enjoyed teaching, didn't push their own agenda, and taught people to think for themselves. I hope retirement is treating you well—you deserve it for a lifetime of service.

Tory Hagen, my graduate mentor and friend. What can I say? You stood by me personally and professionally when few others would. Thank you for always believing in me and sticking by me when things got tough and helping me get through my graduate studies. I couldn't have done it without you. Thank you for everything. Looks like we both achieved our goal.

Fred Lehman, a true friend. It's like we were twins separated at birth. I've always appreciated how you're sure to incorporate fun into everything you do—there's always an adventure to be had when you're around. Thank you for all the great times during our undergraduate. I'd do anything for you and I know you'd do the same.

Mark Levy. Thank you for all the great times and making graduate school bearable and fun. It's been one hell of a good run! You've been a beacon of sanity amongst all the insanity. But most of all, thank you for being such a good friend to me. Good friends are hard to come by but I've definitely found one in you. I wish you all the best in life!

Jamie Rumage. Thank you for all your support, love, and caring, especially in these last days. I don't know if I could have done it without you.

I could go on and on naming names but I'm afraid that would take up more space than I can afford. But let me say to everyone who I didn't mention by name here but who are special in my life—and you know who you are—I thank you for making life so enjoyable and being there when I needed you. I can't imagine life without any of you. And to the all the others who have touched my life in so many ways but that I'm too ignorant to realize it as-of-yet, I thank you as well.

CONTRIBUTION OF AUTHORS

I would like to acknowledge everyone who may have helped me during my tenure as a graduate student, whether it be indirectly through discussions and interactions, or more directly with providing guidance and assistance while conducting my research. I would especially like to acknowledge Shi-Hua “Du” Heath who which I will have co-authored no fewer than three manuscripts with. Her work ethic and “bulldog” approach to conducting experiments in the lab was a constant source of motivation to complete seemingly endless numbers of glutathione analyses. This is besides her seemingly endless amounts of patients and kindness.

I would also like to acknowledge Jung Suh and Robert Kim for being such willing collaborators and providing analyses not directly in this dissertation but that played an essential role in the completion of my studies.

I would like to acknowledge Anil Jaiswal for providing laboratory and research materials as well as providing protocols, guidance, and encouragement during our few candid conversations.

I would like to acknowledge Judy Butler for her role behind-the-scenes, really what is in effect running the laboratory and ensuring all the researchers in the lab have the supplies necessary to complete their studies.

TABLE OF CONTENTS

	<u>Page</u>
Chapter 1. General Introduction.....	1
1.1. Background.....	2
1.2. Dissertation Hypothesis and Aims.....	22
Chapter 2. A Rat Primary Hepatocyte Model for Aging Studies.....	24
2.1. Abstract.....	25
2.2. Introduction.....	26
2.3. Material and Methods.....	27
2.4. Commentary.....	39
Chapter 3. Assessment of Endoplasmic Glutathione is Confounded by Extensive <i>ex vivo</i> Oxidation.....	42
3.1. Abstract.....	43
3.2. Introduction.....	44
3.3. Materials and Methods.....	47
3.4. Results.....	51
3.5. Discussion.....	62
Chapter 4. Age-related Increase of Glutathione Redox Status of the Endoplasmic Reticulum.....	66
4.1. Abstract.....	67
4.2. Introduction.....	68
4.3. Materials and Methods.....	70

TABLE OF CONTENTS (Continued)

	<u>Page</u>
4.4. Results.....	75
4.5. Discussion.....	86
Chapter 5. <i>R</i> -alpha-Lipoic Acid Reverses the Age-related Increase in the Glutathione Redox Status of the Endoplasmic Reticulum.....	90
5.1. Abstract.....	91
5.2. Introduction.....	93
5.3. Materials and Methods.....	96
5.4. Results.....	102
5.5. Discussion.....	115
Chapter 6. General Discussion and Conclusions.....	118
References.....	128

LIST OF FIGURES

<u>Figure</u>	<u>Page</u>
1.1. United States health expenditures as a percentage of gross domestic product (GDP) over the past 45 years.....	4
1.2. Aging increases your likelihood of death over time.....	6
1.3. Metabolic rate and oxidant production are inversely correlated with maximal lifespan.....	9
1.4. Schematic representation of oxidative protein folding in the ER.....	18
1.5. Schematic representation of ER stress response pathways.....	19
3.1. Chromatographic separation of γ -GG, GSH, and GSSG.....	52
3.2. GSH oxidation during microsomal isolation.....	54
3.3. <i>Ex vivo</i> GSH oxidation occurs very rapidly during microsomal isolation.....	57
3.4. Minimal glutathione is present as mixed disulfides with proteins in rat liver microsomes.....	59
3.5. Small changes in GSH redox state markedly affect disulfide bond reduction by PDI.....	61
4.1. Age-related increase in the ER GSH:GSSG redox ratio.....	76
4.2. No age-related change in protein-bound GSH.....	78
4.3. Whole liver GSH:GSSG declines with age.....	80
4.4. Schematic representation of the fluorescent protein redox gel technique.....	82
4.5. False-color image showing gross alterations in the redox status of the soluble ER proteome occurs in aged animals.....	83
4.7. No chronic induction of ER stress response pathways with age.....	85

LIST OF FIGURES (Continued)

<u>Figure</u>	<u>Page</u>
5.1. Plasma levels of R-LA following gavage.....	103
5.2. R-LA rapidly affects the ER glutathione status in microsomes isolated from both young and old rats.....	105
5.3. <i>R</i> -alpha-lipoic acid pair-feeding study.....	107
5.4. Chronic two-week feeding of R-LA reverses the age-related increase in ER GSH:GSSG ratio.....	110
5.5. R-LA supplementation affects the soluble ER proteome.....	111
5.6. R-LA transiently induces ER stress response pathways in both young and old rats.....	113
5.7. R-LA preferentially increases pro-survival ER stress response protein levels in both young and old rats.....	114

The Aging Endoplasmic Reticulum

Chapter 1

General Introduction

1.1. Background

Preamble

“All diseases may be by sure means prevented or cured, not excepting even that of age, and our lives lengthened at pleasure beyond the antediluvian standard”

- Benjamin Franklin, 1780

This is the ultimate goal of this dissertation that in whatever way, large or small, the content herein will in some way contribute to the understanding of the aging process and the means by which we may ultimately increase, not necessarily lifespan, but more importantly, healthspan—the time in one’s life which is free of disease and full of vitality.

The population of the United States is an aging population

The demographics of the United States are rapidly changing. For example, at the beginning of the modern calendar (0 A.D.) mean human lifespan was estimated to be only 35 years of age. Almost 2000 years later at the turn of the twentieth century, the average human lifespan increased to around 53. However, in the past 100 years, thanks to advances in sanitation and medical care, human lifespan saw similar gains wherein the average lifespan of an American is now approximately 80 years of age.

The current demographics of the United States are such that 1 in 5 Americans will be over the age of 65 in just 20 years and that by 2030 it is estimated 72 million Americans will be 65 or older (1). Even though mean lifespan has increased dramatically in recent history, there is a growing concern that human health is not keeping pace with longevity. According to a recent survey by the U.S. Department of Health and Human Services, 40% of Americans over age 65 exhibit at least one chronic disease, disability, or other functional deficit that limits normal daily activity (2). This number rises to over 90% of respondents that are 85 and older or institutionalized in nursing homes. In light of these facts, it comes as no surprise that approximately 75% of all healthcare dollars in the U.S. are spent on the elderly (3, 4).

Adding to the problem, the costs of healthcare are rising at a staggering rate. This is exemplified when you compare total National healthcare dollars spent versus the percentage of the U.S. gross domestic product (GDP) over the last 45 years (Figure 1.1.). In 1960, only about 5% of the GDP went to healthcare cost, tripling to over 15% today. Clearly this trend cannot continue unless dramatic changes are made in the field of geriatric medicine, it likely will.

The aging population and the poor health that afflicts them will require the design of new healthcare strategies to meet the challenges that such a massive increase in both healthcare costs and medical infrastructure will engender. Thus, as the elderly population continues to grow so will the demand on the economy. To avoid this potential healthcare-based implosion on the U.S. economy, it is imperative that geriatric medicine moves from treatment-based approaches to preventative-based interventions to provide cost-effective alternatives that prolong human healthspan. However, to successfully achieve this transition, a better understanding of the underlying mechanisms of the aging process is required.

Aging: a complex and multifactorial process.

Aging is an ill-defined process that can best be described by phenotypic changes at the organismal, tissue, cellular, and subcellular levels relative to their younger counterparts. One definition of aging that encompasses its many varied characteristics is:

The progressive impairment of normal cellular functions that underlie an increasing vulnerability to stresses of all types, which ultimately decreases the ability to survive with time.

This definition emphasizes that the aging process, while underscoring a decline in cellular function, is still a normal biological condition of living animals and not a *pathobiology*; however, declining cellular function associated with aging predisposes the elderly towards diseases traditionally known as “age-related disease”.

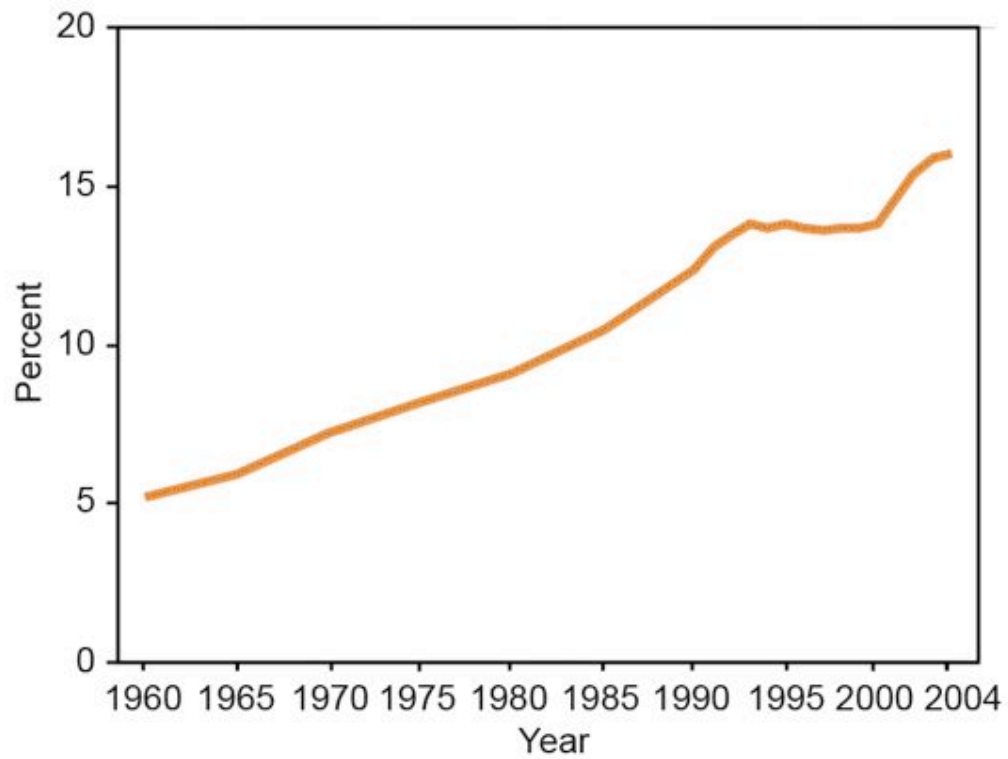


Figure 1.1. United States health expenditures as a percentage of gross domestic product (GDP) over the past 45 years. Source, Centers for Disease Control and Prevention, National Center for Health Statistics, 2006.

The loss of health and increased susceptibility to death that aging causes is dramatically illustrated in Figure 1.2. Here, it is evident that all-cause mortality increases exponentially as a factor of age (Figure 1.2A). For example, an 85 year old person has nearly a 40-fold increased risk of dying versus a middle-aged individual (~45 years-of-age). More telling than this simple age-versus-mortality correlation is shown in Figure 1.2B where it is evident that chronic debilitating diseases, such as cancer, mirror all-cause mortality incidence. This figure illustrates the incidence of all types of cancer increases with the 4th power of age where an elderly person is at an ever-increasing risk for developing cancer over time (Figure 1.2B). Similar correlates can be made with other chronic age-associated pathologies, including cardiovascular diseases, stroke, senile dementias, and diabetes (5, 6). Thus, aging is the leading risk factor for a number of chronic disorders, first leading to morbidity and ultimately to mortality.

Thus, as mentioned above, it is clear that the significant increase in the elder population and the poor health that afflicts them, will require two important and intertwined initiatives: 1) a more definitive understanding of the basic cellular and molecular mechanisms that comprise the aging process as well as 2) the design of new healthcare strategies to meet the challenges that such a significant increase in both healthcare costs and medical infrastructure the aging U.S. population will necessitate.

General characteristics of mammalian aging

As stated above, the hallmarks of aging have largely been characterized as phenotypic decrements relative to those found in young adulthood. Typically, these aging traits can be divided into gross anatomical changes such as the graying of hair and wrinkles; to physiological changes like hearing loss, decreased vision, diminished bone density, and muscle atrophy (sarcopenia); to tissue-specific alterations including decreased absorption of nutrients, lowered lung capacity, and a suppressed immune

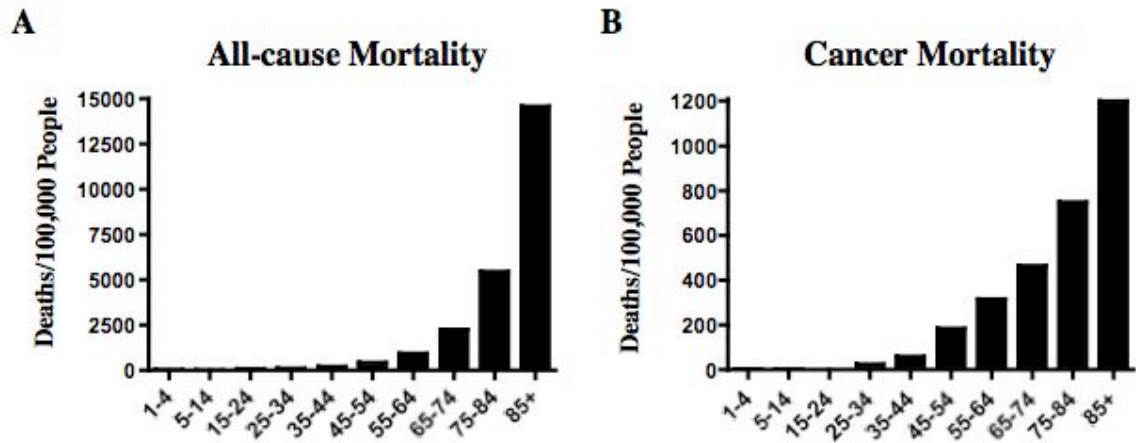


Figure 1.2. Aging increases your likelihood of death over time. Statistics show that mortality incidence increases exponentially with age, whether it is from (A) all causes of mortality combined or (B) from diseases traditionally considered “late age of onset” diseases such as cancer. Statistics collected from the Centers for Disease Control (www.cdc.gov) and users.rcn.com/jkimball.ma.ultranet/BiologyPages/A/Aging.

system (5-7). Of the latter, it is noteworthy that the degree of tissue decline is not uniform. Metabolically active organs such as the brain, heart, eye, and liver tend to decline more significantly than less active organs such as the spleen, thymus, stomach, and intestines. Even among the organs that display significant age-associated deficits, aging *per se* is not uniform. For example, certain brain regions such as the hippocampus and putamen, and the left ventricle of the heart, are far more compromised than other regions of those same organs.

Cellular and molecular aspects of aging

Along with the general physiological changes to organs, significant and multiple age-related alterations to cellular and sub-cellular organelle function have been noted. These changes likely render the cell and tissues they comprise more vulnerable to both endogenous and exogenous stress of all types (8). In turn, these changes would be expected to increase the risk for pathologies associated with aging. Thus, it is likely that dysfunctions at the cellular and molecular level may be responsible for the more overt phenotypes of aging previously described.

A brief overview of the cellular and molecular aspects of aging relevant to this dissertation will now be described.

Cellular and molecular aspects of aging: oxidative stress

It now appears that heightened oxidative insult is a universal aging characteristic in animals. The “Free Radical Theory of Aging” was first proposed by Denham Harmon in 1956. The underlying postulate of this theory is that free radicals produced as a by-product of normal cellular metabolism cause increasing oxidative damage to essential biomolecules, ultimately compromising their function, resulting in the progressive impairment of cellular function (9). This notion that metabolism underlies the aging process is exemplified in Figure 1.3. The group of Sohal *et al.* showed that metabolic rate is inversely correlated to lifespan with few exceptions (10).

That is, relative to body weight, the fewer calories burned, the longer life expectancy (Figure 1.3A). However, Sohal *et al.* took this notion one step further and showed that mitochondrial oxidant (free radical) production *in vitro*, in this case superoxide, was the better correlate in determining lifespan (Figure 1.3B) providing a strong theoretical rationale for the “Free Radical Theory of Aging” (10). This theory has been refined over the years as it has become clear that elevated oxidative stress is due to a variety of factors. Numerous studies note an exponential increase in the appearance of reactive oxygen (ROS) and nitrogen (RNS) species produced and oxidatively modified macromolecules as animals age (11-14).

Cellular and molecular aspects of aging: mitochondria

Mitochondria provide the majority of cellular energy needed for basic metabolic processes. To do this, mitochondria utilize energy from electrons captured from the catabolism of macromolecules in the mitochondrial respiratory chain, ultimately donating those electrons to molecular oxygen (O_2). However, mitochondria have been shown to decay with age and have been strongly implicated in overall cellular declines during aging (15). Decayed mitochondria become increasingly uncoupled and produce large amounts of oxidants with age (15). As an example, Boveris and coworkers suggested that 1% of all O_2 consumed is converted to oxidants (*e.g.*, superoxide) in young adult rats, but this rate increases to as much as 4% of O_2 in aged tissue (16). Primarily, the elevated rate of oxidant production is attributed to a compromised mitochondrial electron transport chain. While the quantitative rate of ROS production from mitochondria is now considered to be much lower than in the original studies by Boveris and Chance, nevertheless the current consensus is that mitochondrial superoxide production significantly increases with age in all tissues studied (17). Oxidative damage has also been noted to occur in the mitochondria. For example, oxidatively modified mitochondrial DNA has been shown to increase with age as well as membrane damage resulting in a decrease in membrane fluidity (15). However, superoxide produced in the mitochondria may not only cause localized

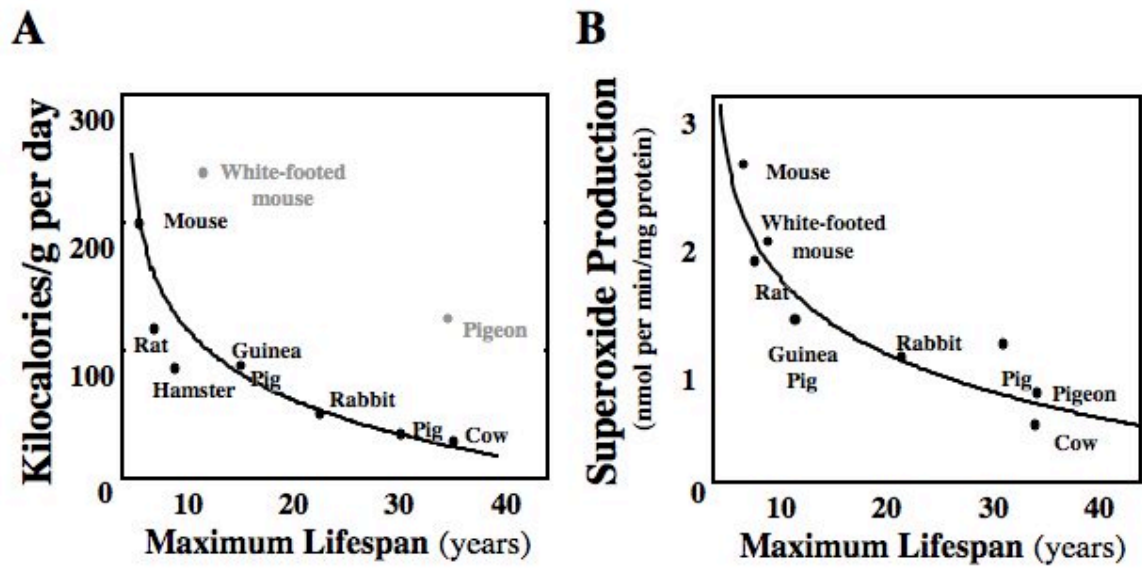


Figure 1.3. Metabolic rate and oxidant production are inversely correlated with maximal lifespan. Data modified from Sohal *et al.* (10).

damage to the mitochondria, but because of its relative stability, would also be able to diffuse and damage biomolecules in other sub-cellular locales. Thus, oxidants produced in the mitochondria could be expected to affect other cellular organelles.

Cellular and molecular aspects of aging: loss of antioxidant status

Exacerbating the increased rate of ROS/RNS production, there is a concomitant decline in levels of low molecular weight antioxidants (18, 19). In particular, the low molecular weight and water-soluble antioxidants, vitamin C and glutathione, significantly diminish with age (20). Of the latter, it appears that there is a significant age-associated decline in the levels of reduced (GSH) versus oxidized glutathione (GSSG), which strongly indicates that aged tissues are chronically experiencing a more pro-oxidant state (15, 21-23). In addition to the loss of low molecular weight antioxidants, certain antioxidant and detoxification enzymes, especially so-called Phase II enzymes (*e.g.*, GSH synthetic enzymes and GSH-S transferases [GST]s) appear to be most affected in aging animals (19, 24). Thus, handling of oxidants and xenobiotic compounds detoxified via GSH-dependent mechanisms in aged tissue appears to be compromised (5, 15, 22, 23, 25). Because of the loss of antioxidant and xenobiotic defenses, there is growing evidence to suggest that aging animals and humans are significantly more vulnerable to oxidative and xenobiotic insult.

Cellular and molecular aspect of aging: protein accumulation

Proteins are known to accumulate within the cell with age and this has been said to be "...the most common molecular symptom of aging" (26). Rodent studies show that steady-state levels of oxidatively damaged lipids, DNA, and protein increase in tissues from old versus young animals. In particular, aged tissues display a chronic accumulation of oxidatively modified proteins. In support of this, accumulation of altered proteins increases significantly with age in all animal species studied (27-35). Dysfunctional proteins can arise from erroneous synthesis, spontaneous deamidation,

inherently unstable amino acids, glycation, and ROS/RNS damage. Further exacerbating this problem, highly modified or oxidized proteins become resistant to proteolysis and can inhibit proteosomal and lysosomal function (26, 36-38).

Cellular and molecular aspects of aging: loss of protein catabolic pathways

Coincident with elevated protein aggregation is a severe decline in protein degradation. Again, increased oxidative damage associated with age has been implicated in this lower rate of protein turnover (37, 38). Thus, a significant and universal aspect of mammalian aging appears to be heightened oxidative stress, which progressively targets the cellular proteome, and ultimately lowers protein turnover (37, 38). The end result is that the cell fills with labile proteins, which become “stuck” in irreversible conformational intermediates that can neither be folded nor unfolded. Once stuck in these misfolded conformations, traditional unfolding pathways can no longer remove these intermediates. As a result, these accumulated proteins compromise normal metabolism, contribute to inefficient house-keeping and repair mechanisms, and can lead to the chronic induction of stress response pathways (26, 37, 38).

However, the cell is not without further defenses. The 20S and 26S proteasomes participate in the selective degradation of altered polypeptide chains (39). Degradation of oxidatively damaged proteins is typically carried out by the 20S proteasome. However, as noted above, proteosomal function declines with age thus compromising the ability of the cell to degrade misfolded proteins with age (37, 38).

Lysosomes provide another route for intra-cellular proteolysis. However, lysosomes also become significantly affected with age, most notably because of the accumulation of lipofuscin, a non-degradable intralysosomal polymeric aggregate (40). Thus, as oxidative stress increases with age, so does the level of oxidatively modified proteins (38). However, a decrease in overall protein catabolic pathways further exacerbates the problem, leading to an accelerated rate of protein accumulation with age, ultimately hindering normal cellular functions (37, 38).

Cellular and molecular aspect of aging: oxidative stress, protein accumulation and the endoplasmic reticulum

The endoplasmic reticulum (ER) is a major site of protein folding that folds up to 1/3 of the total cellular proteome. Proteins folded in the ER tend to be rich in disulfide bonds and facilitate the formation of proper intramolecular disulfide bonding. To achieve proper disulfide bonding, the ER is significantly more oxidizing than other compartments of the cell. For example, the thiol redox state as measured by the reduced glutathione (GSH) to glutathione disulfide (GSSG) ratio has been described to be between 1:1 to 3:1 (41, 42). When compared to the cytosolic glutathione redox ratio of between 30:1 and 100:1, the thiol redox environment of the ER is between 10-100 times more oxidizing than the cytosol (43). However, if the ER becomes either too oxidized or too reduced, this favors the formation of incorrect intramolecular disulfide bonding, resulting in non-native, misfolded protein conformations. Thus, small perturbations in the ER redox status could have dire consequences to overall cellular protein homeostasis.

Accumulating evidence suggests that protein folding results in the generation of ROS as a byproduct of normal ER function and oxidative protein folding. For example, Nuss *et al.* fractionated young and aged liver homogenates and assayed them for oxidatively modified proteins (44). They noted significant age-associated increases in the oxidation of major proteins of the ER including the ER chaperone grp78/BiP, the ER oxidoreductase protein disulfide isomerase (PDI), the ER quality control protein calreticulin, and numerous other chaperones known to specifically localize to the ER. However, whether direct or indirect, this indiscriminate protein damage is not without consequences to cell and organ function. The oxidative modification noted above strongly reduced activity of certain enzymes and was shown to abrogate cell signaling pathways (44). Furthermore, increased protein oxidative damage has been associated with an age-associated impairment in protein folding by inducing irreversible disulfide cross-linking, the formation of insoluble and irreversible protein

folding intermediates, and aberrant protein glycosylation (44-46).

Recent work has also shown that age-related increases in misfolded proteins not only affect specific enzyme activities but may also take on additional cytotoxic qualities, especially if misfolded proteins aggregate. Protein aggregates, as exemplified by ceroid, β -amyloid, huntingtin, CFTR, and lipofuscin are known to undertake detrimental “gain-of-function” activities as their respective diseases progress. That is, over time the more these proteins aggregate the more they compromise cell function (47, 48). The huntingtin protein provides a perfect example. Disease onset and severity is highly correlated with both the expansion of the polyglutamate region in the gene, protein misfolding, and ultimately protein aggregation in the cell (49, 50). Therefore, the larger the repeat, the earlier in life the disease shows clinical manifestations and the more rapid the disease progresses. This case illustrates that any condition that ultimately disrupts protein folding or protein homeostasis (*e.g.*, genetic mutations, oxidative damage, or loss of protein turnover) in the ER increases the potential to cause dire consequences to overall cellular homeostasis.

Protein misfolding in the endoplasmic reticulum

While protein oxidation has been extensively studied as a root-cause for protein aggregation, there is growing evidence that misfolded and aggregated proteins in aged tissues may also develop in a non-oxidative manner (48). Evidence for a non-oxidative component to declines in protein homeostasis come from numerous sources. For example, in the aforementioned decrease in activities of the resident ER chaperone and oxidoreductase, grp78/BiP and PDI, not only did enzyme activity decline with age, but there was an age-related loss in their levels in mouse liver (44). Additional studies now show that amounts of other chaperone proteins involved in nascent protein folding and maintenance also decline with age. Erickson *et al.* showed that ERp55, ERp57, ERp72, grp78/BiP, and calnexin, all critical ER chaperones, decrease between 30%-50% on an age basis in the rat. Considering the role of ER chaperones in ER-dependent protein processing, these data support the concept that their loss could

lead to many of the physiological declines associated with aging. The significant decline in the proper maturation of proteins would also be expected to contribute to toxic protein aggregation both in aged animals as well as pathophysiological processes associated with aging (51, 52). Thus, the relative loss of chaperone-like activities could directly contribute to the age-dependent increase in misfolded and aggregated proteins associated with the endoplasmic reticulum.

The endoplasmic reticulum is an unrecognized site of cellular aging

Because ROS and RNS damage is indiscriminate, it would be expected that the cell as a whole, and all sub-cellular organelles, would be targets of such damage. While theoretically true, most research to date has focused on whole cell, mitochondrial, and lysosomal decay. However, relatively little research has examined the role of the ER as both a target and progenitor of cellular age-related decay. The links between the known cellular hallmarks of aging and the ER include oxidative damage to ER chaperones, decline in protein processing and maturation machinery, accumulation of aberrant proteins, and protein oxidation. Additionally, as the ER has its own sophisticated means of sensing and responding to stresses and accumulation of misfolded proteins further implicates a decay in ER function in aged tissues. Given that the cellular characteristics of aging and the mechanisms responsible for these changes are not well understood, the under-researched nature of the ER is both an obstacle for a more precise understanding of cellular aging as well as an opportunity to define the cellular targets that ultimately lead to organ decline.

The following section will provide a sufficient background related to ER function and the importance of this organelle to overall cellular homeostasis.

The endoplasmic reticulum

The ER is an organelle that comprises 10-30% of overall cellular volume and often greater than 50% of the cellular membrane component (53). The ER plays a vital role in the maturation, processing, and transport of secretory and membrane-associated

proteins. Generally, proteins assembled in the ER are rich in disulfide bonds which help to promote efficient folding and oligomerization of nascent polypeptide chains (54). While disulfide bond formation occurs spontaneously *in vitro*, to ensure proper intramolecular disulfide bonding is achieved, the ER contains numerous chaperones, protein disulfide isomerases, and oxidoreductases to facilitate proper protein folding and to guard against the formation of irreversible folding intermediates (55-59).

Oxidative protein folding in the ER

The activities of resident ER folding enzymes are highly dependent on the local reduction/oxidation (redox) environment and even small perturbations in the redox status can greatly affect enzymatic activity and, as a result, protein folding kinetics (60-63). To help maintain proper protein synthesis, folding, and maturation, the thiol redox status of the ER is significantly more oxidizing than other compartments of the cell (41, 42). This redox environment likely serves to maintain critical enzymes in their preferred redox state to ensure optimal enzymatic activity in the mammalian ER (41, 42, 64). Thus, conditions that disrupt the normal redox environment of the ER would be expected to disrupt the protein folding machinery, other homeostatic ER processes, and even the activation stress response pathways (65).

Endoplasmic protein quality control mechanisms

The eukaryotic ER is unique from prokaryotic protein processing pathways. In bacteria, disulfide bond formation occurs in the periplasm and consists of three distinct pathways (66). In eukaryotes, oxidative protein folding occurs in the ER. However, in contrast with prokaryotic protein processing, the same enzymes that catalyze protein folding in eukaryotes are also responsible for disulfide isomerization, and reduction. Thus, the redox state of the ER must be tightly regulated and maintained within a narrowly defined range to ensure all enzymatic activities are retained (Figure 1.4).

Glutathione is known to be present in high concentrations within the ER (41, 64). The thiol redox state of the ER has been defined by measuring the glutathione thiol redox couple of reduced (GSH) and oxidized (GSSG) species in this organelle. Previous reports have defined the glutathione redox ratio of the ER to be between 1:1 to 3:1 (41, 42). It has been shown *in vitro* that the optimal GSH:GSSG ratio to facilitate efficient and proper protein folding of model proteins is ~2:1 (67). Conversely, it has been shown that optimal unfolding facilitated by ER enzymes occurs at a GSH:GSSG ratio of >5.5:1 (68). Thus, the ER likely compromises both of these activities, maintaining it in a narrowly defined range, to facilitate all activities required in the ER and/or to allow subtle thiol redox modification to favor one function over another (*e.g.*, folding versus unfolding).

While the precise redox ratio and its role in maintaining ER homeostatic mechanisms remains an active area of research, the importance of maintaining the ER redox status is becoming clear. A number of pathophysiologies such as diabetes, liver disease, and emphysema have been described to have an altered ER thiol redox state (48, 62, 63, 65, 69-71). Interestingly, but perhaps counterintuitively, these pathologies are characterized by a reductive shift in the ER thiol redox balance that ultimately alters ER enzymatic function and would be postulated to destabilize higher order proteins structures and result in the misfolding of proteins (Figure 1.4) (63, 72).

To date, there have been only a limited number of studies examining the thiol redox environment of the ER lumen in mammals (41, 42, 64) and whether conditions that alter this redox balance, could adversely affect protein folding. However, to ensure proper redox homeostasis is maintained, the ER possesses a unique set of cell signaling pathways designed to combat and adapt to stresses that specifically target the endoplasmic reticulum.

Endoplasmic reticulum stress

The ER is exquisitely sensitive to alterations in protein homeostasis with perturbations resulting in a number of responses collectively known as ER stress.

Hallmarks of ER stress include: 1) a general inhibition of protein synthesis; 2) transcriptional and translational remodeling of the genome and proteome, respectively; and 3) activation of specific apoptotic pathways (Figure 1.5). The first two functions are aimed at reducing the ER client protein load and, hence, alleviating the stress in the ER. The third is aimed at removing cells damaged beyond repair. Interestingly, these same pathologies observed during ER stress are also observed during the normal aging process suggesting there may be a direct link between the two. However, the role that ER stress, or lack thereof, plays in the normal aging process, and the onset of age-related diseases, is entirely unknown.

Endoplasmic reticulum stress: pro-survival response

To date, the best characterized ER stress response protein is the transmembrane receptor PRK-like ER kinase, or PERK. Upon sensing a stress in the ER lumen, PERK will homodimerize and become autophosphorylated on its cytosolic, extraluminal domains. To date, at least two direct downstream targets of PERK have been identified including the eukaryotic translation initiating factor-2 (eIF2- α) and NFE2-related factor-2 (Nrf2). Phosphorylation of eIF2 α prevents the formation of the eIF2-GTP-tRNA^{Met} initiation complex that is required for translation, ultimately inhibiting novel mRNA transcripts from being translated (inhibition of general protein synthesis). However, PERK-mediated phosphorylation of Nrf2 facilitates translocation of the latter into the nucleus where it initiates the transcription of Phase II (anti-oxidant) genes (73). Furthermore, this group showed that PERK-dependent activation of Nrf2 was essential for survival following the induction of an ER stress (74). Together, these responses (eIF2- α and Nrf2) have the net effect of yielding cytoprotection following an ER stress.

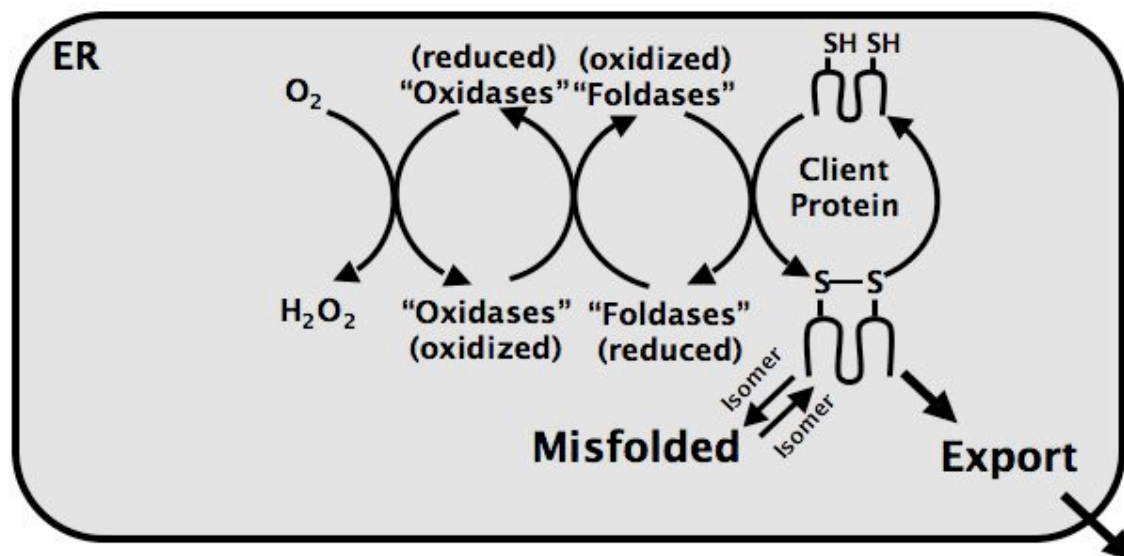


Figure 1.4. Schematic representation of oxidative protein folding in the ER. A nascent peptide is co-translated into the ER where it will be held in its primary structure by molecular chaperones until “folding enzymes” such as the oxidoreductase, PDI, facilitate proper intramolecular disulfide bonding. If the correct folding conformation is achieved, the protein is exported to its next cellular locale. “Oxidases”, such as ER oxidase-1 (ERO1), then re-oxidize the folding enzymes back to their oxidized state. Molecular oxygen has been proposed to be the final electron acceptor, whereby the oxidases become re-reduced and the cycle repeats itself. However, in the eukaryotic ER, these pathways also work in reverse to isomerize incorrectly folded intermediates and/or unfold proteins destined for degradation. These multiple activities underscore the importance of the ER redox state in maintaining proper enzymatic function.

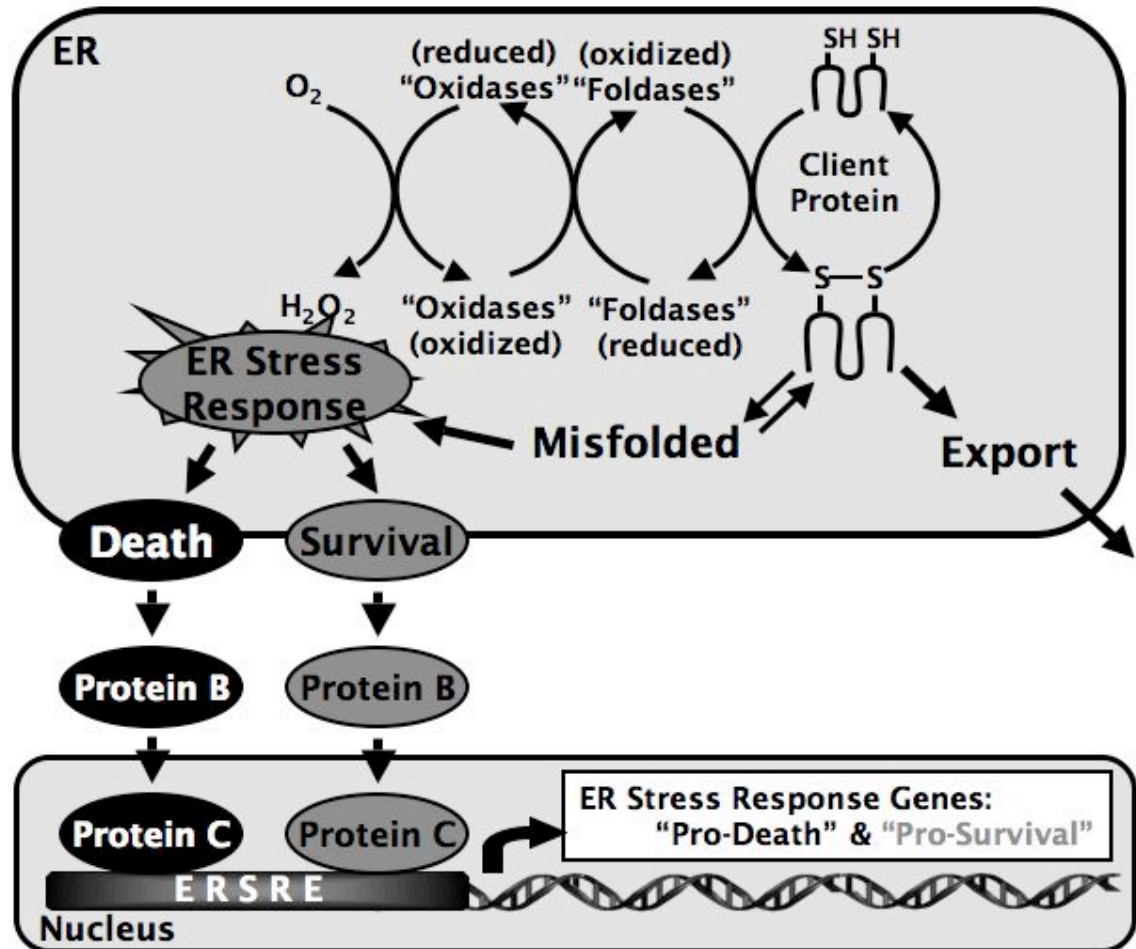


Figure 1.5. Schematic representation of ER stress response pathways. Stressors that disrupt protein folding in the ER and lead to the accumulation of misfolded proteins will elicit an ER stress response. Upon sensing a stress, transmembrane receptors transduce the stress signal to cytosolic intermediates that ultimately activate transcription factors, enter the nucleus, and upregulate ER stress response genes. However, both pro-death and pro-survival pathways are initiated simultaneously. Thus, the severity of the stress dictates which outcome will prevail.

Endoplasmic reticulum stress: pro-death response

As mentioned previously, the ER stress response is a competition between two directly opposing pathways. Upon induction of an ER stress, both pro-survival (discussed above) and pro-death pathways are upregulated. If the stress is mild, the ER will be able to adequately respond to the stress and regain homeostasis. However, if the stress is severe and the ER cannot adequately respond, pro-death pathways will prevail and the cell will undergo apoptosis. One major protein involved in the pro-death pathway is known as growth arrest and DNA damage-inducible gene 153 (*gadd153*) or more commonly known as the C/EBP homologous protein (CHOP) (75, 76). Along with pro-survival pathways, this bZIP transcription factor becomes activated upon an ER stress (77). In addition to its role in inducing the pro-survival genes *grp78/BiP* and *Nrf2*, PERK has also been shown to activate *gadd153/CHOP*. However, the exact mechanism(s) of the pro-apoptotic effects of *gadd153/CHOP* are currently unclear. Recent evidence suggests that *gadd153/CHOP* upregulate and/or activate caspases and pro-apoptotic members of the *bcl-2* family of proteins while simultaneously inhibiting the transcription and activation of anti-apoptotic members of the *bcl-2* family (75, 76).

The endoplasmic reticulum and ER stress response in aging

To date, only three reports have implicated ER stress in the aging process. First, a study using a human diploid fibroblast cellular senescence culture model of aging showed an age-related decline in the expression of the ER chaperone, calnexin, an essential component of ER-dependent protein folding, glycoprotein maturation, processing, and transport machinery. The authors suggested that an age-related decrease in calnexin might contribute to a loss of cytoprotection in a variety of age-related diseases (78). Second, Nuss *et al.* have shown that three key ER resident proteins, *grp78/BiP*, protein disulfide isomerase (PDI), and calreticulin exhibit an age-associated increase in oxidative modifications suggesting an age-associated impairment in protein folding, disulfide crosslinking, and glycosylation in the aged

mouse liver (44). Third, Li and Holbrook showed using cultured hepatocytes isolated from young and old rats that old cells were much more sensitive to cell death following pharmacological induction of ER stress than their young counterparts, in a c-Jun N-terminal protein kinase (JNK) dependent manner (79). However, the precise role the ER and ER stress response mechanisms play in the aging process has never been investigated. Because the ER plays such vital roles in regulating overall protein homeostasis and cellular stress response pathways and because the redox status is essential in regulating these functions, the role of the ER in the normal aging process merits further investigation. Therefore, we hypothesize that the ER is a previously under defined aspect of compromised cellular function known to occur with age and that an age-related ER dysfunction may be a major underlying aspect of the aging process.

1.2. Dissertation Hypotheses and Aims

Based on the previous theoretical rationale, it is the hypothesis of this dissertation that ER dysfunction, specifically, changes in the ER thiol redox status *and* lost ER stress signaling mechanisms may be a significant underlying factor in the aging process. It is further suggested that *R*-alpha-lipoic acid, a dietary compound known to restore age-related changes in redox status *and* activate stress signaling pathways, may be a potent therapeutic agent to maintain ER homeostasis with age. These hypotheses will be explored herein by addressing three specific aims:

Aim 1. Determine if the thiol redox environment of the ER is affected with age. Our laboratory has previously shown that the redox status of the aging liver and mitochondria is adversely affected with age. However, the subcellular redox status of the ER is ill-defined. The goal of this question is two-fold: 1) develop a method to quantify the glutathione redox status in microsomes isolated from rat livers and 2) utilizing this method, determine whether the GSH:GSSG ratio is changing with age. We will then go on to analyze ER stress response pathways *in vivo* to determine whether the rat liver is experiencing a chronic ER stress with age, possibly as the result of an age-related altered ER thiol redox status.

Aim 2. Determine if *R*-alpha-lipoic acid (R-LA) can restore indices shown to decline in the ER with age. Our laboratory has also shown that supplementation with R-LA restores GSH status in old animals *and* beneficially induces stress signaling pathways. The goal of this experimental question is to determine whether or not supplementation with R-LA can reverse any of the above indices shown to be adversely affected with age.

The successful completion of these experimental questions in the following chapters will show: 1) the ER is a cellular target of the aging process and yield a better

understanding of the underlying cellular and molecular mechanisms that contribute to the detrimental indices associated with the aging process and that 2) the ER may be a novel therapeutic target to prevent morbidity and increase healthspan in the elderly.

The Aging Endoplasmic Reticulum

Chapter 2

A Rat Primary Hepatocyte Culture Model For Aging Studies

Swapna V. Shenvi, **Brian M. Dixon**, Kate Petersen Shay, and Tory M. Hagen

Current Protocols in Toxicology

Wiley-Blackwell, Publishers; 10 Ebert Drive; Hillsborough, NJ 08844

In press

2.1. Abstract

The goal of this study was to establish a primary hepatocyte culture system as a suitable model to examine age-related changes in Phase II detoxification gene expression. Hepatocytes were isolated using a two-step collagenase perfusion technique from young (3-6 mo) and old (24-28 mo) rats and placed in primary culture using collagen (Type-I)-coated plates as the extracellular matrix. A supplemented William's E Medium was used as the media. This culture system maintained hepatocyte viability from both young and old rats for approximately 60 hours, as measured by lactate dehydrogenase activity while also maintaining their respective phenotypes relative to Phase II detoxification. We thus conclude that a collagen-based cell culture system is suitable to study age-associated deficits in Nrf2/ARE-mediated Phase II gene regulation provided that experiments can be conducted within 60 hours after cell isolation.

2.2. Introduction

There is growing awareness that Phase II detoxification processes become impaired with age. However, work in this area has been hampered because of the lack of experimental models that maintain the physiological aging phenotype and also allow molecular manipulation to study gene expression reliably. These criteria exclude immortalized cell lines, the main experimental system for molecular biology, as transformed cells cannot adequately mimic the cellular aging phenotype of the liver. Freshly isolated hepatocytes taken from animals of appropriate ages may be an excellent means to study age-related molecular and cellular changes that affect detoxification reactions. Isolated rat hepatocytes only survive for a few hours after collagenase dispersion if they are not placed in culture. Thus, appropriate culture conditions must be discerned in order for differentiated primary hepatocytes to be used as a cellular model for Phase II-dependent reactions. Therefore, we have established a primary hepatocyte culture system that will permit us to address mechanistic questions related to age-associated changes in cell function.

This unit describes procedures for isolating parenchymal hepatocytes from the livers of young and old rats (see Basic Protocol 1), culturing the hepatocytes on collagen-coated plates (see Basic Protocol 2), and for assessing their viability by using the lactate dehydrogenase (LDH) release assay (see Basic Protocol 3).

NOTE: All protocols using live animals must first be reviewed and approved by an Institutional Animal Care and Use Committee (IACUC) and must conform to governmental regulations regarding the care and use of laboratory animals.

NOTE: All solutions and equipment coming into contact with hepatocytes after the isolation procedure is complete must be sterile and aseptic technique used accordingly.

NOTE: All culture incubations should be performed in a humidified 37°C, 5% CO₂ incubator unless specified otherwise.

2.3. Materials and Methods

BASIC PROTOCOL 1

Isolating hepatocytes from young and old rats

This procedure describes the initial isolation of hepatocytes from rat livers and purification for parenchymal cells. Dissection can be conducted on a laboratory surgical table and need not be conducted in an aseptic environment for short-term culture of the hepatocytes. The highest number of healthy viable hepatocytes is achieved by a well-coordinated dissection when materials and solutions are prepared fresh and the total time between anesthesia and purification of isolated hepatocytes is minimized. Hepatocyte isolation from a second rat can be started as soon as the dissociation of liver cells from the first rat is underway.

A liver from a young rat typically provides 400-500 million hepatocytes, while a liver from an old rat yields upwards of 600 million cells. Depending on the experimental protocol, this may be far more hepatocytes than can be conveniently used at once. For example, for viability assessments, gene expression determination, and nuclear extract preparation, hepatocytes are plated at 2 million cells/well of a 6-well plate. Thus, a single rat would provide hepatocytes for hundreds of cultures. Cell suspensions may therefore be cryopreserved and used for other studies (80)

Materials

Young (4-6 months) and/or old (24-28 months) Fischer 344 rats

Hanks' 10X salt solution (see recipe), ice-cold

Pre-Hanks' 1X solution (see recipe), pre-warmed to 37°C and bubbled for 30 minutes with carbogen gas

Hanks' I solution with BSA and EGTA (see recipe)

Hanks' II solution with CaCl₂ (see recipe)

Krebs' 2X stock solution (see recipe)

Krebs' 1X solution, pH 7.4 (see recipe), bubbled for 30 minutes with carbogen gas

Heparin (0.2% in saline; sterile filtered)

Collagenase D (Boeringher-Manheim)

DNase I (Sigma)

37°C water bath

50 ml round bottom flask

Peristaltic pump and tubing

Rotavapor

Glass vial for bubble trap

Inverted microscope

Carbogen tank and tubing

Anesthetizing chamber

Dissecting steel pan

Tape

Dissection tools:

Surgeon's scissors

Cross-action forceps

Iris scissors

Blunt forceps

Butterfly clamp

18 G and 21 G surgical needles for designing cannulae for young and old rats,
respectively

23 G needle for heparin injection

1 ml syringe

Cotton swabs

0.4 mm surgical sutures

Gauze pads

Vacuum aspirator

0.4% (w/v) Trypan Blue

Hemocytometer and cover-slip

Kimwipes

Set-up for surgery

1. Place Pre-Hanks' 1X, Hanks' I, and Hanks' II solutions in a 37°C water bath. Maintain the Krebs' solution at room temperature.
2. Secure the bubble trap in the clamp and arrange tubing through the pump teeth so that tubing is able to reach the water bath and easily reach the bubble trap and surgical area.
3. Adjust the flow rate to 10 ml/min for a young rat and 13 ml/min for an old rat. Transfer the tubing to Pre-Hanks' 1X Solution.

It is very important to adjust the flow rate as a too-low flow rate can lead to incomplete perfusion and low hepatocyte yield, while a too-high flow rate can compromise hepatocyte viability.

4. Fill a 1 ml syringe with 0.4 ml (young rat) or 0.6 ml (old rat) heparin solution, remove any air bubbles and bend the needle to a 90° angle for injection of heparin into the ileac vein.

Preparing animal for surgery

1. Charge the anesthetizing chamber and nose cone with ethyl ether for 5 minutes.
2. Place the animal in the charged anesthesia chamber. Remove the animal after it is immobilized and the eyes stop blinking and place the animal on the sacrifice tray under anesthesia (nose cone) being sure to allow enough anesthesia to maintain unconsciousness but enough air as not to suffocate the animal.

Performing the surgery

1. Secure the animal's limbs to the tray with tape ventral side up. Place the nose cone over the animal's nose so that it receives a mixture of anesthesia and air. Ensure that the animal is insensate before proceeding by pressing firmly on the rear root pads and watching for a reflex response. Use the surgeon's scissors to make a midline incision and lateral incisions on each side.

Note: *take care not to cut through the diaphragm.*

2. Expose the ileac vein by separating the musculature using the forceps to remove the connective tissue. Position the bevel of the 90°-bent needle over the ileac vein and gently slide it in. Slowly inject the heparin (0.4 ml for young, 0.6 ml for old rats). Place a Kimwipe over the injection site to minimize exsanguination while slowly withdrawing the needle.
3. Use the cross-action forceps to place a loose ligature around the vena cava and secure the end of the ligature with a hemostat. Place two more ligatures about 1 cm apart around the portal vein near the base of the liver, also securing loosely with hemostats.
4. Make a small incision between the two portal vein ligatures being careful not to sever the portal vein completely.
5. Quickly place the cannula into the portal vein incision and secure the cannula by tightening the ligature around the portal vein closest to the liver. Tighten the ligature around the portal vein furthest from the liver to secure the cannula to the vein for additional support.
6. Use the surgeon's scissors to cut up completely through the sternum/rib cage. Use the iris scissors to cut the diaphragm and the vena cava above the liver, also tightening the vena cava ligature.
7. Supporting the liver by the cannula, use the iris scissors and the forceps to sever the connective tissue between the liver and the stomach and the spleen. Cut through any adipose, connective, and vasculature tissue beneath the perfusion area. While holding up the liver by the cannula, sever the connective tissue between the liver and the dorsal coelemic area (cut along the spine) to completely free the liver.
Note: use extreme caution to avoid damaging the liver during excision.
8. Let the liver is perfusing with Hanks' I solution for another 2-3 minutes to remove any residual blood.

9. While the liver is perfusing, add collagenase D to the Hanks' II solution (40-45 mg for young and 60-65 mg for old rats in 100 ml Hanks' I solution).
10. Perfuse the liver for 1 minute in the Hanks' II solution, allowing the liquid to flow onto the tray. This will remove any residual EGTA remaining from the Hanks' I perfusion. Transfer the liver to the beaker containing Hanks' II solution and submerge liver completely to maintain temperature and so that the perfusate will continually recirculate; allow the perfusion to continue until the liver feels soft displays a cauliflower-like appearance.

Isolating and purifying the hepatocytes

1. Detach the cannula from the tubing.
2. Using a glass rod, gently massage the liver against the side of the beaker containing the Hanks' II solution and collagenase D to begin to liberate hepatocytes.

Note: the liver massage for extracting hepatocytes can be continued till the liver looks like a transparent sac.

3. Filter the cell mixture through gauze into a 500 ml Erlenmeyer flask to remove any larger contaminants (connective tissue or undissociated liver). Rinse the gauze with approximately 150 ml of Krebs' 1X solution.
4. Allow the cells to settle for 20-30 minutes.

Note: these steps are undertaken to separate the hepatic parenchymal cells from the stellate cells on the basis of differences in their densities. The hepatic parenchymal cells are primarily involved in detoxification reactions.

5. Aspirate the solution above the settled cells.
6. Swirl the cells to resuspend. Add 1-2 mg DNase I directly into to the cell solution. Swirl again gently until the cell suspension is homogeneous.
7. Add 100-120 ml Krebs' 1X solution to the cells, swirling gently to mix.
8. Repeat the wash cycle one more time for a total of three washes.

9. After the final aspiration, measure the volume of the cell suspension (about 20 ml) and then transfer the cell suspension to a round bottom flask, secure the flask to a Rotavapor, and gently rotate the cells.

Measuring cell viability by Trypan Blue exclusion

1. In a 0.5 Eppendorf tube, add 90 μ l Krebs 1X solution + 90 μ l Trypan Blue + 20 μ l cells. Mix well.
2. Put 10 μ l on hemocytometer. Count 4 quadrants.
3. Total cells – blue cells = viable cells.
Cell number x 10,000 x dilution factor = cells/ml.
Cells/ ml x number of ml = Total yield.
4. Viability is typically around 94%. It should not be less than 85% to carry out experiments.

BASIC PROTOCOL 2

Culturing primary rat hepatocytes on collagen coated plates

There is no general consensus for the optimal set of culture conditions for primary rat hepatocytes, in part because the appropriate plating substrate, culture medium, additives, and cell density may vary depending on experimental design. This protocol describes plating of hepatocytes on collagen-coated plastic 6-well culture dishes in William's Medium E containing fetal bovine serum and other supplements. See Background Information for a brief description of the function of each additive in maintaining optimum hepatocyte function. The following should be performed under aseptic conditions.

Materials

Collagen-I (rat tail; Sigma)

50 mM HCl

Hanks' Balanced Salt Solution (HBSS; Sigma)

Hepatocyte cell suspension (see Basic Protocol 1)

Complete William's Medium E (Sigma; see recipe)

Laminar flow hood

6-well plastic cell culture dishes (such as Corning or Nunc brands)

Preparing collagen-coated plates

1. Suspend collagen-I in 50 mM HCl for a final concentration of 1 mg/ml.
2. Incubate the collagen-HCl suspension in a 37°C water bath until the collagen-I is completely dissolved.
3. Dilute the collagen solution in sterile water for a concentration of 60 µg/ml.
4. Place 6-well culture plates in a laminar flow hood.
5. Pipet 1 ml of collagen solution into each well, replace lids and place in the 37°C incubator for 4 hours.

Note: Many other substrates are used for hepatocyte culture, including fibronectin, laminin, and combinations of these with collagen. Several companies also sell pre-

coated dishes (e.g., Biocoat™ dishes from BD Biosciences). Other substrates used as matrices in hepatocyte cell culture include proprietary formulations like Matrigel™ (BD Biosciences) and AlgiMatrix™ (Invitrogen) provide a three dimensional matrix.

6. Rinse each well three times with 2 ml HBSS to neutralize the acid. Aspirate the last rinse.

Note: if dishes are to be used immediately, proceed to cover the wells with media. However, dishes may be used for ≥ 2 weeks after coating, if they are stored dry at 4°C.

Culturing hepatocytes

1. Dispense 2 ml of complete William's Medium E into each well and leave in the incubator for 30 minutes to equilibrate with the matrix.
2. Determine the desired number of cells per well and calculate the volume of hepatocyte suspension needed to achieve this number. In the laminar flow hood, using sterile pipet tips, pipet the appropriate volume of cell suspension into each well containing complete William's Medium E.

Note: the hepatocyte cell density is crucial for toxicological studies. For a high density plating, two-million cells per well of a 6-well plate was found to be an appropriate number.

Note: the hepatocytes will settle to the bottom of the flask before they are plated. If necessary, gently resuspend the cells before drawing them into the pipet.

3. Replace the medium after 4 hours. *This step is especially important for high density hepatocyte cultures to remove debris produced during collagenase digestion and cell dissociation. Perform all subsequent experiment only after an overnight incubation.*
4. Replace the medium every 24 hours of the entire cell culture period.

BASIC PROTOCOL 3

Determination of hepatocyte viability by lactate dehydrogenase (LDH) release

Cytotoxicity in primary culture of rat hepatocytes can be measured by two methods: cytosolic enzyme leakage, and detachment of damaged cells from the monolayer culture. Leakage of LDH, an intracellular enzyme, is typically used for hepatocyte viability measurements. The lactate dehydrogenase method is simple, accurate, and yields reproducible results. When a cell is damaged, LDH is released into the culture medium. Thus, by measuring the intracellular LDH activities of cells that remain intact and attached to the collagen substrate, hepatocyte survival in culture can be determined. The protocol presented here is a modification of the method developed by Moldeus and co-workers (81). In this assay, LDH activity is measured by following the consumption of NADH during the conversion of pyruvate to lactate.

Materials

Phosphate buffered saline (PBS)

Potassium phosphate buffer (0.1 M, pH 7.4)

10% Triton X-100

NADH, 20 mM

20 mM sodium pyruvate

UV spectrophotometer

1. Wash each well twice with 2 ml of PBS.
2. Add 10 μ l of 10% Triton X-100 in 1 ml potassium phosphate buffer to each well to lyse hepatocytes.
3. Scrape cells and transfer to 1 ml Eppendorf tube.
4. Incubate on ice for 30 minutes.
5. Pre-warm the spectrophotometer to 37°C and turn on UV bulb to allow beam to stabilize.

6. Add 50 μ l of cell lysate to 2.85 ml of reaction buffer (0.1 M phosphate buffer, pH 7.4, 5 mM NADH).
7. Initiate the reaction by adding 100 μ l of 20 mM sodium pyruvate solution.
8. Measure the rate of decreasing absorbance at 340 nm.
9. A unit of LDH activity is defined as an optical density change of 0.001 per minute.

Reagents and solutions

Use Milli-Q purified distilled or deionized water in all recipes and protocol steps. All reagents and chemicals in the recipes are from Sigma unless otherwise specified.

1 L Hanks' 10X stock solution

80 g NaCl
4 g KCl
0.6g Na₂HPO₄
0.6g KH₂PO₄

500 ml Pre-Hanks' 1X solution

50 ml 10X Hanks' stock solution
3 g HEPES
1 g NaHCO₃

Hanks' I solution, pH 7.4

100 ml Pre-Hanks' 1X solution
2 g bovine serum albumin
0.5 ml 120 mM EGTA

Hanks' II solution, pH 7.4

100 ml Pre-Hanks' 1X solution
1 ml 0.4 M CaCl₂

1 L Krebs' 2X Stock Solution

13.8 g NaCl
0.72 g KCl
0.59 g MgSO₄·7H₂O
4 g NaHCO₃
0.26 g KH₂PO₄

500 ml Krebs' 1X solution, pH 7.4

250 ml Krebs' 2X stock solution

1.5 g HEPES

0.18 g Glucose

0.5 g Glutamate

Complete William's Medium E (in William's E base medium)

5% FBS

1:100 (v/v) antibiotic/antimycotic mix containing 10,000 U penicillin, 10 mg streptomycin, and 25 μ g amphotericin B per ml (ATCC)

2 mM *L*-glutamine

100 ng/ml insulin

1 μ M dexamethasone

2.4. COMMENTARY

Background Information

A progressive age-associated decline in stress response mechanisms has been noted in many animal species, which leads to heightened risk for both morbidity and mortality (6, 14, 82, 83). However, the molecular mechanisms leading to this overt aging phenotype have yet to be elucidated. In part, this is because of a lack of *in vitro* models that can be molecularly manipulated to discern the precise lesion(s) involved in the aging cellular environment. The present protocol describes a primary hepatocyte culture system that fills this gap. Using this protocol, hepatocytes from young and old rats can be kept in primary culture for at least 60 hours. Thus, this model provides a sufficient experimental window to carry out cellular and molecular studies related to detoxification mechanisms during aging.

Methods for culturing rat hepatocytes have been established for a number of years, but to our knowledge no definitive studies have described conditions showing this model is suitable for toxicological research related to aging. Holbrook and coworkers successfully used cultured rat hepatocytes to monitor age-associated changes to cell signaling cascades. They found that a similar culture system as described herein was suitable for discerning age-related differences in mitogen-activated protein kinase (MAPK) signaling mechanisms (84) and endoplasmic reticulum stress response (79). In addition to this, studies from other groups utilized the collagen matrix in combination with various media to demonstrate that the aging phenotype was maintained in culture in a caloric restriction model as well as under growth factor stimulation (85, 86). Thus, these previous studies combined with the present method suggest that culturing hepatocytes from old rats is an appropriate model to examine a variety of age-dependent changes that affect cell signaling and stress response mechanisms.

Critical Parameters and Troubleshooting

Acclimatization of animal colonies

It is important that animals be acclimatized in the animal facilities for at least 1 week prior to the experimental procedures. Since a major application of the isolation and cell culture of the hepatocytes is to assess age-associated differences in detoxification capacity, it is critical that the transportation-induced stress does not affect these parameters.

Cell isolation and culture

Cell damage and death begin as soon as the animal is anesthetized. Therefore, speed of surgery as well as timely dissociation and purification of cells is of utmost importance. To minimize cell damage, avoid contact with the perfusing liver either by hand or pointed surgical instruments. Instead, support the perfusing liver by the cannula and use a cotton swab to reposition the liver if necessary. After isolation, resuspend hepatocytes in buffer by gently swirling the flask. Do not pipet too vigorously or through a narrow-bore pipet. Viability of hepatocytes before plating is the single-most important predictor of suitability for culture. Discard a hepatocyte preparation that has < 85% viability as the survival in culture will not be optimum. This is especially true for hepatocytes isolated from old rats.

Be sure that the medium is replaced 4 hours after plating. It is also critical that experiments be initiated only after an overnight culture. After isolation, levels of stress-induced transcription factors are especially high, thus confounding differences in the aging phenotype. After the initial 4 hour medium replacement, replace media every 24 hours thereafter for the maintenance of cultures.

Anticipated Results

The percent viability of the final hepatocyte preparation will typically be $\geq 85\%$ with a greater percentage of viable hepatocytes from younger rats than from older rats. Thus, there may be a greater sensitivity to collagenase disruption of aged liver and subsequent cellular damage. In this unit, cellular release of lactate dehydrogenase (LDH) was used as means of assessing hepatocyte viability over the culture period. Experiments have shown that almost no cells from old rats remained viable after 60

hours in culture whereas nearly 50% of cells from young rats were alive at this time point. Hence, hepatocytes from old rats can be cultured under similar conditions acceptable for maintaining viability for cells from young rats. However, experimentation on isolated hepatocytes from old rats should be conducted within 60 hours after isolation.

Time Considerations

Prepare reagents and set up for isolation and culture ideally a day before the surgery. The first step in this process should be the preparation of collagen solution and coating of the plates, so that they have sufficient time to set and be used the next day. If a series of isolations is planned for the whole week, coat all the plates at one time and store them appropriately. Apply the same considerations for the preparation of the media.

Start the surgery and isolation procedure early in the day to leave enough time for plating and the first media change. This also gives a sufficient overnight incubation time for the hepatocytes before the start of experiments. Plate the hepatocytes within 3 hours of isolation to prevent a loss of initial viability prior to plating.

The Aging Endoplasmic Reticulum

Chapter 3

Assessment of Endoplasmic Glutathione Redox Status is Confounded by Extensive *Ex Vivo* Oxidation

Brian M. Dixon, Shi-Hua D. Heath, Robert Kim, Jung Suh, and Tory M. Hagen

Antioxidants and Redox Signaling

Mary Ann Liebert, Publishers; 140 Huguenot Street; New Rockelle, NY 10801

May, 2008 10(5):963-972

3.1. Abstract

Glutathione (GSH) and glutathione disulfide (GSSG) form the principal thiol redox couple in the endoplasmic reticulum (ER); however, few studies have attempted to quantify GSH redox status in this organelle. To address this gap, GSH and GSSG levels and the extent of protein glutathionylation were analyzed in rat liver microsomes. Because of the likelihood of artifactual GSH oxidation during the lengthy microsomal isolation procedure, iodoacetic acid (IAA) was used to preserve the physiological thiol redox state. Non-IAA-treated microsomes exhibited a GSH:GSSG ratio between 0.7:1 to 1.2:1 compared to IAA-treated microsomes that yielded a GSH:GSSG redox ratio between 4.7:1 and 5.5:1. The majority of artifactual oxidation occurred within the first 2 h of isolation. Thus, the ER GSH redox ratio is subject to extensive *ex vivo* oxidation and when controlled, the microsomal GSH redox state is significantly higher than previously believed. Moreover, *in vitro* studies showed that PDI reductase activity was markedly increased at this higher thiol redox ratio versus previously reported GSH:GSSG ratios for the ER. Lastly, we show by both HPLC and Western blot analysis that ER proteins are highly resistant to glutathionylation. Together, these results may necessitate a re-evaluation of GSH and its role in ER function.

3.2. Introduction

The endoplasmic reticulum (ER) plays essential roles in many vital cellular functions including synthesis of macromolecules, regulation of cellular calcium homeostasis, and the maturation, processing, and transport of secretory and membrane-associated proteins (87). Generally, proteins assembled in the ER are rich in disulfide bonds which help to promote efficient folding and oligomerization of nascent polypeptide chains (54). While disulfide bond formation occurs spontaneously and independently of enzymatic processes, to ensure correct intramolecular disulfide bonding is achieved, the ER contains chaperones and oxidoreductases to ultimately produce a properly folded protein (55-59). The activities of resident ER folding enzymes are highly dependent on the reduction/oxidation (redox) environment and even small perturbations in redox status greatly affects enzymatic activity and, as a result, protein folding kinetics (60-63).

To ensure protein processing, the ER lumen appears to be more oxidizing than other compartments of the cell (41, 42). This environment likely serves to maintain critical enzymes in their preferred redox state to ensure optimal enzymatic activity in mammals (41, 42). For example, members of the ryanodine receptor superfamily, responsible for Ca^{2+} release from ER stores, contain sulfhydryl groups that function as a redox “switch” which either induces or inhibits Ca^{2+} release (88-92). Generally, oxidation activates these receptors while thiol reduction is inhibitory (88). Furthermore, protein disulfide isomerase (PDI) requires its active site thiols to be oxidized to catalyze disulfide bond formation for activity and only a slight reductive shift in the ER converts PDI to a reduced state (63).

Due to its sheer amount, GSH is the principal thiol compound of the ER and has been implicated in maintaining the ER thiol redox environment (65). However, the precise role of GSH in the ER remains unclear. For example, GSH may act as an antioxidant in scavenging reactive oxygen species (93), as a reductant to maintain protein sulfhydryls in a reduced state (54), or conversely, as an adjunct in forming

native disulfide bonds within proteins entering the secretory pathway (94). Despite the lack of a consensus regarding its precise role in the ER, there is a general appreciation that GSH is directly tied to normal ER function and changes in the GSH redox state have been associated with pathophysiologies that target and disrupt the ER (62, 63, 65).

Because of its importance to the ER, it is surprising that only a few studies have attempted to directly quantify ER GSH levels and determine its redox state. An initial study by Hwang *et al.* used a tetrapeptide probe to measure the general ER redox environment in a hybridoma cell line (42). This group determined the probe's thiol redox ratio, and thus the ER GSH:GSSG ratio, to be between 1.5:1 to 3.3:1 (42). Recently, a more direct measurement of rat liver microsomal ER GSH redox status was made using monobromobimane as a thiol derivatizing agent in isolated rat liver microsomes (41). The GSH:GSSG ratio was more precisely estimated to be 3:1, which again suggested that the ER was a generally more oxidizing environment than other compartments of the cell (41). However, both studies failed to control for *ex vivo* oxidation during sample preparation. Thus, the potential exists that thiol oxidation occurs during cell culture (95) and microsomal isolation, which may be a confounding factor in the proper assessment of thiol redox status. Given the importance of GSH redox state as a determinant in ER function, it is the goal of the current study to more accurately define the ER glutathione redox status by controlling for the likelihood of *ex vivo* oxidation.

By modifying an established method previously used to quantify glutathione in other subcellular organelles (25, 96-102), we show that both GSH and GSSG can be quantified simultaneously in microsomes isolated from rat liver. As such, iodoacetic acid (IAA) was incorporated into the microsomal isolation procedure to preserve the GSH redox state. Herein we show that *ex vivo* oxidation is extensive during microsomal isolation and its control reveals the ER GSH:GSSG ratio to be significantly higher than previously reported. Moreover, we show that ER protein glutathionylation, which was previously shown to be extensive (2), is actually quite

small with only a select number of proteins modified. These results may necessitate a re-evaluation of the precise role that microsomal GSH:GSSG redox state plays in normal ER function.

3.3. Materials and Methods

Materials

High performance liquid chromatography (HPLC) solvents were all HPLC grade (Fisher Scientific, Pittsburgh, PA). All other chemicals were reagent grade or the highest quality available from Sigma-Aldrich (St. Louis, MO).

Isolation of rat liver microsomes

Fischer 344 rats (8-11 mo old; National Institute on Aging animal colonies) were anesthetized with diethyl ether, the livers perfused with ice-cold phosphate buffered saline, pH 7.5 (PBS), to remove blood, and then sacrificed according to IACUC-approved guidelines. The livers were quickly excised and placed on ice. Microsomes were isolated as previously reported with some modifications (103). Briefly, liver was homogenized 1:7 [w/v] in ice-cold homogenization buffer (10 mM potassium phosphate [monobasic], 10 mM potassium phosphate [dibasic], 150 mM HEPES, 75 mM potassium chloride, 1 mM EDTA; pH 7.5) and microsomes isolated by differential centrifugation. The microsomal pellet was further washed (100 mM potassium pyrophosphate and 1 mM EDTA, pH 7.4) to remove heme and spun again at 100,000 x g for 95 min at 4°C. The microsomal pellet was resuspended in 750 µl of 100 mM potassium phosphate buffer containing 30% glycerol [v/v] and 1 mM EDTA, pH 7.25. Only freshly isolated microsomes were used for experimentation. Assays for purity revealed that microsomal preparations using this procedure had minimal contamination of Golgi using the 59 kDa Golgi protein (Abcam #ab23932) as a marker) but were highly enriched for Calnexin (Abcam #ab22595) (data not shown). Thus, the procedure employed in this study results in microsomes relatively free of contaminating membranes.

Incorporation of iodoacetic acid

In some experiments, the portal veins of rats were cannulated, immediately perfused with homogenization buffer containing 70 mM iodoacetic acid (IAA; Sigma-Aldrich) to immediately arrest thiol/disulfide exchange at the time of animal sacrifice, and microsomes were isolated. In other studies, livers were perfused to remove blood and then homogenized in buffer containing 70 mM IAA. To determine if and when artifactual thiol oxidation occurred during microsome isolation, timecourse experiments were undertaken where IAA (70 mM, final concentration) was added at 2 h intervals throughout the ~6 h microsomal isolation procedure.

Preparation of microsomal samples for free glutathione analysis

Immediately following isolation of microsomes, 300 μ l of the microsomal suspension was added directly to an equal volume of 15% (v/v) perchloric acid (PCA; Fisher Scientific) containing 10 mM diethylenetriaminepentaacetic acid (DTPA; Sigma-Aldrich), and incubated on ice for 15 min. Acidified samples were then spun at 15,000 \times g for 15 min, the supernatant removed, and stored at -20°C until derivatization and glutathione analysis. PCA (300 μ l of a 15% stock, containing 10 mM DTPA) was then added back to the pellet, snap-frozen in liquid nitrogen, and stored at -80°C for protein-bound glutathione analysis (described below).

Determination of protein glutathionylation

To determine the amount of glutathione present as mixed disulfides with proteins, three validation protocols were followed. First, freshly isolated microsomes treated with or without IAA were incubated with dithiothreitol (DTT; 0.1 mM) for 1 h at room temperature and the extent of GSH liberated was quantified by HPLC. Second, a stronger thiol reductant, tris(2-carboxyethyl)phosphine hydrochloride (TCEP; 10 mM), was similarly used to release GSH bound to proteins (104). Lastly, acid-precipitated protein pellets were re-solubilized in 0.1 M phosphate buffer, and the

pH adjusted to 7.4 with 3 M KOH. These samples were then incubated in the presence of 1 mM DTT for 24 h at 4°C and the amount of GSH released determined.

High performance liquid chromatography for glutathione

GSH quantification was performed as described using dansyl chloride as a fluorophore and γ -glutamylglutamate (γ -GG) as an internal standard for derivatization efficiency (100, 102). Analyte separation was achieved using a 3-aminopropyl column (200 mm x 2.6 mm i.d.; Custom LC, Houston, TX) using a gradient of two buffers (Buffer A, 80/20 methanol/water (v/v); Buffer B, 62.5% MeOH (v/v), 20% acetate stock (217.6 g sodium acetate trihydrate [Fisher Scientific] in 400 ml glacial acetic acid) and 17.5% glacial acetic acid (v/v)). By this means, both GSH and GSSG can be simultaneously separated and quantified relative to authentic standards from a single biological sample.

Western blot analysis for glutathionylated ER proteins

As a negative control, microsomes were incubated in 50 mM Tris buffer, pH 7.25, containing 5 mM EDTA, 1% Triton-X 100, and 1 mM DTT for 1 h at 25°C to release and remove all glutathione present as mixed disulfides. As a positive control, microsomal samples were incubated with 1 mM or 10 mM GSSG in identical conditions as described above. Freshly isolated rat liver microsomes were added directly to 3X loading buffer (0.5 M Tris-HCl, pH 6.8, 10% SDS [w/v], 25% glycerol [v/v], and 0.5% bromophenol blue [w/v]). Protein was separated on 10% polyacrylamide gels (Pierce, Rockford, IL) and transferred to PVDF membranes (Millipore). The levels of glutathionylated proteins were detected using a mouse monoclonal antibody (Fitzgerald Industries, Concord, MA), standardized to BiP/Grp78 levels as a loading control (Stressgen, Ann Arbor, MI), visualized using appropriate horseradish peroxidase-conjugated secondary antibodies (Amersham

Pharmacia Biotech, Buckinghamshire, UK) in conjunction with a chemiluminescent substrate (Amersham Pharmacia) and Enhanced Chemiluminescent Film (Amersham Pharmacia).

Insulin turbidity assay

The insulin turbidity assay, a means to assess how modulating GSH redox state affects PDI-catalyzed reduction of insulin disulfides, was performed essentially as described (105). Briefly, 0.25 μ M recombinant PDI (RayBiotech, Norcross, GA) was incubated in 0.1 M HEPES buffer, pH 7.25, containing 2 mM EDTA. Aliquots of the protein suspension were incubated with 5 mM GSH equivalents but the GSH:GSSG ratio in each aliquot was varied from 1:1 to 15:1. The resulting mixture was allowed to equilibrate at 25°C for 1 h whereupon the reaction was initiated by the addition of insulin (1 mg/ml, final volume). The rate of disulfide bond reduction was monitored spectrophotometrically at 650 nm in kinetic mode for 60 min using a DU800 spectrophotometer (Beckman-Coulter, Fullerton, CA). The rate of the reaction was monitored relative to control preparations where either PDI and/or insulin were omitted from the reaction mixture.

Statistical analysis

Statistical significance between means of two independent groups was determined by Student's *t* test, assuming equal variances. For comparison of treatment effects, one-way analysis of variance (ANOVA) with Tukey's *post hoc* test was used. All of the results were considered significant if the *p* value was < 0.05. Statistical analysis was performed using PRISM 4.0b software (GraphPad Software, San Diego, CA).

3.4. Results

Analytical method for microsomal glutathione

The well-known method first established by Reed and coworkers was chosen to monitor ER GSH status (100, 102). This HPLC technique allows the simultaneous determination of both GSH and GSSG from a single sample. Adapting this protocol to monitor ER GSH was achieved with minimal changes from the published method (see Materials and Methods). As assessed using γ -GG as an internal standard to monitor the efficiency of analyte derivatization, acid-soluble thiol-containing compounds of the ER were reproducibly derivatized with near complete efficiency (data not shown). Baseline separation of both GSH and GSSG standards were also reproducibly achieved (Figure 3.1A and B) and easily detectable in microsomal samples (Figure 3.1C). These results show that the method employed in this study is acceptable to quantify free GSH and GSSG in complex microsomal mixtures.

Ex vivo oxidation occurs during isolation of microsomes

Quantification of the total microsomal glutathione pool (GSH + 2GSSG) shows that the ER contains significant quantities of this tripeptide. Overall microsomal GSH equivalents were calculated to be 0.32 nmols/mg protein with a notably small (20%) coefficient of variation (data not shown). In contrast to the highly stable nature of the overall GSH pool, both GSH and GSSG levels varied markedly, with a calculated coefficient of variance of 69% and 34%, respectively (data not shown). Variability in the GSH:GSSG ratios ranged over 114% (0.12:1 to 3.0:1; $N \geq 11$). The extensive range in values was in accordance with Hwang *et al.* (42) who also observed significant variability in the ER thiol redox state. Because of this marked variability, the rapid nature of thiol-disulfide exchange, and the long isolation procedure, *ex vivo* oxidation was suspected as a confounding factor in quantifying the GSH:GSSG ratio in microsomal preparations.

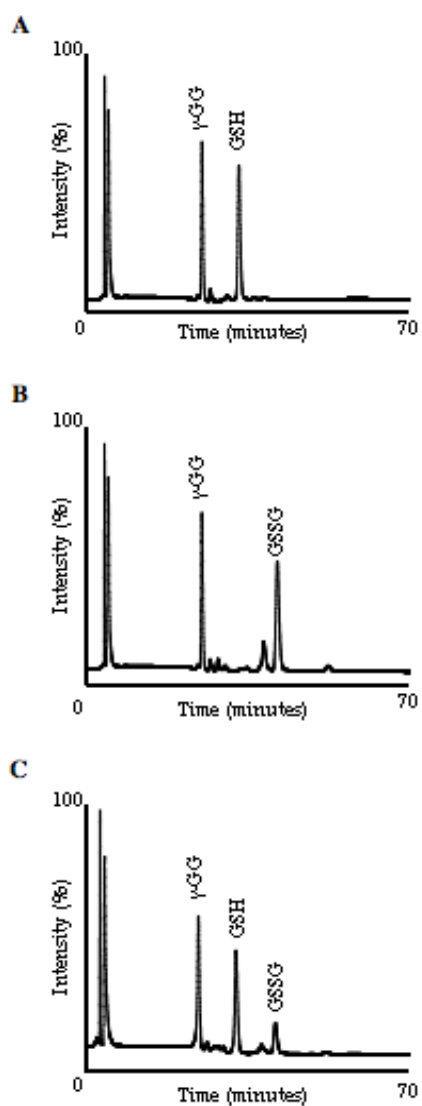


Figure 3.1. Chromatographic separation of γ -GG, GSH, and GSSG. GSH and GSSG standards were prepared and injected (50 μ l) onto a 3-aminopropyl column for HPLC separation and fluorescence detected at 315 nm excitation/585 nm emission. Depicted are representative chromatograms for (A) GSH and (B) GSSG. γ -GG was used as an internal standard to monitor derivatization efficiency. (C) Baseline separation of microsomal GSH and GSSG by HPLC with fluorescence detection. Microsomes (6 mg protein) were acidified with PCA and acid-soluble thiols derivatized as described. Results show that baseline separation of the analytes is easily achieved using this method.

Use of iodoacetic acid to preserve ER glutathione and its redox ratio

Iodoacetic acid (IAA) is used routinely as a thiol acetylating agent, which would chemically preserve GSH redox status by protecting free thiolates from oxidation or thiol-disulfide exchange (106, 107). Homogenization of rat livers in the presence of 70 mM IAA did not adversely interfere with the chemical derivatization method for quantifying glutathione, which was shown by the complete separation of γ -GG, GSH, and GSSG from IAA-treated microsomes (data not shown). Moreover, incorporating IAA into the microsomal isolation method resulted in markedly higher reduced GSH levels (0.07 nmoles/mg protein without IAA versus 0.26 nmoles/mg protein with IAA), and significantly lower GSSG concentrations (0.12 nmoles/mg protein without IAA versus 0.06 nmoles/mg protein with IAA) than observed in nonIAA-treated samples (Figure 3.2A and B). This IAA trapping method resulted in a microsomal GSH:GSSG ratio over 5-fold higher (4.7:1) than untreated controls (0.7:1) (Figure 3.2C). These results reveal that the GSH redox couple in IAA-treated microsomes is in a more reduced state than previously observed.

Ex vivo oxidation occurs rapidly during the microsomal isolation procedure

To determine the rapidity of *ex vivo* oxidation, IAA was either directly perfused into the liver at the time of sacrifice or added to liver homogenates at different stages of microsomal isolation and the GSH:GSSG ratio determined. Figure 3.3A shows a schematic of the isolation procedure and the times when IAA was added to microsomes. Overall, microsomal isolation required 6 h to complete and IAA could be conveniently added by perfusion, directly into the homogenization buffer, and at 2 h intervals thereafter. Immediate perfusion of rat livers with IAA followed by microsomal isolation resulted in a GSH:GSSG ratio of 5.6:1 (Figure 3.3B). Furthermore, homogenization in the presence of IAA resulted in a GSH:GSSG ratio of 4.8:1 (Figure 3.3B), which was not significant ($p > 0.05$) from the observed ratio found in the perfusion experiments. Thus, microsomal GSH and its redox state appear to be much higher than previously reported in the literature.

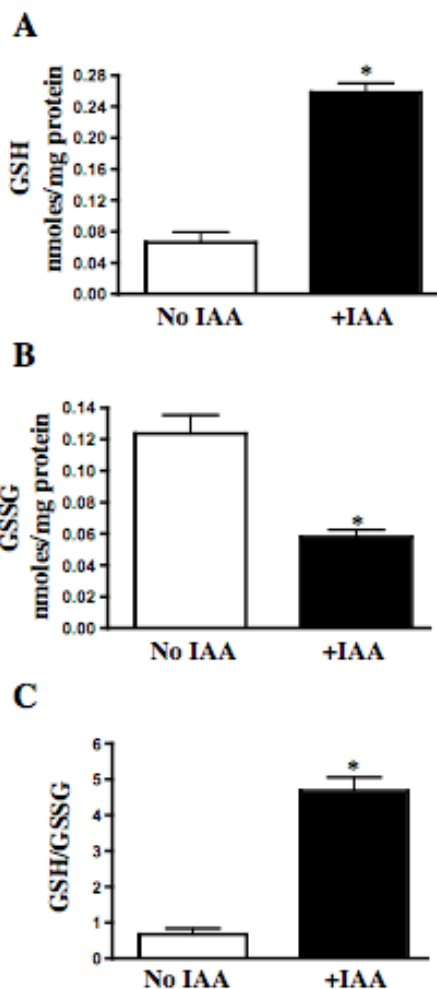


Figure 3.2. GSH oxidation during microsomal isolation. Microsomes (6 mg protein) were isolated in the presence or absence of IAA and GSH and GSSG monitored by HPLC and quantified relative to standards. The presence of IAA resulted in significantly (A) higher GSH and (B) lower GSSG than observed when IAA was omitted. (C) Calculation of the GSH:GSSG ratio revealed that IAA results in an ~5-fold higher GSH redox ratio in microsomes containing IAA versus nonIAA-treated control samples. Results are expressed as mean \pm SEM; $N \geq 11$ animals per group. Asterisks indicate $p < 0.01$ versus nonIAA-treated samples.

Adding IAA at times increasingly closer to final microsome purification revealed that extensive *ex vivo* oxidation occurred rapidly, mostly within the first 2 h of the isolation procedure (Figure 3.3B; $p < 0.05$). Thereafter, only minimal oxidation was observed which indicates that steps need to be taken early in microsome isolation to minimize *ex vivo* oxidation and to accurately assess glutathione status.

To determine if a loss of GSH and/or an increase in GSSG was responsible for the low GSH:GSSG ratio when no IAA is present (compare Figure 3.2C and 3.3B), free GSH and GSSG were quantified. To achieve this, IAA was again introduced into tissue by immediate perfusion or at various times throughout the isolation procedure as described in the Materials and Methods. We observed an initial nonsignificant ($p > 0.05$) loss of GSH within the first 2 h which became significant by 4 h post-isolation (Figure 3.3C). This loss was accompanied by a concomitant increase in GSSG (Figure 3.3D) which did not decline further following the 2 h timepoint (Figure 3.3C), and plateaued after 4 h (Figure 3.3D). The final result reflected the GSH:GSSG ratio as observed in Figure 3.2B when no IAA was added.

To further gauge the impact of GSH oxidation during microsomal isolation, total GSH equivalents (GSH + 2GSSG) was calculated. Results showed that overall GSH levels were lowest in microsomes treated with IAA for the shortest time (2 h and 0 h timepoints), becoming significant ($p < 0.05$) at the 0 h timepoint (Figure 3.3E). Taken together, samples either directly perfused or homogenized in 70 mM IAA display significantly higher levels of GSH, lower levels of GSSG, and increased total GSH equivalents relative to non-treated preparations.

Minimal glutathionylation of ER proteins

A previous report by Bass *et al.* indicates that the majority of GSH in rat liver microsomes is present as mixed disulfides with proteins (41). However, the general loss of GSH and increase in GSSG evident in Figures 3.3C and D suggest that ER protein glutathionylation may be a by-product of *ex vivo* oxidation. First, to understand the extent of GSH-protein mixed disulfides in our system, freshly isolated

microsomes treated with or without IAA were incubated with dithiothreitol (DTT; 0.1 mM) and the extent of GSH liberation was quantified. Approximately 5% of total ER GSH was bound to proteins in IAA-treated microsomes (data not shown). Second, to determine whether this relatively low percentage of glutathionylation was because of inadequate reducing power of DTT, a stronger thiol reductant, tris(2-carboxyethyl)phosphine hydrochloride (TCEP), was used to release protein-bound GSH (104). Again < 5% of the total GSH found in the ER was bound to proteins (data not shown). Lastly, to further verify low levels of glutathionylation, resolubilized PCA-precipitated proteins were incubated with DTT (1 mM) to liberate any protein-bound GSH. Using this method, only 3.3% of the total ER glutathione is present as mixed disulfides with proteins in IAA-treated samples (Figure 3.4A). Interestingly, nonIAA-treated microsomes displayed similar amounts of protein glutathionylation (5.7%) as IAA-containing controls (Figure 3.4A). This was contrary to expectations from the increase in GSSG noted when microsomes were isolated without IAA (see Figure 3.3).

To further corroborate that only a small percentage of GSH is present as mixed disulfides, the soluble ER proteome was quantified immunochemically. Figure 3.4B shows a representative blot confirming that there is very little glutathione bound to proteins when compared to DTT-treated samples as a negative control (Figure 3.4B, DTT lane). Furthermore, this blot also indicates that microsomal proteins may be relatively resistant to glutathionylation. When microsomes were incubated with a physiological concentration of GSSG (1 mM) as a positive control, only two bands near 40 kDa become glutathionylated. It is not until microsomes were incubated with a supraphysiological concentration of GSSG (10 mM) that significant glutathionylation became overt. Together, these results indicate that there is only a small amount of glutathione found present as mixed disulfides with proteins in microsomes isolated from rat livers. Furthermore, it appears that the proteins of the ER are not easily glutathionylated indicating this may be a highly regulated process.

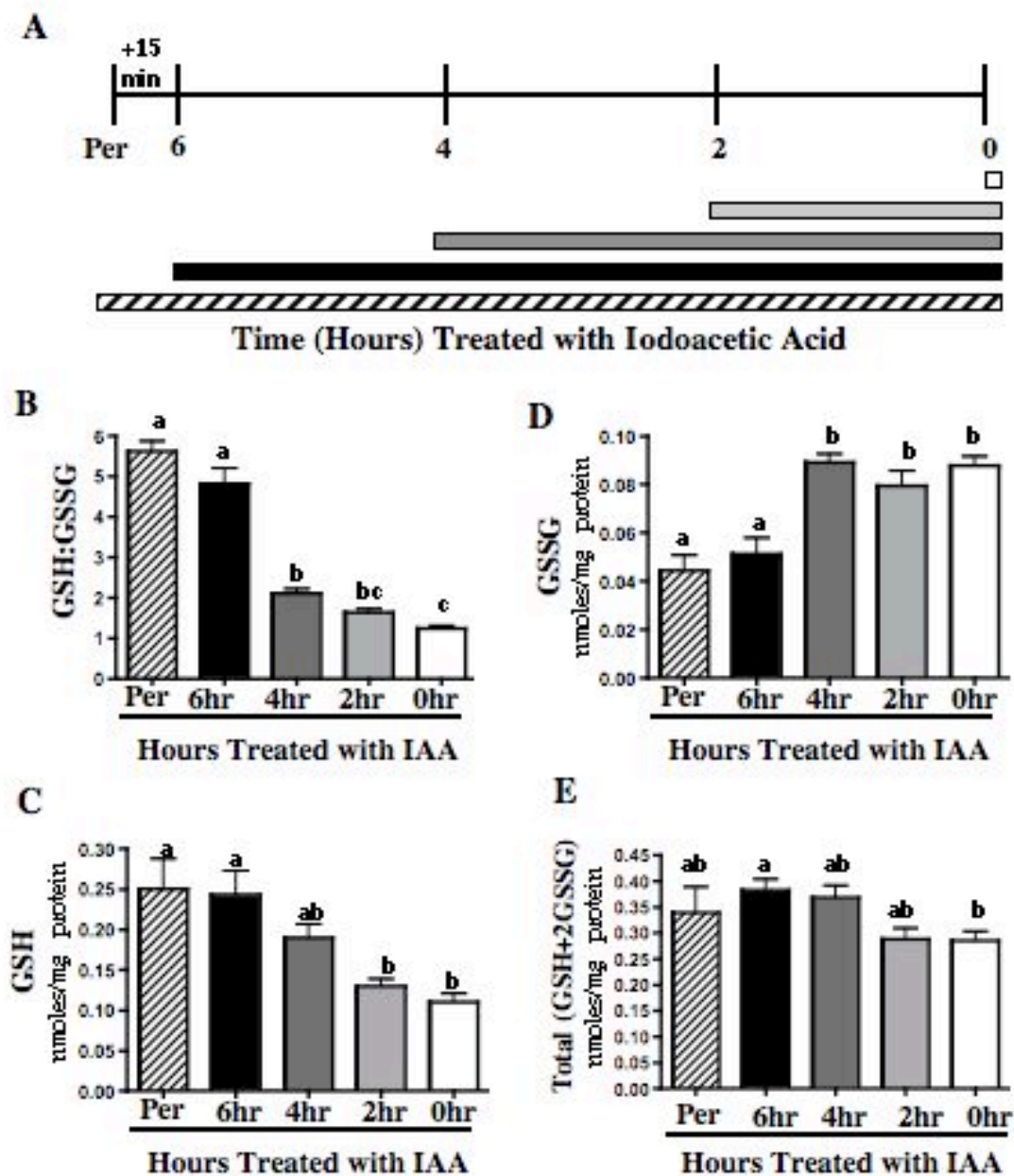


Figure 3.3. *Ex vivo* GSH oxidation occurs very rapidly during microsomal isolation.

(Figure legend continued on next page)

Figure 3.3. *Ex vivo* GSH oxidation occurs very rapidly during microsomal isolation. Rat liver homogenates or microsomal preparations were treated with IAA at different times during the isolation of microsomes and GSH redox state monitored by HPLC. (A) Schematic representation of the microsomal isolation procedure and the times at which IAA (70 mM, final concentration) was added (at perfusion (Per), homogenization, or at 2 h intervals). Bars under the timeline indicate the length of time that a particular sample was incubated with IAA. (B) The GSH redox ratio falls rapidly when liver homogenates are not immediately treated with IAA. Results show that the GSH:GSSG ratio was highest when liver tissue was either directly perfused or immediately homogenized in IAA-containing buffer (see Per and 6 h timepoints). However, significantly lower ($p < 0.05$) ratios were observed in all samples that were not initially treated with IAA (see 4 to 0 h timepoints). (C) Results show loss of GSH within the first 2 h of the microsomal isolation procedure when IAA is not present which becomes significant at the 2 h and 0 h timepoints ($p < 0.05$). (D) The initial loss of GSH corresponds to a significant increase in the levels of GSSG ($p < 0.05$). (E) Nonprotein-bound total glutathione (GSH + 2GSSG) levels become lower in the last timepoint (0 h) versus longer IAA treatment (6 h timepoint) ($p < 0.05$). Results are expressed as mean \pm SEM; $N = 3$ animals for perfusion group and $N = 6$ animals for all other groups. Different letters indicate statistical significance ($p < 0.05$).

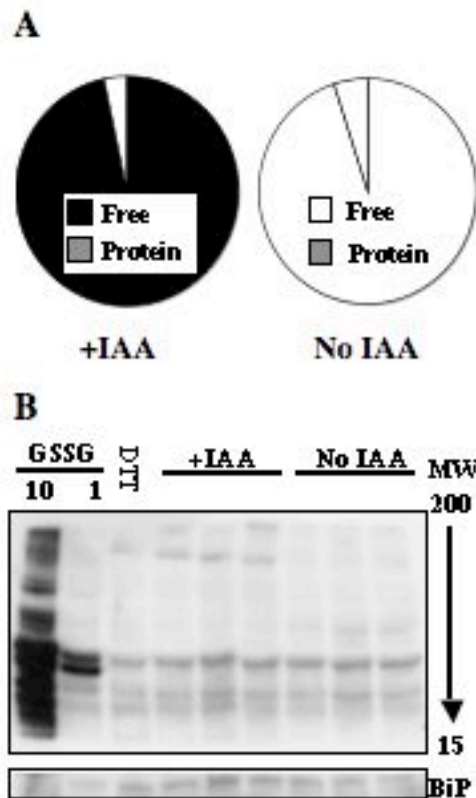


Figure 3.4. Minimal glutathione is present as mixed disulfides with proteins in rat liver microsomes. Acid precipitated protein pellets were re-solubilized and incubated with DTT (1 mM) to liberate any glutathione bound to proteins. (A) Results show the distribution of free versus protein-bound GSH. Only minimal glutathione was observed bound to protein regardless of the presence or absence of IAA. (B) Western blot analysis of microsomal glutathionylated proteins. When compared to the DTT control, very little glutathione is bound to proteins regardless of IAA treatment. Furthermore, incubation of microsomes with 1 mM GSSG resulted in minimal glutathionylation and only addition of supraphysiological GSSG concentrations (10 mM GSSG) resulted in extensive glutathione-protein mixed disulfides. ($N = 3$ animals per group).

Modulating GSH:GSSG ratios significantly alters protein disulfide isomerase (PDI) activity

To determine the biological relevancy of a higher thiol redox state residing in the ER, we performed experiments to directly monitor the consequences of a higher GSH:GSSG ratio to protein disulfide reduction, a basic function of ER-dependent protein processing. Specifically, an assay was used to determine the effect of varying the GSH:GSSG ratio on PDI-dependent reduction of intramolecular disulfide bonds in insulin. Results showed that PDI activity increased rapidly as the GSH:GSSG ratio also increased (Figure 3.5A and B). The maximal rate of reduction occurred at a GSH:GSSG ratio $\geq 9:1$ (Figure 3.5B). Interestingly, the rate of disulfide reduction was only 23% lower than the maximum rate when PDI was incubated with a GSH:GSSG redox state of 5:1, the approximate ratio observed in our studies. In contrast, PDI-dependent reduction was significantly impaired when PDI was given a GSH:GSSG redox environment at levels previously observed for microsomes (41, 42). As shown in Figure 3.5B, when the GSH:GSSG ratios were clamped at either 3:1 or 1:1, the rate of disulfide bond reduction was 67% and 76% lower than the maximal activity, respectively. Thus, the seemingly small change in the GSH:GSSG ratio described herein versus previous literature reports (2, 17) may have profound effects on disulfide reductase activity and ER function.

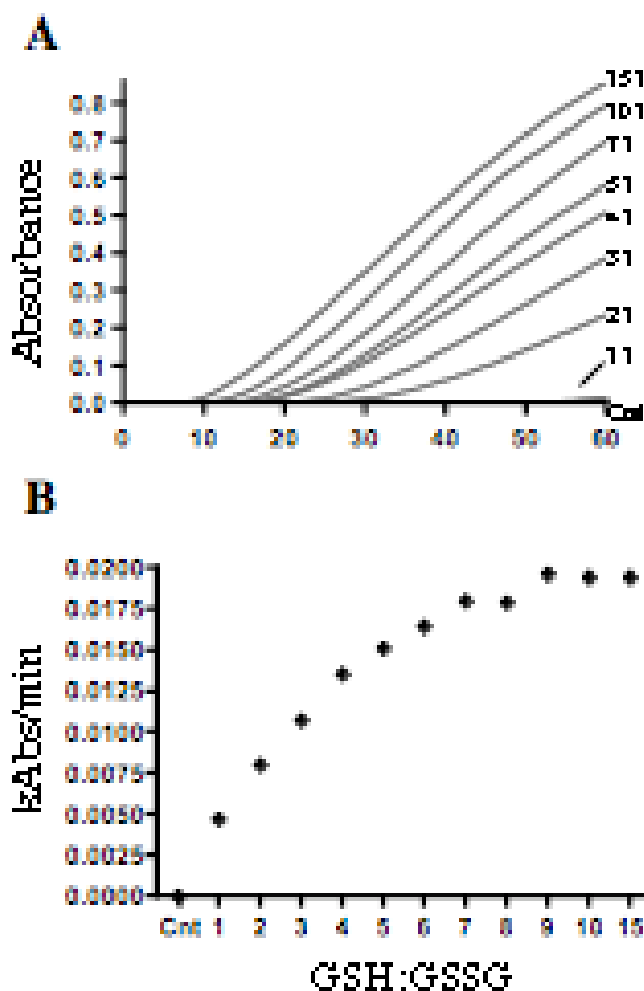


Figure 3.5. Small changes in GSH redox state markedly affect disulfide bond reduction by PDI. PDI reductase activity was monitored using the insulin turbidity assay of Holmgren (105). PDI (0.25 μ M), insulin (1 mg/ml), and glutathione (5 mM) concentrations were kept constant while altering the GSH:GSSG ratio (1:1 to 15:1) and changes in turbidity was monitored spectrophotometrically at 650 nm. (A) Kinetic traces of PDI reduction of insulin intramolecular disulfide bonds. (B) Rates of PDI reductase activity were calculated and plotted against varying GSH:GSSG ratios.

3.5. Discussion

The present work establishes that rat liver microsomes contain very high amounts of GSH equivalents. Based on our data showing total ER glutathione (GSH + 2GSSG) to be between 0.34 and 0.38 nmol/mg protein and literature reports indicating that microsomal ER volume is $\sim 4.5 \mu\text{l}/\text{mg}$ protein (108, 109), we estimate that microsomal GSH levels are approximately 4.5 mM. Considering parenchymal hepatocellular GSH concentrations have been variously reported to be between 1-11 mM (110), our results suggest that ER GSH levels largely reflect that found in the cell as a whole. Thus, GSH may be considered the most abundant low molecular weight thiol present in the ER. Even though this has been suggested previously, to our knowledge, this is the first report that actually quantifies microsomal GSH.

Despite both the cytosolic and microsomal GSH pools being similar in concentration, it is thought that the ER GSH redox status may be far more oxidized than the cellular thiol redox environment. This was most recently shown by Bass *et al.* who reported a GSH:GSSG ratio to be 3:1. Their results also support those of Hwang *et al.* who indicated that the microsomal thiol redox ratio ranged between 1:1 to 3:1. Although we observed a significantly higher GSH:GSSG ratio, our data confirm that the ER is indeed a much more oxidizing environment than the cytosol and thus may be a uniquely regulated GSH pool. Thus, GSH may also have specific role(s) unique for the ER though these putative functions are still ill-defined.

The poorly defined role(s) of ER GSH is in part a reflection of the limited information on its overall levels and redox state. By incorporating IAA into the microsomal isolation procedure, we show that the GSH:GSSG ratio is significantly higher than that observed for nonIAA-treated samples. IAA-protected microsomes displayed 60% higher GSH, and concomitantly lower GSSG (see Figure 3.3). Overall GSH levels (GSH + 2GSSG) were also 30% higher over nonIAA- treated samples (see Figure 3.3). It is possible that GSH may have been converted to higher oxidation states which could not be detected by the HPLC technique employed or lost during isolation.

However, this discrepancy remains unelucidated and subject to future analysis. Our data suggests that the unaccounted for GSH equivalents are not the result of artifactual protein glutathionylation as there were no differences evident in protein-GSH mixed disulfides with or without IAA. One possibility is that GSSG may be exported from the ER when levels increase beyond a specific threshold. This is generally supported by our data showing that free GSSG levels plateau despite the continued loss of GSH during our timecourse experiments (see Figure 3.3). However, much work remains in order to elucidate the mechanisms governing steady-state ER glutathione. Regardless, the use of IAA provides a strikingly different profile of both the GSH:GSSG redox ratio and the overall concentrations of glutathione in the ER.

The differences in microsomal GSH redox state reported here versus literature values are not trivial. This may best be illustrated by estimating the differences in GSH reducing capacity in microsomes with and without IAA treatment. Using the Nernst equation ($\Delta E = \Delta E_{\text{pH}7.5} - RT/F(2) \log [GSH]^2/[GSSG]$) and a calculated E_o at pH 7.5 for the GSH:GSSG redox couple of -255 mV, our data would estimate the microsomal GSH reducing capacity at -205 mV and -176 mV in microsomes with or without IAA treatment, respectively. This 30 mV difference suggests a significantly higher reducing capacity in the ER than previously believed which would be expected to have a significant impact on the protein dithiol/disulfide ratio. Considering a midpoint potential of -200 mV, a more accurate microsomal protein dithiol/disulfide ratio would thus be near 1:1 versus 1:10 if the 2GSH:GSSG couple were 30 mV more oxidized. For example, protein disulfide isomerases have two active sites with similar CXXC motifs and, depending on whether the active site sulfhydryls are in a disulfide or dithiol form, converts the enzyme from an oxidase involved in disulfide formation to a reductase involved in reducing disulfides (62, 111, 112). Thus, it is important to note that the estimated GSH reducing capacity places the GSH:GSSG redox couple in closer equilibrium with the midpoint potential of PDI than previously believed.

These theoretical calculations are supported by our *in vitro* studies showing that a GSH:GSSG of 5:1 yields a significantly increased reductase activity for PDI

versus its activity when the GSH:GSSG redox ratio is clamped at 3:1 or lower. Furthermore, it has also previously been reported that PDI-dependent refolding/isomerization is optimal at a GSH:GSSG ratio of 5:1 (56, 68, 113). Thus, there is little controversy regarding the consequences of glutathione levels and thiol redox status on enzymes of the ER. It is our contention that the greater unknown is the precise physiological thiol redox status of the ER by which to put these *in vitro* studies into context.

Our HPLC studies indicate that protein/glutathione mixed-disulfides to be only approximately 5% of the total glutathione found in the ER regardless of the presence or absence of IAA. This was further confirmed using Western blot analysis. Because only specific proteins appeared to be glutathionylated and that high levels of GSSG are needed to increase glutathionylation, one interpretation of these results is that steady-state protein glutathionylation in the ER is a highly regulated process. This concept is not only consistent with our results but also fits with other work showing that mixed disulfides between GSH and ER client proteins is the rate-limiting step in enzyme catalyzed folding (68). Therefore, glutathionylation may be normally kept to a minimum to limit protein transit time through the secretory pathway; conversely, conditions that induce protein/GSH mixed disulfides may increase protein transit time. Thus, protein glutathionylation may be a yet heretofore underappreciated aspect of regulating both protein maturation and degradation in the ER. However, more work will be necessary to understand the potential role of glutathionylation in the ER.

Future perspective

The goal of this study was to develop proper methodologies for assessing the GSH and the GSH redox balance in the ER. Based on our results, there is the distinct possibility that the general function and precise redox nature of microsomal GSH may have to be re-evaluated in light of its more reduced state. For instance, outside of protein processing, the GSH:GSSG ratio may be a potent “redox switch” that senses, and ultimately initiates, an ER stress response through affecting redox sensitive

proteins (65). Furthermore, perturbations in the ER thiol redox balance have been noted during diabetes and in protein aggregation diseases (48, 62, 63, 65, 70, 71). Interestingly, these pathologies have noted a reductive shift in the ER thiol redox balance (63). Thus, not controlling for *ex vivo* oxidation during microsomal isolation may fail to detect a critical nuance in the ER GSH:GSSG ratio under normal and pathophysiological conditions. Whether alterations in the thiol redox status are a cause or consequence for these pathologies remains unknown and should be the focus of future studies.

The Aging Endoplasmic Reticulum

Chapter 4

Age-related Increase in the Glutathione Redox Status of the Endoplasmic Reticulum

4.1. Abstract

One hallmark of the aging process is an accumulation of misfolded and aggregated proteins. Protein folding, isomerization, and unfolding are dependent on oxidation/reduction (redox) processes in the endoplasmic reticulum (ER). To help balance these opposing reactions, the redox status of the ER is significantly tilted more towards an oxidizing environment than other cellular compartments. Glutathione is known to be present at low millimolar concentrations within the ER. As such, the reduced glutathione (GSH) to glutathione disulfide (GSSG) ratio likely represents the most important thiol redox couple of the ER. Utilizing a method we have shown to minimize *ex vivo* oxidation of ER GSH (Chapter 4) (64), we sought to determine if the ER thiol redox status is altered with age. Microsomes were isolated from young (3-4 mo) and old (24-26 mo) F344 rat livers and the glutathione status determined. Results show a significant *increase* (60%; $p < 0.01$) in the GSH:GSSG ratio with age, which was the result of increased GSH levels ($p < 0.01$) rather than a loss of GSSG ($p > 0.05$). To determine if this age-related increase in the GSH:GSSG ratio affected the thiol oxidation state of ER proteins, a fluorescent technique that monitors the extent of protein thiol oxidation was employed. Results showed gross alterations in the redox status of the soluble ER proteome. A more precise examination of two quintessential ER proteins, protein disulfide isomerase (PDI) and ER oxidase-1L alpha (ERO1L-alpha), showed PDI was more reduced, while ERO1 was more oxidized, with age. However, these significant age-associated changes in ER thiol redox environment failed to activate ER stress response basally with age. Together, the results indicate a significant age-related dysfunction in thiol redox environment occurring in the ER.

4.2. Introduction

The accumulation of misfolded and aggregated proteins is a hallmark of the aging process and is thought to play a significant role in the pathogenesis of age-related diseases such as diabetes, cardiovascular, and neurodegenerative diseases (47, 48, 114). However, the molecular events that lead to aberrant protein handling during aging are not fully understood. One explanation may be a degradation of endoplasmic reticulum function (ER) with age.

The ER plays essential roles in many vital cellular functions including synthesis of macromolecules, regulation of cellular calcium homeostasis, and the maturation of secretory and membrane-associated proteins. In fact, the ER processes between 10-30% of the total cellular proteome (115, 116). Proteins folded in the ER tend to be rich in disulfide bonds and facilitate the formation of proper intramolecular disulfide bonding. Disulfide bonding is critical for the formation of higher order protein structures and ensures stability and proper enzymatic activity (115, 116). To achieve proper disulfide bond formation, the ER provides a highly oxidizing environment relative to the rest of the cell (41, 42).

The eukaryotic ER is unique from prokaryotic protein processing pathways. In bacteria, disulfide bond formation, isomerization, and reduction occur in the periplasm and consists of three distinct pathways for each of these functions (66). However, in eukaryotes, oxidative protein folding occurs in the ER and the same enzymes are also responsible for both disulfide isomerization and reduction (65, 115, 116). Molecular switching of enzymes from “foldases” (oxidases) to isomerases to “unfoldases” (reductases) is controlled by the thiol reduction/oxidation (redox) environment of the ER (117). Thus, the redox state of the ER must be tightly regulated and maintained within a narrowly defined range to ensure that desired enzymatic function is retained. To ensure client and resident protein fidelity, the lumen of the ER is significantly more oxidizing than other compartments of the cell (Chapter 4) (41, 42, 64). This redox environment likely serves to maintain quintessential ER enzymes in their preferred

redox state to ensure optimal enzymatic activity and to facilitate proper intramolecular disulfide bond formation, isomerization, or unfolding.

Glutathione is present in millimolar concentrations within the ER (Chapter 4) (41, 64). Considering that glutathione represents the largest redox active sulfhydryl pool in the ER, it significantly defines the overall ER thiol redox environment. Previous reports have defined the thiol redox ratio of the ER to be between 1:1 to 5:1 (Chapter 3) (41, 42, 64). *In vitro* work has shown that the optimal reduced (GSH) to oxidized (GSSG) ratio (GSH:GSSG) ratio to facilitate efficient and proper protein *fold*ing of the model protein, ribonuclease-1, is ~2:1 (67). Conversely, optimal *un*folding activity occurs at a GSH:GSSG ratio of >5.5:1 (Chapter 3) (64, 68). Thus, the regulation of the ER GSH:GSSG ratio must be elastic to facilitate ER folding and unfolding.

While the precise ER redox ratio and its regulation is not well understood, it is clear that perturbations of ER thiol redox has been described as an underlying factor in some chronic diseases. A number of pathophysiologies such as diabetes, liver disease, and emphysema have been described to have an altered ER thiol redox state (48, 62, 63, 65, 69-71). Interestingly, but perhaps counter-intuitively, considering that oxidative stress is part of these disease etiologies, the perturbation in the thiol redox environment tends toward a *reductive shift* in the ER thiol redox balance. This “reductive stress” would be expected to markedly influence protein chaperone and oxidoreductase function to favor disulfide reduction and lead to destabilized higher order protein structures (63, 72).

To date, there have been only limited studies examining the thiol redox environment of the ER lumen in mammals (Chapter 4) (41, 42, 64) either on a basal level or during disease states, and none have examined the ER GSH:GSSG ratio on an age basis. To fill this important gap in knowledge, we sought to determine if the ER thiol redox state changes on an aging basis. To this end, the thiol redox status was determined in rat liver microsomes isolated from young and old animals and whether ER stress signaling pathways were basally induced on an aging basis.

4.3. Materials and Methods

Materials

High performance liquid chromatography (HPLC) solvents were all HPLC grade (Fisher Scientific, Pittsburgh, PA). All other chemicals were reagent grade or the highest quality available from Sigma-Aldrich (St. Louis, MO).

Isolation of rat liver microsomes

Young (3-4 mo) and old (24-26 mo) Fischer 344 rats (National Institute on Aging animal colonies) were anesthetized with diethyl ether, the livers perfused with ice-cold phosphate buffered saline (PBS), pH 7.5, to remove blood, and then sacrificed according to Institutional Animal Care and Use Committee (IACUC) approved guidelines. The livers were quickly excised, weighed, and placed on ice. Microsomes were isolated as previously reported with some modifications (64, 103). Briefly, half of each liver (~6-7 g) was homogenized 1:7 [w/v] in ice-cold homogenization buffer (10 mM potassium phosphate [monobasic], 10 mM potassium phosphate [dibasic], 150 mM HEPES, 75 mM potassium chloride, 1 mM EDTA; 70 mM iodoacetic acid (IAA) pH 7.5) and microsomes isolated by differential centrifugation. The microsomal pellet was further washed (100 mM potassium pyrophosphate and 1 mM EDTA, pH 7.4) to remove heme and spun again at 100,000 x g for 95 min at 4°C. The microsomal pellet was resuspended in 750 µl of 100 mM potassium phosphate buffer containing 30% glycerol [v/v] and 1 mM EDTA, pH 7.25. Only freshly isolated microsomes were used for GSH analysis. Western blot assays for purity revealed that microsomal preparations using this procedure had minimal contamination of Golgi using the 59 kDa Golgi protein (Abcam #ab23932) as a marker but were highly enriched for Calnexin (Abcam #ab22595) (data not shown). Thus, the procedure employed in this study results in microsomes relatively free of contaminating membranes.

Preparation of microsomal samples for free glutathione analysis

Immediately following isolation of microsomes, 300 μ l of the microsomal suspension was added directly to an equal volume of 15% (v/v) perchloric acid (PCA; Fisher Scientific) containing 10 mM diethylenetriaminepentaacetic acid (DTPA; Sigma-Aldrich), and incubated on ice for 15 min. Acidified samples were then spun at 15,000 \times g for 15 min, the supernatant removed, and stored at -20°C until derivatization and glutathione analysis. PCA (300 μ l of a 15% stock, containing 10 mM DTPA) was then added back to the pellet and snap-frozen in liquid nitrogen, and stored at -80°C for protein-bound glutathione analysis (described below).

Determination of protein glutathionylation

To determine the amount of glutathione present as mixed disulfides with proteins, acid-precipitated protein pellets from free GSH analysis (described above) were re-solubilized in 0.1 M phosphate buffer, and the pH adjusted to 7.4 with 3 M KOH. These samples were then incubated in the presence of 1 mM DTT for 24 h at 4°C and the amount of GSH released determined by HPLC.

High performance liquid chromatography for glutathione

GSH quantification was performed as described using dansyl chloride as a fluorophore and γ -glutamylglutamate (γ -GG) as an internal standard for derivatization efficiency (64, 100, 102). Analyte separation was achieved using a 3-aminopropyl column (200 mm \times 2.6 mm i.d.; Custom LC, Houston, TX) using a gradient of two buffers (Buffer A, 80/20 methanol/water (v/v); Buffer B, 62.5% MeOH (v/v), 20% acetate stock (217.6 g sodium acetate trihydrate [Fisher Scientific] in 400 ml glacial acetic acid) and 17.5% glacial acetic acid [v/v]). By this means, both GSH and GSSG can be simultaneously separated and quantified relative to authentic standards from a single biological sample.

Quantitative real-time PCR

Tissues (approximately 200 mg liver) were immediately placed in RNALater (Ambion, Foster City, CA) and stored according to manufacture's instructions. Total RNA was isolated using RNeasy kit (Qiagen, Valencia, CA) according to manufacture's instructions, quantified spectrophotometrically (260 nm), and assaying for purity by determining the 260/280 nm ratio. cDNA was prepared from 12.5 µg of total RNA using SuperScript II (Invitrogen, Carlsbad, CA) and oligo(dT) primers (Operon, Huntsville, AL) in a 50 µl reaction according to manufacture's instructions. Quantitative real-time PCR (qPCR) analyses were performed using mRNA-specific primers spanning exon/exon boundaries using the DNA Engine Opticon II system (BioRad, Hercules, CA). Specifically, 62.5 ng of each cDNA pool, 0.3 µM of each primer (forward and reverse) and Finnzymes' DyNAmo Master Mix containing SYBR Green (Finnzymes, Espoo, Finland) were used for each qPCR reaction in accordance with manufacturer's instructions.

Primer Sequences (Operon):

gadd153/CHOP-F; 5'-CAGCTGAGTCTCTGCCTTTCG-3'

gadd153/CHOP-R; 5'-GATTCTTCCTCTTGCTTTCCTGG-3'

grp78/BiP; F; 5'-CAAGTTCTTGCCATTCAAGGTGGTTGA-3'

grp78/BiP; R; 5'-CAGCTGCTGTTGGCTCATTGATGATC-3'

beta-actin-F; 5'-CCTTCCTTCCTGGGTATGGAATCC-3'

beta-actin-R; 5'-GAGCAATGATCTTGATCTTCATGGTG-3'

Thermocycler conditions included an initial incubation at 95.0°C for 00:10:00 followed by 45 cycles of 94.0°C for 00:00:10; 58.0-61.0°C for 00:00:20 (primer/gene specific; see below); incubation at 72.0°C for 00:00:20 followed by a plate read. Cycling conditions concluded with a final incubation at 72.0°C for 00:07:00; a melt

curve analysis (65.0°C to 95.0°C, reading every 0.2° with a 00:00:01 hold) and a final extension step at 72.0°C for 00:10:00. Annealing temperatures were as follows: gadd153/CHOP, 58.0°C; grp78/BiP, 61.0°C; and beta-actin; 58.0°C - 61.0°C (compatible for all conditions and all genes examined). To obtain appropriate template concentrations, samples were run concurrently with standard curves generated using plasmid standards (Topo Cloning Kit; Invitrogen). Beta-actin was used as the housekeeping control for RNA recovery, reverse transcription efficiency, and template concentration. Gene expression was normalized to beta-actin mRNA levels and expressed as arbitrary units. Agarose gel electrophoresis and thermal denaturation (melt curve analysis) were used to confirm specific replicon formation.

Western blot analyses

Whole tissues were homogenized, spun at 15,000 x g for 15 min, and the supernatant collected. Whole tissue homogenates or microsomal samples were added directly to 3X loading buffer (0.5 M Tris-HCl, pH 6.8, 10% SDS [w/v], 25% glycerol [v/v], and 0.5% bromophenol blue [w/v]). Protein was separated on 10% polyacrylamide gels (Pierce, Rockford, IL) and transferred to PVDF membranes (Millipore, Billerica, MA). The levels of proteins were detected using a polyclonal antibody for grp78/BiP (Stressgen, Ann Arbor, MI) and gadd153/CHOP (Santa Cruz Biotechnology; Santa Cruz, CA) and standardized to PDI (Stressgen), grp/78 (Stressgen), or beta-actin (Sigma-Aldrich) levels when appropriate as a loading control. Proteins were visualized using appropriate horseradish peroxidase-conjugated secondary antibodies (Cell Signaling Technologies, Danvers, MA) in conjunction with a chemiluminescent substrate (Amersham Pharmacia Biotech, Buckinghamshire, UK) and Enhanced Chemiluminescent Film (Amersham Pharmacia).

Determination of ER protein redox state by fluorescent detection

IAA-treated microsomes were incubated in 300 mM HEPES buffer (Sigma) containing 10 mM tris(2-carboxyethyl)phosphine hydrochloride (TCEP; Sigma) for 1

hr to reduce any thiol disulfides present. 1 mM of a Texas Red-conjugated maleimide (Invitrogen) was then added to label any free thiols reduced by the use of TCEP for 2 hr. Reactions were then added to an appropriate volume of dye-free loading buffer, heated for 5 min at 95°C, and loaded onto a 10% SDS-PAGE gel. Fluorescent proteins were visualized using a BioRad FX Molecular Imager. Proteins were then transferred onto PVDF membranes (Millipore) and the levels of grp78/BiP (Stressgen) detected as a loading control.

Statistical analysis

Statistical significance between means of two independent groups was determined by Student's *t* test, assuming equal variances. For comparison of treatment effects, one-way analysis of variance (ANOVA) with Tukey's *post hoc* test was used. All of the results were considered significant if the *p* value was < 0.05. Statistical analysis was performed using PRISM 4.0b software (GraphPad Software, San Diego, CA).

4.4. Results

Age-related increase in GSH:GSSG redox ratio

To determine potential age-related differences in ER GSH status, microsomal acid-soluble thiol compounds were derivatized and quantified using the well-known method of Reed and coworkers (100, 102). This HPLC technique, with only slight modifications (Chapter 4), allows the simultaneous determination of both GSH and GSSG from a single microsomal sample when *ex vivo* oxidation is properly controlled (Chapter 4) (64). Results showed that the microsomal GSH:GSSG ratio significantly ($p < 0.01$) increased by 60% with age from 3.8 (± 0.23 ; N=6) in microsomes isolated from young rats to 6.4 (± 0.63 ; N=6) in microsomes isolated from old rats (Figure 4.1A). The increase in the GSH:GSSG ratio was the result of a significant ($p < 0.01$) 42% increase in the concentration of GSH (0.21 nmols/mg protein in the young versus 0.30 nmols/mg protein in the old; Figure 4.1B) and only minimally as a non-significant ($p > 0.05$) 15% loss of GSSG (0.056 in the young versus 0.047 in the old; Figure 4.1C). As a result of the increase in GSH, the total acid-soluble glutathione concentration (GSH + 2GSSG) also significantly ($p < 0.05$) increased by 22% with age (Figure 4.1D). These results show there is an age-related *reductive* shift in the thiol redox status of the ER where the aging ER contains higher overall levels of free glutathione.

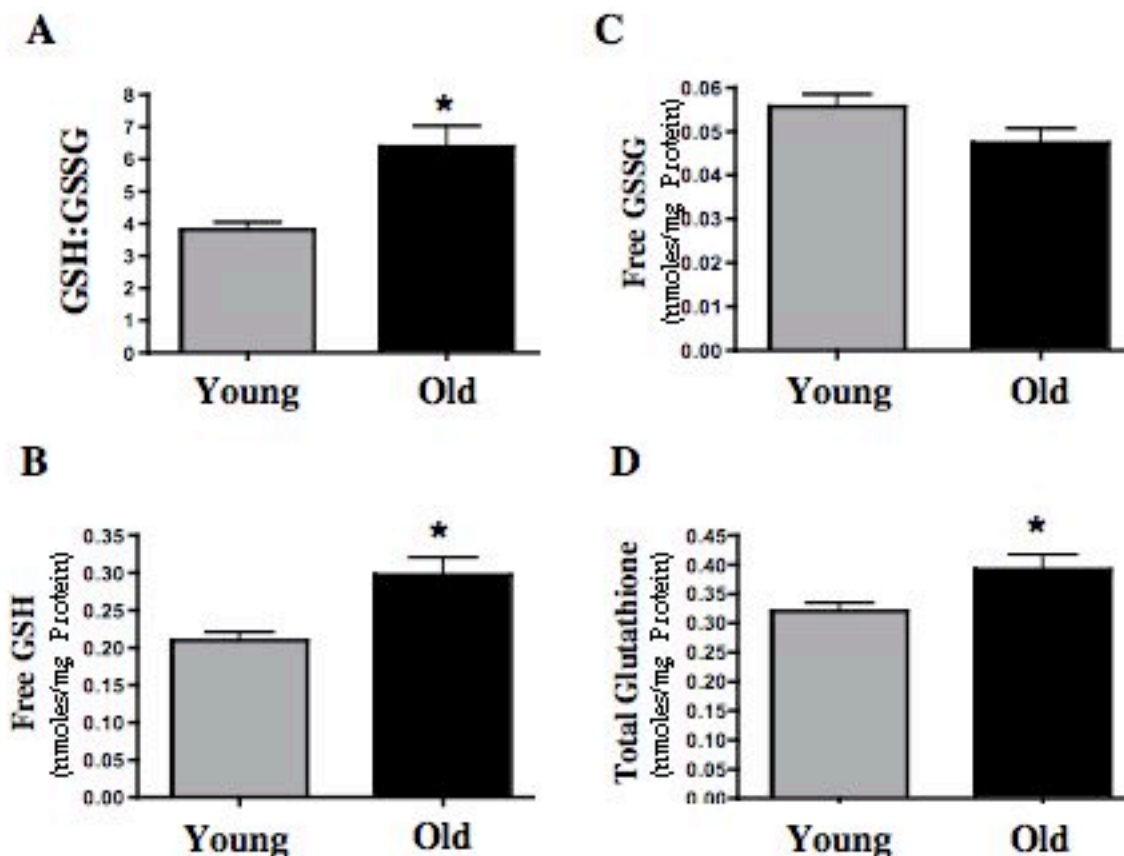


Figure 4.1. Age-related increase in the ER GSH:GSSG redox ratio. Microsomes were isolated from young and old rats and glutathione quantified by HPLC. (A) The GSH:GSSG ratio significantly ($p < 0.01$) increased by 60% with age. (B) The increase in the GSH:GSSG ratio was the result of a significant 42% increase ($p < 0.01$) in the concentration of GSH and (C) only minimally because of a non-significant, 15% loss of GSSG with age ($p > 0.05$). (D) As a result of the increase in GSH, the total acid-soluble glutathione concentration (GSH + 2GSSG) increased by 22% in microsomes isolated from old animals ($p < 0.05$). N=6 for all groups; asterisks (*) indicates statistical differences as indicated in the text.

Minimal glutathionylation of ER proteins

A previous report indicated that most microsomal GSH is present as mixed disulfides with proteins (41). However, as shown in Chapter 4, we demonstrated that only a small amount of the total ER GSH is bound to proteins (64). To determine whether the amount of GSH present as mixed disulfides with proteins in the ER changes with age, acid-precipitated protein pellets were re-solubilized, incubated with 1 mM DTT, and the amount of GSH liberated determined by HPLC as described in the Materials and Methods. Despite increases in both the ER GSH redox status and overall GSH levels, no significant age-dependent changes were observed in the amounts of GSH bound to proteins ($p > 0.05$). Results showed that 11.4% and 10.4% of total ER GSH was bound to proteins in young and old rat liver microsomes, respectively (Figures 4.2A and B). These results confirm our previous study that only a small percentage of the total GSH present in the ER is found a mixed disulfides (Chapter 4) (64). Thus, aging does not affect the protein-bound ER GSH pool.

Whole liver GSH:GSSG declines with age

Previous work in the Hagen Laboratory as well as others show that there is a significant age-associated decline in both hepatic GSH levels and GSH redox state (19, 22, 23, 25, 97, 99, 101, 118, 119). As the previous results indicate (see Figure 4.1), microsomal GSH levels and redox status *increase* with age. Because this effect is contrary to previous reports in whole liver tissue, to rule out differences in overall tissue levels of GSH in our specific samples as a confounding factor, we determined whole liver GSH status in the same liver samples used for microsomal analysis. This

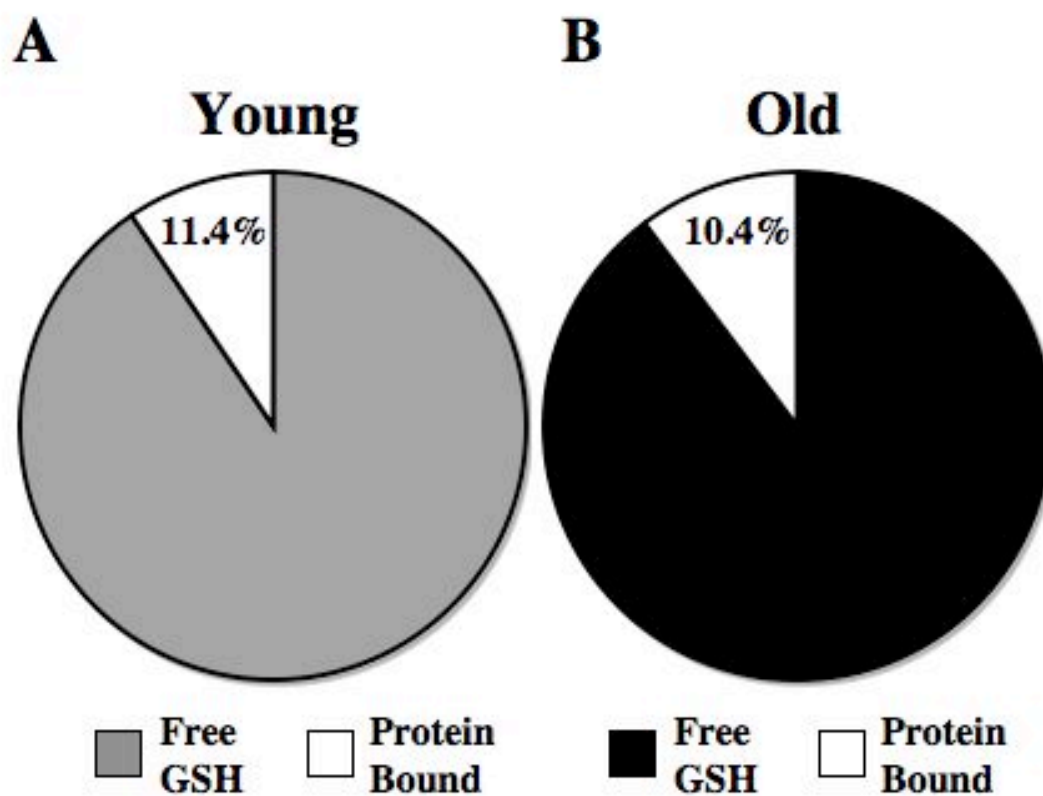


Figure 4.2. No age-related change in protein-bound GSH. Acid precipitated protein pellets were re-solubilized and incubated with 1mM DTT to liberate GSH bound to proteins and GSH levels quantified by HPLC. Results show the distribution of free versus protein-bound GSH in microsomes isolated from (A) young and (B) old rats. Only minimal GSH was observed present as mixed disulfides in both young and old microsomes with no significant differences ($p > 0.05$) between the two groups. N=6 animals per group.

comparison revealed a significant ($p < 0.05$) 45.1% decline in the GSH:GSSG ratio in whole liver with age (Figure 4.3A). Also, contrary to the results found for GSH levels in rat liver microsomes, whole tissue GSH levels were not significantly different in young versus old rats (Figure 4.3B). In summary, these results indicate that on a whole tissue basis, there is an *oxidative* shift in the GSH:GSSG ratio, but microsomal GSH redox state is affected counter to this oxidative shift, and the ratio actually *increases* in microsomes isolated from old rats. Together, these results suggest that the ER GSH pool is unique relative to the cytosol, or at least able to differentially regulate its GSH status.

Redox state of the soluble ER proteome is grossly affected with age

To determine whether the redox status of proteins found in the ER are influenced by the age-related increase in the GSH:GSSG ratio, a fluorescent gel technique was employed to assess ER protein thiol redox status. Here, ER protein thiol redox state can be generally determined by reducing protein disulfides followed by labeling with a fluorescent maleimide as described in the Materials and Methods. Thus, microsomes isolated in the presence of iodoacetic acid (IAA) were then reduced with 10 mM tris(2-carboxyethyl) phosphine hydrochloride (TCEP) and labeled with a Texas Red-conjugated maleimide (see reaction scheme; Figure 4.4). Because of the charge added by IAA and the likely heterogeneity of IAA-labeled proteins utilizing this method, 1D gel electrophoresis was chosen over 2D gel electrophoresis. Unfortunately, this method does not yield high resolution and thus it becomes impossible to discern how specific proteins

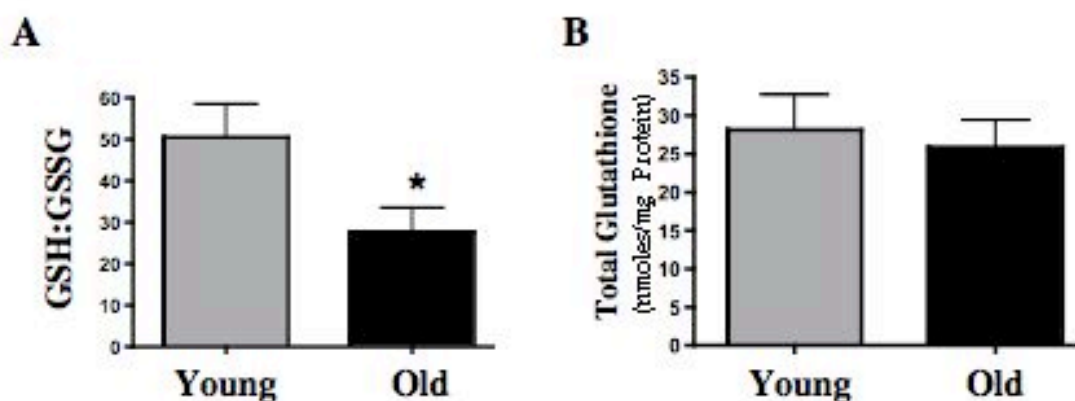


Figure 4.3. Whole liver GSH:GSSG declines with age. Glutathione status was determined in whole hepatic tissue isolated from the same young and old liver samples utilized to determine the microsomal GSH status (see Figure 4.1). (A) Results show a significant ($p < 0.05$) 45.1% decline in the GSH:GSSG ratio in old relative to young rats. (B) Measurement of total hepatic GSH (GSH + 2GSSG) indicated that there was no significant change of total GSH equivalents on an aging basis. N=6 per group; asterisk (*) indicates statistical significance ($p < 0.05$).

are affected. However, we only sought to determine if the alterations seen in the GSH:GSSG ratio were a surrogate for overall protein redox status.

Our results show that the redox status of the ER proteome is significantly affected with age (Figure 4.5) and shows at least four molecular weight regions of approximately 200, 75, 50, and 35 kDa that were differentially fluorescent on an aging basis, thus indicating altered protein redox status (Figure 4.5; arrows). Interestingly, these four regions of the soluble ER proteome were not affected equally. Contrary to our hypothesis that the ER proteome should be increasingly reduced with age as the result of the *increased* GSH:GSSG ratio, the three highest molecular weight regions (200 kDa, 75 kDa, and 50 kDa) appear to be more oxidized with age (increased fluorescence versus young) with only the lowest molecular weight region (35 kDa) becoming more reduced with age (Figure 4.5; arrows). To confirm that altered loading of the gel could not account for the differences observed, levels of protein disulfide isomerase (PDI) were determined by Western blot analysis following fluorescent imaging. Together, these results indicate that the redox status of the proteome in the aging ER is dramatically affected by age but that there appears to be a disconnect of the redox circuitry between GSH and the proteome in the ER.

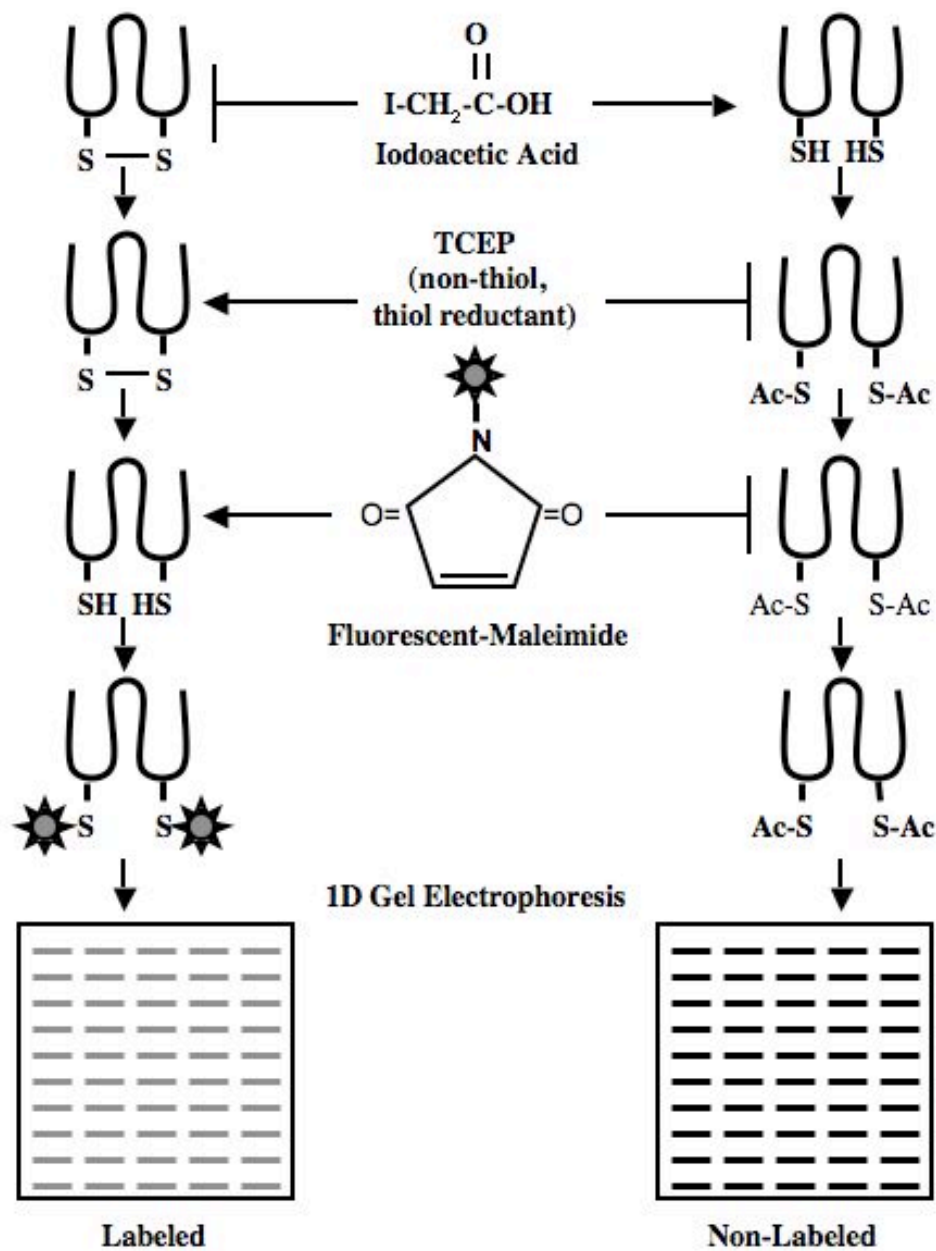


Figure 4.4. Schematic representation of the fluorescent protein redox gel technique. Utilizing this method, because microsomes were initially isolated in the presence of IAA to alkylate free thiols, increased fluorescence is interpreted as a protein being more oxidized while a diminution in fluorescence is interpreted as more reduced.

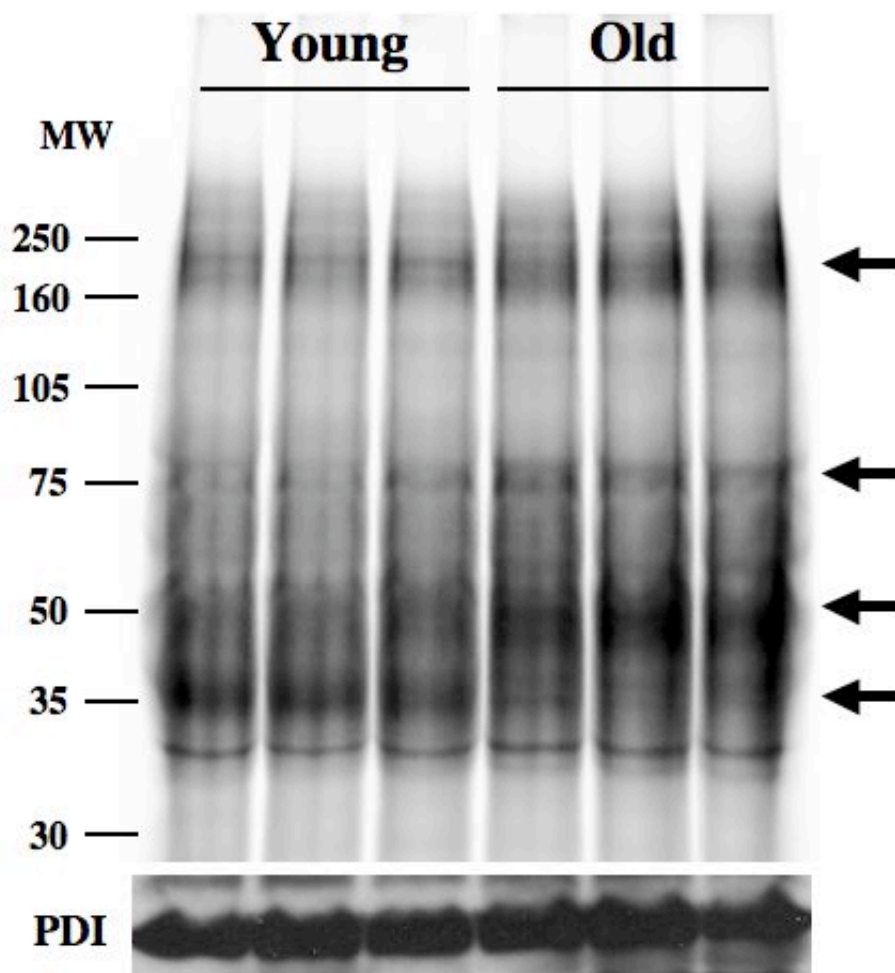


Figure 4.5. False-color image showing gross alterations in the redox status of the soluble ER proteome occurs in aged animals. A fluorescent gel technique was utilized to visualize the redox status of ER proteins (see schematic; Figure 4.4) to determine whether alterations in the redox state of the ER proteome mirrored the age-related changes seen in the ER GSH:GSSG ratio. Arrows indicate general regions on the false-color image where redox status (fluorescence) was varied in old versus young animals. Relative to young, the three highest molecular weight regions (200 kDa, 75 kDa, and 50 kDa) showed increased fluorescence (more oxidized) but the lowest molecular weight region (35kDa) showed less fluorescence (more reduced). N=3 per group.

No chronic induction of ER stress response pathways with age

Because the ER redox states of GSH, the proteome, and specific oxidoreductases were drastically altered with age, we hypothesized that the aging ER may be under a chronic ER stress. ER stress response is collectively a well-defined set of cell signaling cascades that, among other responses, induces the upregulation of so-called ER stress response genes. To determine if there was an induction of ER stress response during aging, mRNA and protein levels of two well-known ER stress response genes, gadd153/CHOP and grp78/BiP, were determined. Using quantitative real-time PCR (qPCR) to determine mRNA levels, results showed that there was no significant ($p > 0.05$) increase in either gadd153/CHOP gene expression (Figure 4.6A) or protein levels (Figure 4.6B). There was also no significant increase observed for the ER stress response gene grp78/BiP in terms of mRNA levels (Figure 4.6C) or protein concentration (Figure 4.6D). These results indicate that despite the gross age-related changes seen in the overall redox status of the aging ER, there is no induction of an ER stress response with age.

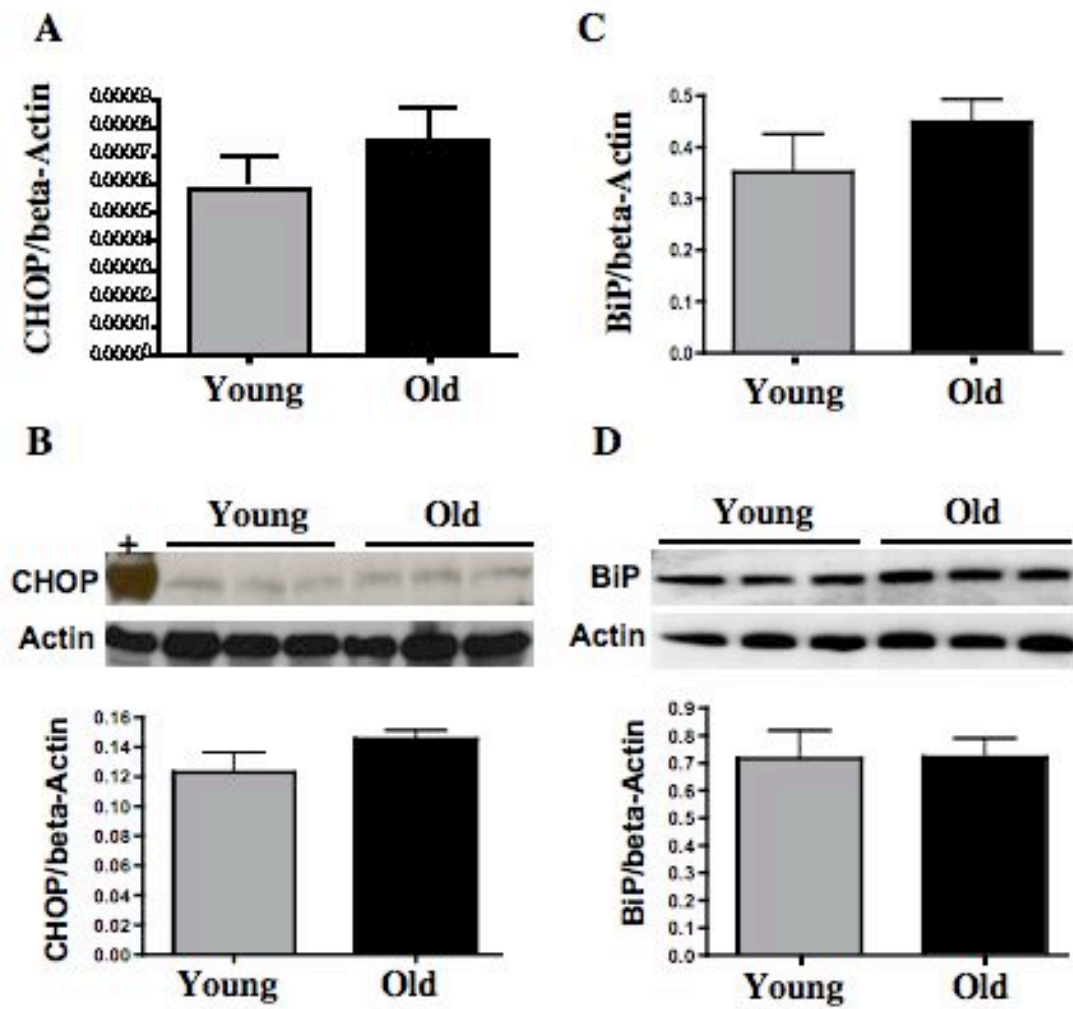


Figure 4.6. No chronic induction of ER stress response pathways with age. To determine if ER stress response mechanisms are chronically activated during the aging process, expression of known ER stress response genes was determined using quantitative real-time PCR. (A) No significant increase in either mRNA or (B) protein levels of gadd153/CHOP was observed. Furthermore, a similar trend was shown for the ER stress response gene *grp78*/BiP for (C) *grp78*/BiP mRNA levels or (D) protein expression. N=3 per group; plus sign (+) indicates positive control.

4.5. Discussion

We have previously shown that *ex vivo* oxidation is a major confounding factor in the assessment of microsomal glutathione status and that when controlled, the GSH:GSSG redox status is significantly higher than previously reported (41, 42, 64). Utilizing this method, the present work establishes that the redox status of the ER is compromised with age.

One of the most important observations of the present study is the discovery of a *reductive* shift in the thiol redox status in the endoplasmic reticulum. This is contrary to expectations, given that previous studies examining redox state in whole liver show a more oxidizing environment with age and a progressive accumulation of oxidatively damaged biomolecules (12-15, 34, 35). Elevated oxidative damage and resultant oxidative stress is evident both in tissues and in specific subcellular compartments (15, 22, 23, 25, 97-99, 101, 120). Thus, an opposing reductive shift in the microsomal redox environment is surprising and exemplifies the need to characterize the redox state of specific sub-cellular compartments to fully understand the nuances of normal cellular aging.

In retrospect, a reductive stress for the aging ER fits with previous reports showing a similar elevated reducing environment occurs in “age-accelerated” diseases or in some chronic pathologies. For example, Nardai *et al.* showed that in a chemically induced mouse model of diabetes, the ER of these animals experienced a significant reductive shift in the thiol redox status (62, 63). Furthermore, this same group showed total oxidoreductase activity was also negatively affected stemming from this reductive stress. These authors went on to show that oxidizing equivalents (dehydroascorbic acid and GSSG) could reverse the reductive shift they observed. Together, the authors concluded that diseases causing an overall oxidative stress such as diabetes nevertheless resulted in a reductive stress in the ER, and compromised

enzymes of the ER. In addition to diabetes, reductive shifts in the ER have been noted in liver disease, emphysema (72) and now the normal aging process.

Despite the elevated reducing environment, ER protein redox status was differentially affected with age (see Figures 4.3 and 4.4). Specifically, the three highest molecular weight regions (200 kDa, 75 kDa, and 50 kDa) were more oxidized with age (increased fluorescence versus young) with only the lowest molecular weight region (35 kDa) becoming more reduced with age (loss of fluorescence; see Figure 4.5). Nardai *et al.* also noted heterogeneity in the ER protein redox state in the context of an increased thiol redox state in their diabetes model (63). This group used a gel retardation assay where free thiols were modified with 4-acetamido-40-maleimidylstilbene-2,20-disulfonic acid (AMS) to assay for protein redox state, and found that generally ER oxidoreductases were more reduced but the ER oxidase, ERO1L-alpha, was found to be in a more oxidized state. Utilizing the fluorescent redox technique described herein, our findings agree with these previous results (data not shown). We found that the ER oxidoreductase PDI, was 69.7% more reduced in old versus young microsomes but that ERO1L-alpha was 57.1% more oxidized. However, due to the inherent variability induced by this methodology and low relative low number of samples (N=3), neither value reached statistical significance in old versus young microsomes (data not shown). Nonetheless, these results are intriguing and suggest that, because ERO1L-alpha is the direct oxidase of PDI and in light of our findings above, PDI and ERO1L-alpha are no longer efficiently interacting whereby ERO1L-alpha no longer maintains PDI redox status. While the mechanisms associated with an altered protein redox state was neither explored by Nardai *et al.* nor in the present study, it is interesting to speculate that the increased concentration of reduced GSH, total GSH (GSH + 2GSSG), and increased GSH:GSSG ratio seen in the ER with age may be responsible for facilitating this lesion. Thus, a future avenue of research should be to explore the causes and its implications of altered ER enzyme redox status.

Because the oxidizing environment of the ER is essential for the proper (poly)peptide folding and processing and any alteration in protein homeostasis induces

an ER stress (115, 116), this organelle has specific stress signaling mechanisms to respond to perturbations in its redox environment. We thus hypothesized that ER stress response pathways should be chronically activated during aging. This hypothesis was developed based not only on the present results but also from previous reports showing that altered expression of pro-apoptotic ER stress proteins sensitizes aged tissues to xenobiotics and cell death (79, 121). However, no age-associated activation of ER stress response was observed. This lack of activation can be interpreted two ways. First, it is possible that the increase in the ER redox status is a compensatory and protective mechanism. Proteins have been shown to accumulate with age, and during the pathogenesis of some diseases; in some cases, specifically in the ER (48). However, whether these proteins are functional proteins or proteins which have been irreversibly modified remains unclear. The increase in the redox status may be a means to help remove accumulated and misfolded proteins from the cell by favoring protein unfolding over protein folding by enzymes like protein disulfide isomerase (PDI) (64, 68). However, it has also been shown in a transgenic mouse model of protein misfolding where a reductive shift was noted in both the thiol redox status and in PDI, that unfolding activity was significantly reduced in the ER of these animals (72). Thus, a reductive shift may not be indicative of favoring protein unfolding pathways but a symptom of compromised ER homeostasis (63, 72).

The second interpretation of these results is that the aging ER is experiencing a chronic stress but fails to adequately adapt. It is well-known that a loss of stress response mechanisms occur with age (19, 79, 122). Thus, it is feasible that the ER is indeed compromised with age but fails to activate ER-dependent stress signaling pathways to ultimately restore homeostasis. Based on literature precedent, the second scenario is more likely. For example, during certain conditions that would be expected to activate ER stress response mechanisms, ER stress pathways were not induced (72, 123-126). It has also been shown that compounds which elicit a mild ER stress can be protective by upregulating ER stress response proteins (74, 127, 128). Thus, it is interesting to speculate that if dietary compounds could be identified that had similar

effects, these compounds might be protective when reduction of the ER is found to occur either during certain disease states or during the normal aging process.

In summary, this work indicates that the redox circuitry of the ER is a much more complicated and a highly regulated process and warrants further studies to determine the effects an altered ER redox status has both on ER and overall cellular homeostasis. Whether alterations in the ER thiol redox status are a cause or consequence also remains unknown but is intriguing to speculate that the ER may be a potential therapeutic target for protein aggregation diseases, diabetes, and aging.

The Aging Endoplasmic Reticulum

Chapter 5

***R*-(alpha)-Lipoic Acid Reverses the Age-related Increase in the Glutathione Redox Status of the Endoplasmic Reticulum**

5.1. Abstract

The aging ER displays an increase in the reduced (GSH) to oxidized (GSSG) glutathione ratio, dysregulated ER protein redox, and a failure to activate ER stress response mechanisms (Chapter 5). To determine if *R*-(α)-lipoic acid (R-LA), a dietary compound shown to preserve cellular glutathione status, reverses the age-related increase in the ER GSH:GSSG ratio, a single bolus of R-LA (gavage; 120 mg/kg) was administered to young and old rats. Supplementation to young rats revealed that R-LA initially increased the GSH:GSSG ratio to the levels seen in old, unsupplemented animals. This initial R-LA-induced pro-reductive environment was followed by a rapid oxidation of ER GSH 6 hr post-gavage. This significant oxidation persisted for at least 18 hr and was followed by a slow recovery. In contrast to the young animals, R-LA supplementation of old rats did not initially induce a further increase in the GSH:GSSG redox ratio but mirrored the oxidation of ER GSH identical to that seen in the young. At 48 hr post-gavage, *both* the young and old ER GSH:GSSG redox status returned to levels initially seen in young rats. To determine the effects of long-term R-LA supplementation, young (3-4 mo) and old (24-26 mo) rats were pair-fed R-LA (0.2% w/w) in the diet for 2 wk prior to sacrifice and microsomal isolation. R-LA supplementation led to a more oxidizing environment in the ER of old rats, with no significant changes noted in the redox environment of the young such that *both* R-LA supplemented young and old animals were no longer different versus young unsupplemented rats. To determine if R-LA also reversed age-associated differences in ER protein thiol redox status (Chapter 5), a fluorescent probe was utilized to determine protein thiol redox status from rats gavaged R-LA (120 mg/kg) and monitored for 48 hr. Initial results showed R-LA reversed the overall protein redox changes observed in aged animals. Furthermore, R-LA induced an ER stress response over this same time-course, preferentially inducing the pro-survival ER stress response gene, *grp78/BiP* over the pro-apoptotic ER stress response gene *gadd153/CHOP*. These results show that R-LA supplementation reverses the

detrimental aging ER phenotypes related to altered thiol redox state and stress response mechanisms. Together, these results suggest pharmacological treatment of R-LA may be an effective strategy to treat conditions associated with a dysfunctional ER observed during the normal aging process.

5.2. Introduction

On average, the ER is responsible for the synthesis of approximately one-third of the total cellular proteome. Eukaryotic ER enzymes that facilitate protein folding also catalyze protein refolding, isomerization, as well as unfolding and degradation. The conundrum as to how these enzymes take on multiple catalytic roles has perplexed researchers examining ER-dependent protein maturation and processing. It is now clear that protein processing enzymes switch catalytic roles depending on the thiol redox environment of the ER (64, 68, 117). The endoplasmic reticulum (ER) maintains a significantly more oxidizing environment than other cellular locales (Chapter 4) (41, 42, 64). Even very small changes in the GSH:GSSG ratio can have profound effects on ER enzyme function. For example, it has been shown that optimal protein folding *in vitro* occurs at a GSH:GSSG ratio approximately 2:1 (67). We and others have also shown that optimal reductase activity occurs at a GSH:GSSG greater than 5:1 (Chapter 3) (64, 68). Interestingly, the ER GSH:GSSG ratio typically exists somewhere in between these two values to tightly regulate all three essential activities (*e.g.*, folding, isomerization, and unfolding). Thus, small perturbations in the ER GSH:GSSG ratio would favor protein maturation at the expense of degradation or protein degradation at the expense of proper protein maturation.

As shown in Chapters 4 and 5, the ER GSH:GSSG redox ratio tilts toward a more reduced state with age. Briefly, the GSH:GSSG ratio in rat microsomes was approximately 4:1, 5.5:1, and 7:1 in microsomes isolated from young (3-4 mo), middle-aged (9-11 mo), and old (24-26 mo) rats, respectively. In terms of protein processing activity, these results suggest that the catalytic role of ER enzymes may shift toward protein disulfide reduction and away from oxidative protein folding. Thus, it could be envisioned that the aging ER protein processing machinery is more involved in protein refolding (isomerization) and degradation (unfolding), ultimately at the expense of nascent peptide synthesis and fidelity.

Proteins are generally considered to accumulate on an aging basis. Recent work showed that age-related increases in misfolded proteins, and coincident loss of protein degradation, not only affect specific enzyme activities, but can even take on toxic gain-of-function qualities, especially if the misfolded proteins aggregate (see General Introduction). Protein aggregates, as exemplified by ceroid, β -amyloid, huntingtin, cystic fibrosis transmembrane conductance regulator (CFTR), and lipofuscin, have been shown to progressively compromise cell function in accordance with their rate of accumulation (26, 37, 38, 49, 129, 130). Hence, one therapeutic strategy currently being employed for protein folding diseases is to pharmacologically induce endogenous cellular chaperones and antioxidant gene expression to restore both protein and redox homeostasis. Indeed, there is evidence that inducing chaperone expression prevents the accumulation of cytotoxic misfolded intermediates and improves cellular function in these diseases. Moreover, upregulation of antioxidant genes function to protect proteins from oxidative modification that have been shown to disrupt protein folding and also restore redox balance (8, 19, 74, 131). One compound which has shown great promise to induce cellular tolerance is trans-4,5-dihydroxy-1,2-dithiane (DTTox). DTTox is a dithiol compound that specifically upregulates the ER chaperone grp78/BiP while simultaneously protecting cells against oxidative injury, and thereby providing cytoprotection (127, 128). Moreover, previous studies show that other thiol-reactive substances such as 3H-1,2-dithiole-3-thione (D3T), pyrrolidine dithiocarbamate (PDTC), sulforaphane, and *R*-alpha-lipoic acid (1,2-dithiolane-3-pentanoic acid; R-LA) act as potent chemoprotective agents (19). In particular, R-LA is also known to directly affect cellular and subcellular redox status (25, 97, 132, 133). Thus, we pondered whether the dithiol compound, R-LA, would also prove to be beneficial in regards to the ER endpoints shown to decline herein (Chapters 3 and 5).

To this end, based on the structural and chemical similarities between DTTox and R-LA, and because R-LA is known to directly affect cellular and subcellular glutathione status (25, 97, 132, 133) *and* upregulate stress response mechanisms (19), we sought to determine whether R-LA can restore redox homeostasis in the ER of old animals following both acute and chronic dietary administration and induce endogenous chaperones and antioxidant enzymes

5.3. Materials and Methods

Materials

High performance liquid chromatography (HPLC) solvents were all HPLC grade (Fisher Scientific, Pittsburgh, PA). All other chemicals were reagent grade or the highest quality available from Sigma-Aldrich (St. Louis, MO).

Lipoic acid pair-feeding study

Young (3-4 mo) and old (24-26 mo) Fischer 344 rats (National Institute on Aging animal colonies) were pair-fed as *R*-alpha-lipoic acid (R-LA) is a well-known appetite suppressant (134). Nonsupplemented rats were pair-fed relative to the food intake of R-LA-supplemented animals to avoid possible confounding results from differences in caloric intake. Following acclimatization at the OSU animal facilities, rats were placed on AIN-93M diet supplemented \pm R-LA (0.2% [w/w]) for 2 wk (N=5-6 animals per group). Rats were sacrificed 4 per day (one from each experimental group) for 6 d and liver microsomes isolated as described below.

Isolation of rat liver microsomes

Young (3-4 mo) and old (24-26 mo) Fischer 344 rats (National Institute on Aging animal colonies) were anesthetized with diethyl ether, the livers perfused with ice-cold phosphate buffered saline (PBS), pH 7.5, to remove blood, and then sacrificed according to Institutional Animal Care and Use Committee (IACUC) approved guidelines. The livers were quickly excised, weighed, and placed on ice. Microsomes were isolated as previously reported with some modifications (64, 103). Briefly, half of each liver (~6-7 g) was homogenized 1:7 [w/v] in ice-cold homogenization buffer (10 mM potassium phosphate [monobasic], 10 mM potassium phosphate [dibasic], 150 mM HEPES, 75 mM potassium chloride, 1 mM EDTA; 70 mM iodoacetic acid (IAA) pH 7.5) and microsomes isolated by differential centrifugation. The microsomal pellet was further washed (100 mM potassium pyrophosphate and 1 mM EDTA, pH

7.4) to remove heme and spun again at 100,000 x g for 95 min at 4°C. The microsomal pellet was resuspended in 750 µl of 100 mM potassium phosphate buffer containing 30% glycerol [v/v] and 1 mM EDTA, pH 7.25. Only freshly isolated microsomes were used for GSH analysis. Assays for purity revealed that microsomal preparations using this procedure had minimal contamination of Golgi using the 59 kDa Golgi protein (Abcam #ab23932) as a marker but were highly enriched for Calnexin (Abcam #ab22595) (data not shown). Thus, the procedure employed in this study results in microsomes relatively free of contaminating membranes.

Preparation of microsomal samples for free glutathione analysis

Immediately following isolation of microsomes, 300 µl of the microsomal suspension was added directly to an equal volume of 15% (v/v) perchloric acid (PCA; Fisher Scientific) containing 10 mM diethylenetriaminepentaacetic acid (DTPA; Sigma-Aldrich), and incubated on ice for 15 min. Acidified samples were then spun at 15,000 x g for 15 min, the supernatant removed, and stored at -20°C until derivatization and glutathione analysis. PCA (300 µl of a 15% stock, containing 10 mM DTPA) was then added back to the pellet and snap-frozen in liquid nitrogen and stored at -80°C for protein-bound glutathione analysis (described below).

High performance liquid chromatography for glutathione

GSH quantification was performed as described using dansyl chloride as a fluorophore and γ -glutamylglutamate (γ -GG) as an internal standard for derivatization efficiency (64, 100, 102). Analyte separation was achieved using a 3-aminopropyl column (200 mm x 2.6 mm i.d.; Custom LC, Houston, TX) using a gradient of two buffers (Buffer A, 80/20 methanol/water (v/v); Buffer B, 62.5% MeOH (v/v), 20% acetate stock (217.6 g sodium acetate trihydrate [Fisher Scientific] in 400 ml glacial acetic acid) and 17.5% glacial acetic acid [v/v]). By this means, both GSH and GSSG can be simultaneously separated and quantified relative to authentic standards from a single biological sample.

Lipoic acid gavage study

A single bolus of R-LA (gavage; 120 mg/kg in PBS) was given to both young and old rats, the rats sacrificed over-time (0.5, 1, 6, 12, 24, and 48 hr post-gavage), microsomes isolated, and the ER GSH:GSSG ratio monitored as described above. The remaining liver tissue not utilized for microsomal isolation was either snap frozen on liquid nitrogen or stored in RNALater (Ambion) for mRNA analysis of ER stress response genes.

Determination of plasma lipoic acid concentrations

Plasma levels of R-LA were determined as described previously (135). Briefly, 100 μ l plasma was immediately placed in an equal 15% perchloric acid and 100 μ l mobile phase (50 mM NaH₂PO₄ 30% acetonitrile, and 20% methanol [pH 2.7]). Using a Supelco Discovery C18 column (15cm x 4.6 mm, 5 μ m), 50 μ l of analyte was injected at a flow rate of 1 ml/min. ESA CoulArray EC detector voltage was set at 0.85-.90 V and plasma concentrations of lipoic acid determined relative to authentic standards (Asta Medica; Frankfurt, Mainz, Germany).

Quantitative real-time PCR

Tissues (approximately 200 mg liver) were immediately placed in RNALater (Ambion, Foster City, CA) and stored according to manufacture's instructions. Total RNA was isolated using RNeasy kit (Qiagen, Valencia, CA) according to manufacture's instructions, quantified spectrophotometrically (260 nm), and assaying for purity by determining the 260/280 ratio. cDNA was prepared from 12.5 μ g of total RNA using SuperScript II (Invitrogen, Carlsbad, CA) and oligo(dT) primers (Operon, Huntsville, AL) in a 50 μ l reaction according to manufacture's instructions. Quantitative real-time PCR (qPCR) analyses were performed using mRNA-specific primers spanning exon/exon boundaries using the DNA Engine Opticon II system (BioRad, Hercules, CA). Specifically, 62.5 ng of each cDNA pool, 0.3 μ M of each primer (forward and reverse) and Finnzymes' DyNAmo Master Mix containing SYBR

Green (Finnzymes, Espoo, Finland) was used for each qPCR reaction in accordance with manufacturer's instructions.

Primer Sequences (Operon):

gadd153/CHOP-F; 5'-CAGCTGAGTCTCTGCCTTTCG-3'

gadd153/CHOP-R; 5'-GATTCTTCCTCTTGCTTTCCTGG-3'

grp78/BiP; F; 5'-CAAGTTCTTGCCATTCAAGGTGGTTGA-3'

grp78/BiP; R; 5'-CAGCTGCTGTTGGCTCATTGATGATC-3'

beta-actin-F; 5'-CCTTCCTTCCTGGGTATGGAATCC-3'

beta-actin-R; 5'-GAGCAATGATCTTGATCTTCATGGTG-3'

Thermocycler conditions included an initial incubation at 95.0°C for 00:10:00 followed by 45 cycles of 94.0°C for 00:00:10; 58.0-61.0°C for 00:00:20 (primer/gene specific; see below); incubation at 72.0°C for 00:00:20 followed by a plate read. Cycling conditions concluded with a final incubation at 72.0°C for 00:07:00; a melt curve analysis (65.0°C to 95.0°C, reading every 0.2° with a 00:00:01 hold) and a final extension step at 72.0°C for 00:10:00. Annealing temperatures were as follows: gadd153/CHOP, 58.0°C; grp78/BiP, 61.0°C; and beta-actin; 58.0°C - 61.0°C (compatible for all conditions and all genes examined). To obtain appropriate template concentrations, samples were run concurrently with standard curves generated using plasmid standards (Topo Cloning Kit; Invitrogen). Beta-actin was used as the housekeeping control for RNA recovery, reverse transcription efficiency, and template concentration. Gene expression was normalized to beta-actin mRNA levels and expressed as arbitrary units. Agarose gel electrophoresis and thermal denaturation (melt curve analysis) were used to confirm specific replicon formation.

Western blot analyses

Whole tissues were homogenized, spun at 15,000 x g for 15 min, and the supernatant collected. Whole tissue homogenates or microsomal samples were added directly to 3X loading buffer (0.5 M Tris-HCl, pH 6.8, 10% SDS [w/v], 25% glycerol [v/v], and 0.5% bromophenol blue [w/v]). Protein was separated on 10% polyacrylamide gels (Pierce, Rockford, IL) and transferred to PVDF membranes (Millipore, Billerica, MA). The levels of proteins were detected using a polyclonal antibody for grp78/BiP (Stressgen, Ann Arbor, MI) and gadd153/CHOP (Santa Cruz Biotechnology; Santa Cruz, CA) and standardized to PDI (Stressgen), grp78 (Stressgen), or beta-actin (Sigma-Aldrich) levels when appropriate as a loading control. Proteins were visualized using appropriate horseradish peroxidase-conjugated secondary antibodies (Cell Signaling Technologies, Danvers, MA) in conjunction with a chemiluminescent substrate (Amersham Pharmacia Biotech, Buckinghamshire, UK) and Enhanced Chemiluminescent Film (Amersham Pharmacia).

Determination of ER protein redox state by fluorescent detection

IAA-treated microsomes were incubated in 300 mM HEPES buffer (Sigma) containing 10 mM tris(2-carboxyethyl)phosphine hydrochloride (TCEP; Sigma) for 1 hr to reduce any thiol disulfides present. 1 mM of a Texas Red-conjugated maleimide (Invitrogen) was then added to label any free thiols reduced by the use of TCEP for 2 hr. Reactions were then added to an appropriate volume of dye-free loading buffer, heated for 5 min at 95°C, and loaded onto a 10% SDS-PAGE gel. Fluorescent proteins were visualized using a BioRad FX Molecular Imager. Proteins were then transferred onto PVDF membranes (Millipore) and the levels of grp78/BiP (Stressgen) detected as a loading control (Stressgen, Ann Arbor, MI). To determine the redox states of specific proteins, immunoprecipitations for protein disulfide isomerase (PDI) or ER oxidase 1L alpha (ERO1L-alpha) were performed using Seize-X Immunoprecipitation Kit (Pierce, Rockford, IL) followed by the reaction scheme, visualization, and Western blotting scheme described above.

Statistical analysis

Statistical significance between means of two independent groups was determined by Student's *t* test, assuming equal variances. For comparison of treatment effects, one-way analysis of variance (ANOVA) with Tukey's *post hoc* test was used. All of the results were considered significant if the *p* value was < 0.05. Statistical analysis was performed using PRISM 4.0b software (GraphPad Software, San Diego, CA).

5.4. Results

Plasma concentrations of R-LA following an acute single bolus dose

Based on previous results from our laboratory that dietary supplementation of R-LA results in reversal of the age-related loss in overall GSH and its redox state, we hypothesized that orally administered R-LA would also alter ER GSH status. However, again, based on data from our laboratory for whole liver tissue, R-LA increased GSH levels and the GSH:GSSG ratio. Thus, it could be hypothesized that feeding R-LA to old rats may actually exacerbate the age-related elevation in GSH levels and its reduced state.

To determine whether oral supplementation of R-LA reverses the age-related increase and GSH:GSSG ratio in microsomes isolated from old rats, or further adversely affect the ER GSH environment, young and old rats were given a bolus of R-LA (120 mg/kg) by gavage. To determine the extent of R-LA absorption following a single dose (120 mg/kg), plasma was isolated from each rat 0.5, 1, 1.5, 2, 6, and 12 hr post-gavage, and R-LA concentrations measured via HPLC. Results show that R-LA was detected as early as 0.5 hr post gavage, at which time it reached maximal plasma levels in both the young (3.0 pmol/ml plasma [\pm 0.6]) and old (5.7 pmol/ml plasma [\pm 0.7]) and quickly declined thereafter. By 6 hr post-gavage almost no R-LA was detectable in the plasma (Figure 5.1). These results confirm previous reports showing that R-LA is rapidly absorbed into the bloodstream and that maximal plasma concentrations are observed 0.5-2 hr post-consumption (136-138).

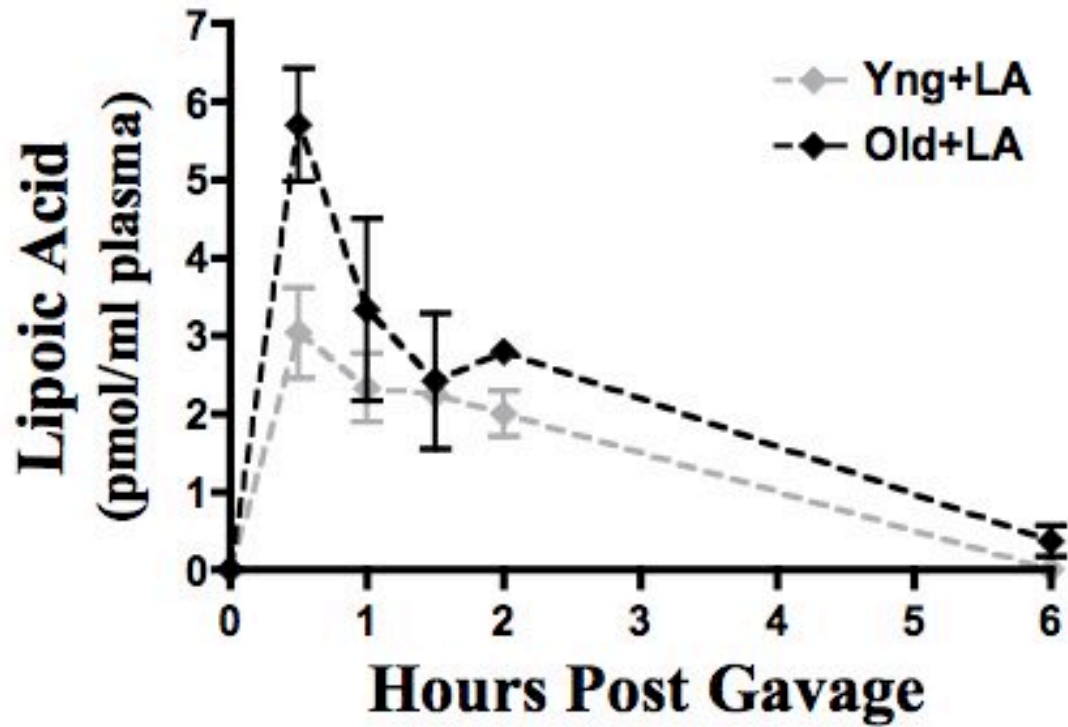


Figure 5.1. Plasma levels of R-LA following gavage. R-LA was detected as soon as 0.5 hr post-gavage. Thereafter, R-LA concentrations rapidly declined, becoming only negligibly detectable by 6 hr post-gavage. N=3 animals per group.

Acute R-LA supplementation rapidly affects the ER glutathione status

To determine whether a single oral dose of R-LA affected ER GSH redox status, rats were sacrificed over a timecourse following R-LA gavage, liver microsomes isolated, and the GSH:GSSG ratio monitored by HPLC determination. HPLC analysis demonstrated that R-LA rapidly affected ER GSH status as early as 0.5 hr post-gavage. Initially, a reduction in the ER GSH:GSSG ratio was observed in young rat microsomes, which was significant ($p < 0.05$) relative to sham-gavaged controls. The reduction of GSH redox state was so extensive such that the ER GSH redox environment in young R-LA-treated rats was similar to GSH:GSSG ratio in microsomes of old, untreated animals. Thereafter, a rapid and significant ($p < 0.05$) *loss* in the ER GSH:GSSG ratio was observed at 6 h and persisted for 18 hr thereafter (24 h post-gavage; Figure 5.2A). By 48 hr post-gavage, the GSH:GSSG ratio had returned to the initial baseline value (Figure 5.2A).

In contrast, R-LA treatment to old rats resulted in no immediate reduction in GSH redox state. Rather, R-LA induced a marked decline in the GSH:GSSG ratio which reached its maximum 12 hr post-gavage. At this time, the GSH:GSSG ratio was 71.4% lower than pre-gavage levels (Figure 5.2A). Thereafter, there was a small trend towards a more reducing GSH:GSSG ratio for the remainder of the timecourse. However, even after 48 hr post-gavage, the ER GSH:GSSG ratio was still significantly lower than that observed prior to R-LA gavage. In fact, R-LA administration ultimately produced a microsomal GSH:GSSG redox environment that was remarkably similar to ER GSH:GSSG values normally seen in young untreated rat microsomes (Figure 5.2A).

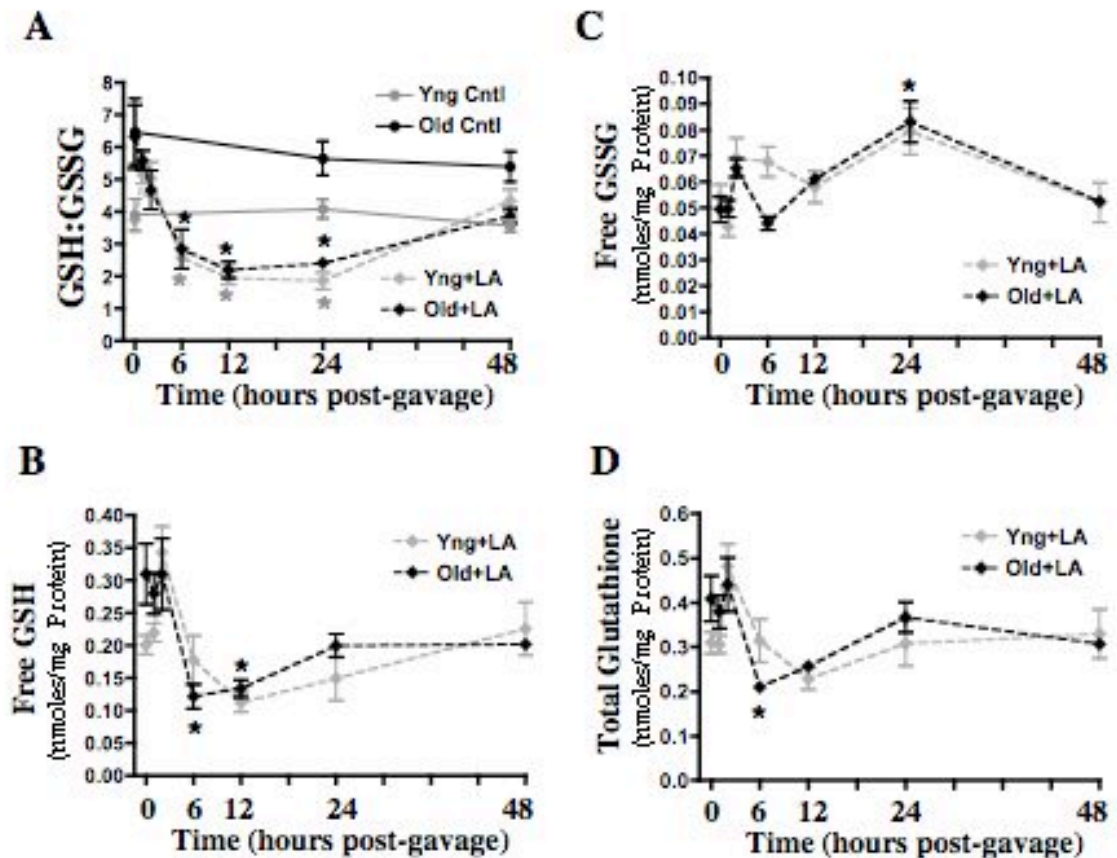


Figure 5.2. R-LA rapidly affects the ER glutathione status in microsomes isolated from *both* young and old rats. To determine how rapidly R-LA affects the ER glutathione pool, R-LA was administered in a single bolus via gavage (120mg/kg) to young and old rats and the ER GSH:GSSG ratio monitored over time. (A) An initial reduction was seen in young rat microsomes followed by a rapid loss in the ER GSH:GSSG ratio in both young and old rats at 6 hr post-gavage and persisted for 18 hr thereafter (24 hr post-gavage). At 48 hr post-gavage, the GSH:GSSG ratio had returned to the baseline value initially seen in the young for microsomes isolated from *both* young and old rat liver. To control for diurnal variations of glutathione, the GSH:GSSG ratio was also determined in untreated control animals at 0, 24, and 48 hr, and no significant change relative to time 0 controls was observed. (B) The loss of the ER GSH:GSSG was the result of both a significant lowering of GSH and (C) a significant increase in GSSG levels. (D) A significant loss of total ER glutathione was also initially observed but ultimately returned to the levels seen at time 0 for *both* the young and old. N=3 for all groups; asterisks (*) denotes significance ($p < 0.05$) versus young controls.

To control for diurnal variations of glutathione, the GSH:GSSG ratio was also determined in untreated control animals at 0, 24, and 48 hr (Figure 5.2A). Because no differences were observed at any of these timepoints examined, we concluded that this effect was the result of R-LA supplementation and not rhythmic variations in ER GSH status. The loss of the ER GSH:GSSG was the result of both a significant lowering of GSH (Figure 5.2B) and a significant increase in GSSG levels (Figure 5.2C) indicating that R-LA is either acting directly or indirectly to provide oxidizing equivalents to the ER. Furthermore, a significant loss of total ER glutathione was also initially observed but ultimately returned to the levels seen at time 0 in the young (Figure 5.2D).

Together, these results suggest that R-LA acts as an overall oxidizing agent to ER thiols in both young and old rats. However, for old rats, this decline is more persistent where R-LA caused a reversal of the age-related increase in GSH:GSSG ratio, even 48 hr post-gavage.

Lipoic acid pair-feeding study

Because a single oral R-LA dose resulted in a reversal of the age-related increase in microsomal GSH:GSSG ratio even 48 hr post-gavage, we hypothesized that a long term supplementation regimen would maintain the ER GSH redox state in old rats at levels normally seen in the ER of young rats. To this end, young and old rats were pair-fed AIN-93M diet +/- 0.2% R-LA for 2 wk. Analysis of food consumption show that rats fed R-LA in the diet (0.2% w/w) resulted in a significant decline in food intake (Figure 5.3A). Caloric intake was reduced by 34.8% and 29.1% in young and old rats, respectively, from the first day on supplemented diet versus just prior to sacrifice. This LA-induced anorectic effect has also been observed previously (134).

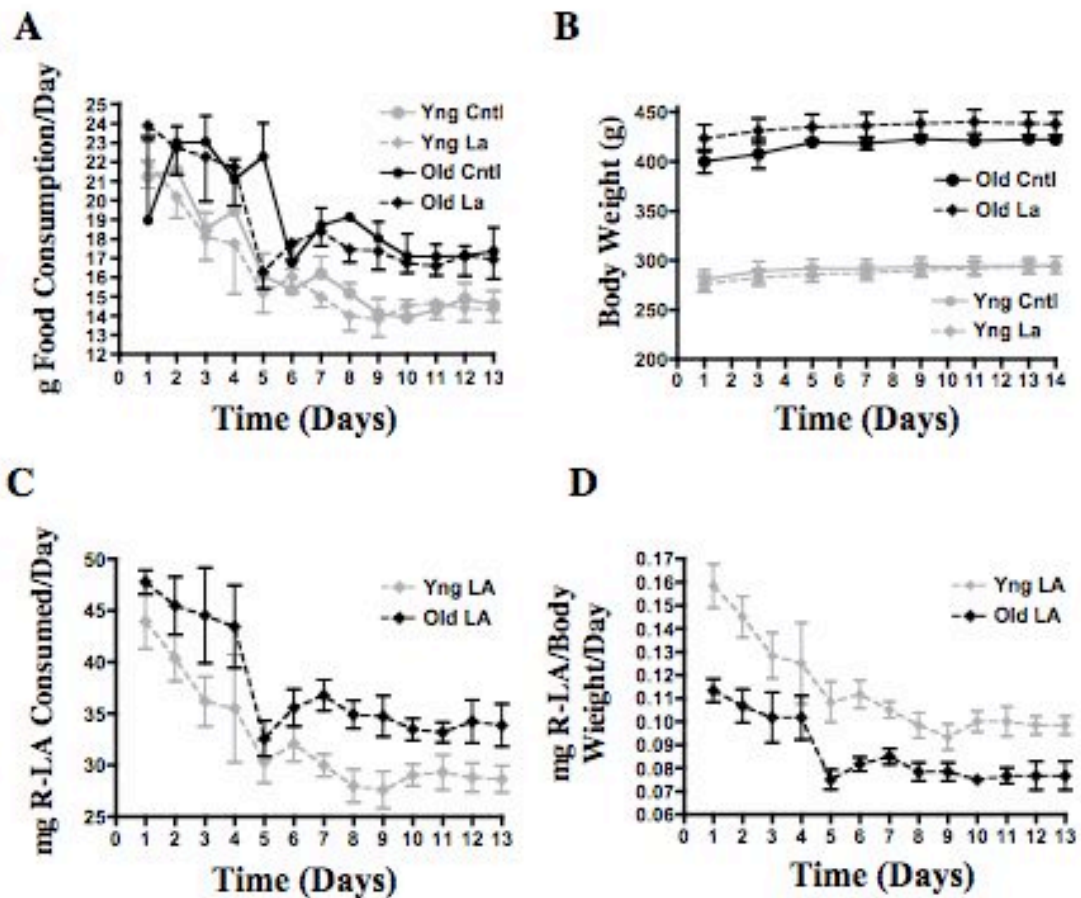


Figure 5.3. R-alpha-lipoic acid pair-feeding study. Because R-LA is known to suppress appetite, young and old rats were pair-fed AIN-93M diet (\pm 0.2% LA) for two-weeks. (A) Results show that R-LA had an anorectic affect on food intake but (B) there was no significant change in rat body weight over the course of the two-week feeding time period. (C) Because food consumption declined so did the amount of R-LA consumed over the course of the study but (D) even though the old rats consumed more total R-LA over the 2 wk study, they actually ate less relative to their larger mass. N=6 animals per group.

Despite the consumption of fewer calories, no change in rat body weight relative to respective pair-fed controls, over the course of the two-week feeding study, was observed (Figure 5.3B). Average R-LA intake for the young was 39.0 mg/day (+/- 1.7) for the first 4 days and 29.1 mg/day (+/- 0.5) from days 6-13. Thus daily R-LA intake was calculated to average 32.3 mg/day (+/- 0.8) over the course of the feeding study (Figure 5.1C). Old rats consumed an average of 45.3 mg/day (+/- 1.6) for the first 4 days and 34.6 (+/- 0.6) from days 6-13, averaging to 37.7 mg/day (+/- 0.8) for the course of the feeding study (Figure 5.3C). While the old animals ate more R-LA than the young, on a body weight basis the young actually consumed more R-LA, having consumed an average of 0.11 mg R-LA/gram b.w./day (+/- 0.003) compared to the old who averaged 0.09 mg R-LA/gram b.w./day (+/- 0.002) (Figure 5.3D). Together these results confirm previous studies that R-LA acts as an appetite suppressant but that relatively similar amounts of both total calories and R-LA was consumed by young and old animals.

A two week lipoic acid supplementation regimen reverses the age-related increase in ER GSH:GSSG ratio

We have previously shown that supplementation of R-LA improves both whole cell and mitochondrial GSH status to the levels originally seen in the young (25, 97, 132, 133, 139). We also showed in Figure 5.2 (A-D) that a single oral dose of R-LA ultimately produced an ER GSH:GSSG redox status no different than young untreated *and* treated rat microsomes. To determine if supplementation of R-LA for two-weeks in the diet could also remediate ER GSH status, microsomes were isolated from rats pair-fed R-LA for 2 wk and the GSH status determined. Old rats exhibit a significantly ($p = 0.02$) higher GSH:GSSG ratio in the ER (Figure 5.4A) that was the result of increased GSH (Figure 5.4B) and not a loss of GSSG (Figure 5.2C). However, supplementation with R-LA for two-weeks in the diet completely reversed the age-related increase in the ER GSH:GSSG ratio (Figure 5.4A). Whether directly or indirectly, it appears that R-LA is delivering oxidizing equivalents to the ER as seen

by the increase in GSSG in the young supplemented with R-LA (Figure 5.4B and C) and a reduction in the levels of GSH in the old supplemented animals (Figure 5.4B). However, pair-feeding with R-LA had no effect on total GSH levels (Figure 5.4D). These results show that longer-term supplementation with R-LA may be an effective way to maintain the ER glutathione status with age.

R-LA supplementation affects the soluble ER proteome

To determine whether R-LA supplementation affects the redox status of ER proteins in aged rats, we used a fluorescent gel technique (see reaction scheme Figure 5.4) to assess ER protein thiol redox status up to 48 hr following R-LA supplementation (gavage; 120mg/kg). To determine whether the oxidation of ER GSH:GSSG ratio induced by R-LA supplementation (Figure 5.2) also affected ER protein redox status, microsomal proteins from 0, 12, and 48 hr post gavage were fluorescently labeled and visualized. Preliminary results show that R-LA appears to affect the redox status of the ER proteome (Figure 5.5). When two of the four molecular weight regions previously shown to change with age (35 and 50 kDa; Figure 5.5) were examined by densitometry (Figure 5.5; arrows), a reversal of the alterations seen in protein thiol redox state was observed following R-LA supplementation. Together, these results provide evidence that the redox status of the proteome in the aging ER is affected with age but that R-LA supplementation may shift the redox status of the ER proteome of old rats towards that observed in young rats.

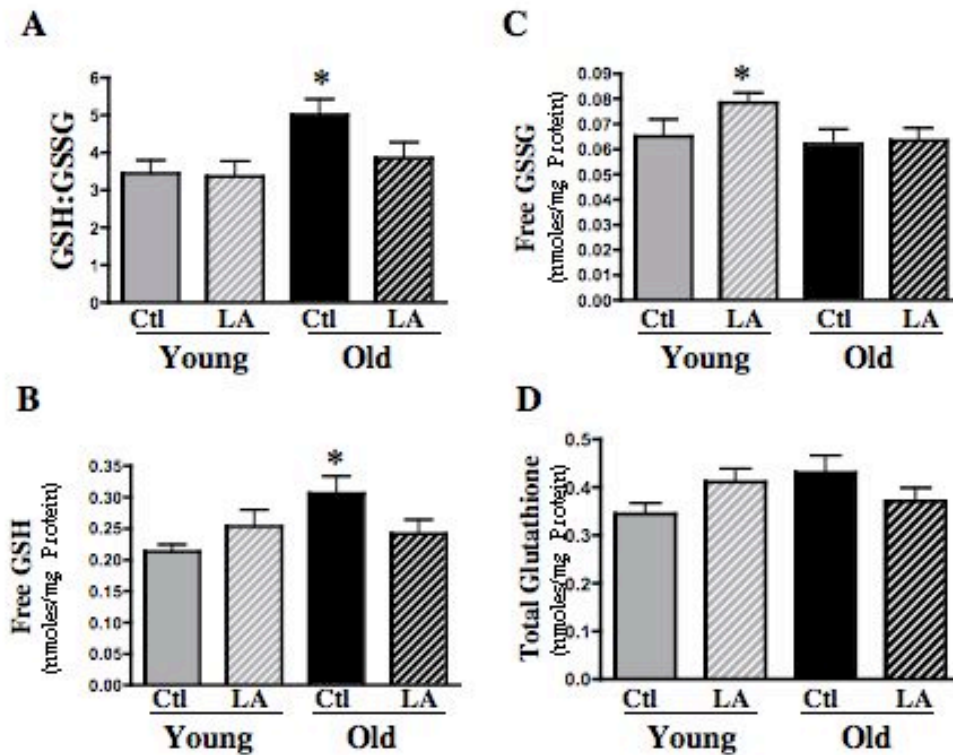


Figure 5.4. Chronic two-week feeding of R-LA reverses the age-related increase in ER GSH:GSSG ratio. To determine if R-LA beneficially affects ER glutathione, young and old rats were pair-fed AIN-93M diet (+/- 0.2% LA) for two-weeks. (A) R-LA reversed the 30% increase in ER GSH:GSSG ratio seen in old rat microsomes to levels observed in young animals. (B) In old rats, GSH was significantly ($p < 0.05$) elevated relative to young controls but R-LA supplementation completely reversed this phenomenon. (C) R-LA dietary supplementation significantly increased free GSSG concentrations in the young but had no effects on the old rats. (D) Total GSH (GSH + 2 GSSG) was not affected by R-LA supplementation in young or old rats. N=5-6 animals per group; asterisks (*) denotes statistical significance ($p < 0.05$) relative to young controls.

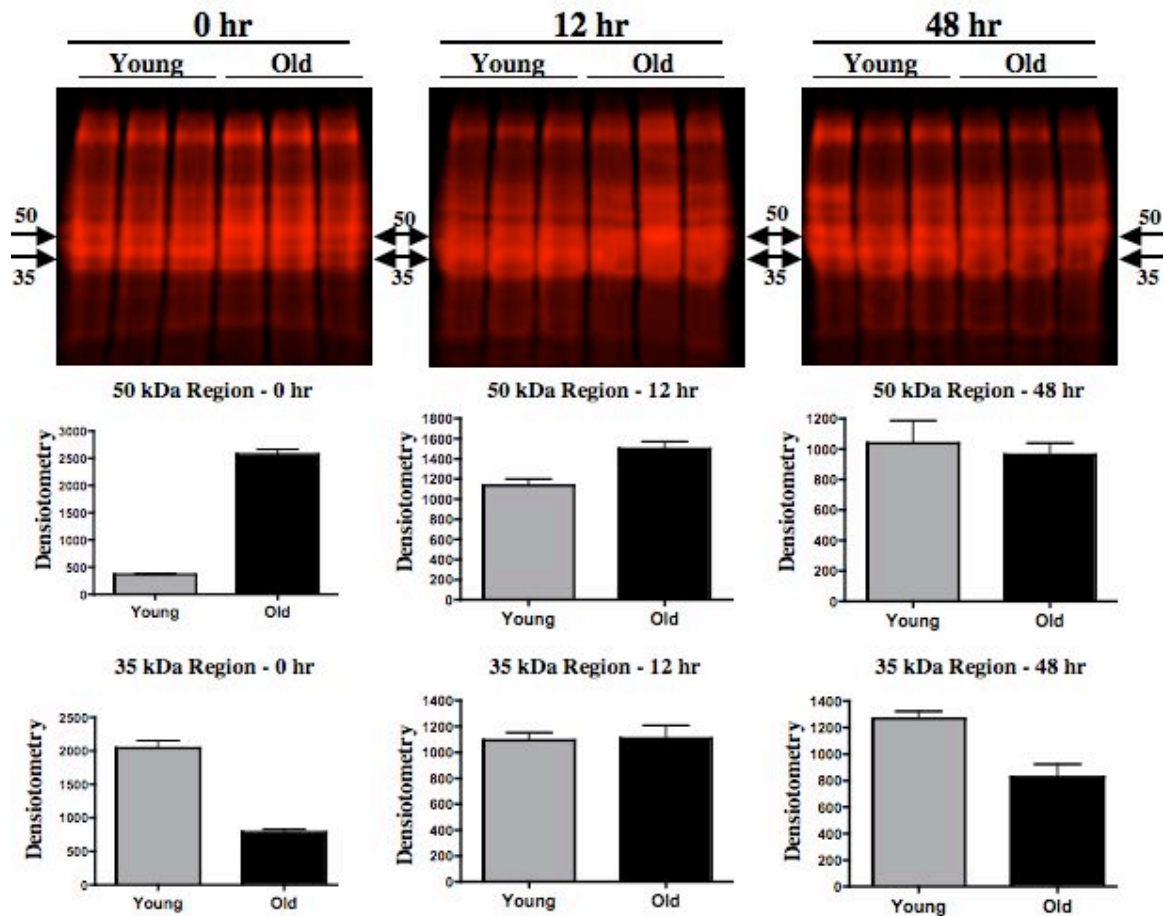


Figure 5.5. R-LA supplementation affects the soluble ER proteome. Preliminary studies were conducted to determine if R-LA can influence the redox status of ER proteins. Microsomal proteins collected at 0, 12 and 48 hr post-gavage (120mg/kg) were fluorescently labeled and visualized (false color image shown). When fluorescence of the molecular weight regions at 35 and 50 kDa were analyzed by densitometry results showed that R-LA appears to at least temporarily reverse any age-related changes seen in the protein thiol redox status of the proteome in these molecular weight regions (35 and 50 kDa; 12 and 48 hr). N=3 animals per group, at each timepoint.

Lipoic acid induces ER stress response pathways

Because the R-LA-induced changes in the ER GSH redox ratio are consistent with that of a thiol oxidizing agent, we hypothesized that R-LA may act as a weak stressor that would also be expected to induce a protective ER stress response. Thus, quantitative real-time PCR (qPCR) was used to measure message levels of known ER stress activated genes following R-LA administration (gavage; 120 mg/kg). Initially, there was a significant increase in *gadd153/CHOP*, a gene associated with induction of pro-apoptotic pathways, at 1 and 2 hr post-gavage in liver tissue of young rats (Figure 5.6A). A similar induction was also observed for old rats except induction of *gadd153/CHOP* mRNA persisted up to 6 hr following LA treatment (Figure 5.6A). For both age groups *gadd153/CHOP* message levels returned to baseline by 12 hr (Figure 5.6A). However, despite the increases in message levels, no significant increases in *gadd153/CHOP* protein levels were observed for any of the timepoints examined (Figure 5.7A). Interestingly, message levels of the pro-survival ER chaperone, *grp78/BiP*, also increased significantly following administration of LA in both young and old rat liver and this induction persisted up to 24 hr post-gavage (Figure 5.6B). Contrary to *gadd153/CHOP*, increases in *grp78/BiP* mRNA levels resulted in increased protein levels in livers of both young and the old rats treated with R-LA (Figure 5.7B). These results indicate that even though R-LA acutely acts as a pro-oxidizing agent to ER sulfhydryls, it also induces a largely protective ER response to this initial stress.

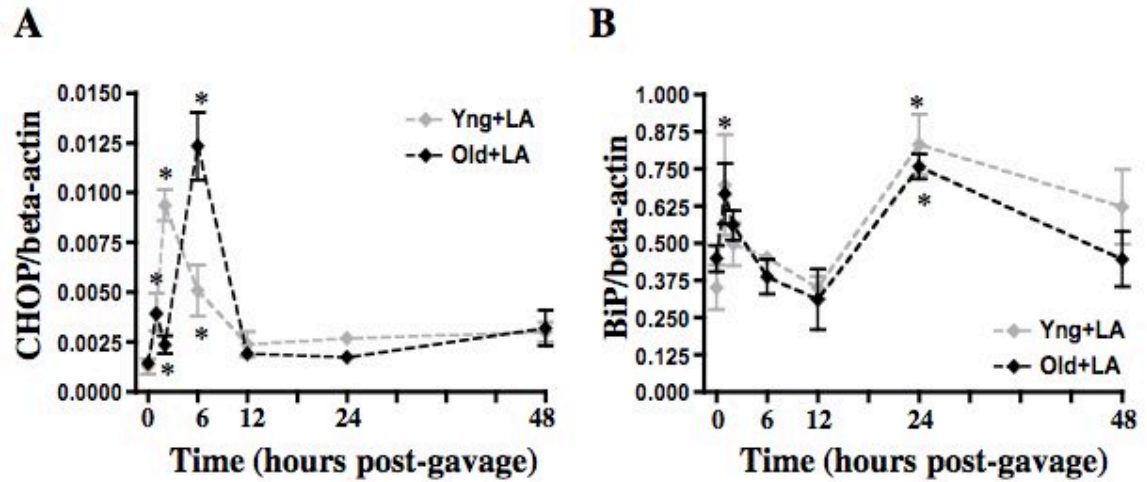


Figure 5.6. R-LA transiently induces ER stress response genes in both young and old rats. To determine if ER stress response pathways are activated following administration of R-LA (gavage:120mg/kg), quantitative real-time PCR for message levels of known ER stress response genes was performed. (A) There was an initial significant increase in gadd153/CHOP at 1 and 2 hr post-gavage in the young and 1, 2, and 6 hr post-gavage in the old, returning to baseline by 12 h. (B) grp78/BiP mRNA was also significantly increased following administration of LA at 1 and 24 hr post-gavage. N=3 for all groups; asterisks (*) denotes significance ($p < 0.05$) versus young controls.

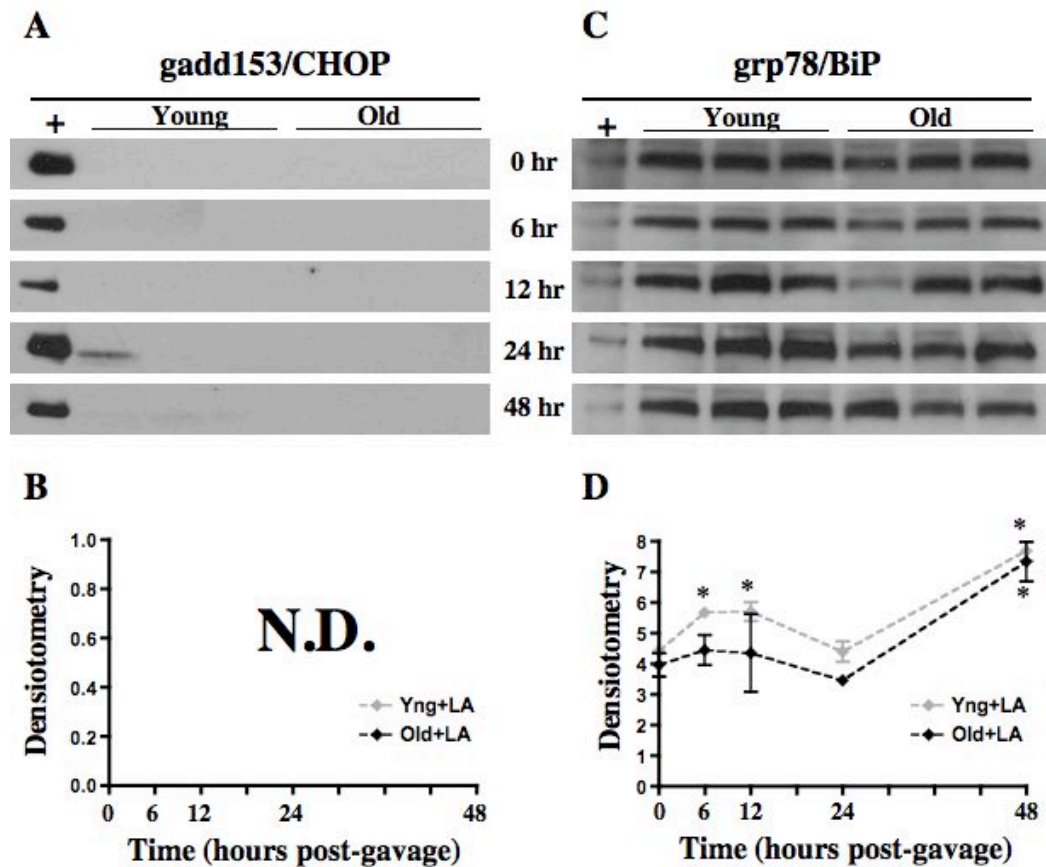


Figure 5.7. R-LA preferentially increases pro-survival ER stress response protein levels in both young and old rats. To determine if ER stress response pathways are activated following administration of R-LA (gavage:120mg/kg), Western blot analysis for protein levels of known ER stress response genes was performed. (A) Despite the increases in message levels of gadd153/CHOP no significant increase in protein expression was observed for any of the timepoints examined. (B) Because no protein levels of gadd153/CHOP were detected following R-LA supplementation, no densitometry (N.D.) was performed. (C) and (D) levels of grp78/BiP were significantly increased in *both* the young (6, 12, and 48 hr) and the old (48 hr). N=3 for all groups; asterisks (*) denotes significance ($p < 0.05$) versus young controls.

5.5. Discussion

To facilitate protein homeostasis, the cell and ER possess macromolecular complexes including chaperones, oxidoreductases, and antioxidant enzymes to minimize aggregation (45). To respond when the proteome becomes challenged, the cell uses stress sensing mechanisms and inducible pathways to adapt to the stress. These include ER stress response pathways that counter unfolded, misfolded, and accumulated proteins or under severe stresses, induce apoptosis. As we have shown, despite the age-related *increase* in the thiol redox status of the ER, ER stress signaling pathways are not upregulated in older rats. Therefore, treatments aimed at restoring redox status, protein homeostasis, and stress signaling pathways in disease states, and during the normal aging process, could prove to beneficially influence healthy aging.

It is well documented that R-LA can restore both glutathione levels and the redox potential in aging animals to that seen in their younger counterparts (19, 25, 97, 132, 133, 139, 140). Results from our laboratory have shown that R-LA works through NFE2-related factor 2 (Nrf2) to upregulate glutathione synthesizing genes (19). Interestingly, Nrf2 is known to be activated, and essential for survival, following chemical induction of the ER stress response (73, 74). Thus, it is interesting to speculate that the ER possesses a “redox switch” to activate stress response pathways and further that R-LA may be activating these beneficial stress response genes via modulation of the thiol redox status.

Previous studies have shown that pharmacological intervention with dithiol compounds can beneficially induce stress response pathways, including those originating from the ER. The present study, however, goes one step further into gaining mechanistic insight into how dithiol compounds, including R-LA, may confer cytoprotection against certain toxicants. Perturbations of the thiol-disulfide and/or NAD(P)H/NAD(P)⁺ redox potential in the cytosol or ER is known to activate stress-response genes (141-143). Herein we show that following a single acute administration of R-LA, the ER GSH:GSSG ratio becomes significantly oxidized.

However, the likelihood that this effect is mediated by a perturbation in the ER NADPH/NADP⁺ ratio is unlikely since in the ER pyridine nucleotides and thiol redox status are uncoupled (144). That is, pyridine nucleotides remain reduced despite the oxidizing thiol redox status (144). Thus, more direct effects of R-LA, such as thiol-disulfide exchange, may be the more likely mechanism. Regardless of the precise mechanism, this is the first time that R-LA has been shown to work as a cellular oxidant as opposed to its traditional role as an antioxidant.

To this end, Nardai *et al.* have shown that exposing isolated rat liver microsomes to oxidizing equivalents such as dehydroascorbic acid and glutathione disulfide could reverse the appearance of reductive shifts in protein thiol status in a mouse model of diabetes (63). Herein we show that following a single acute administration of R-LA, the ER GSH:GSSG ratio becomes significantly oxidized. Thus, as shown *in vitro* (63), if agents such as R-LA can deliver oxidizing equivalents to the ER, this may prove to be a novel therapeutic target and a potent means in reverse detrimental indices of aging.

The mechanism for the R-LA-induced ER-oxidation is entirely unknown. Normally, compounds which induce a severe oxidative stress are toxic but in the context of the oxidizing environment of the ER, and the reductive shift with age, in this case it appears to be beneficial. However, whether this effect is direct or indirect would only be speculation. The kinetics of R-LA absorption and excretion are very rapid. In fact, >80% of a dietary bolus is excreted via the urine within 24 hr. Furthermore, plasma levels only reach <150 μ M at peak plasma levels, 0.5-2 hr post-prandial (see Figure 5.1) (20, 138, 145). Thus, a direct oxidizing effect of R-LA is unlikely based on concentration alone. For example, the GSH content in the ER is in the low millimolar range (41, 64). Furthermore, the ER is rich in thiol-containing proteins. Together, the total thiol content of the ER would be estimated to be in the middle-to-high millimolar range. Thus, it seems unlikely that R-LA is acting to directly oxidize compounds in the ER. However, whether the ER is a direct cellular target of R-LA and whether R-LA will at least transiently accumulate in the ER is

entirely unknown but in light of the current studies (Chapter 5), should be the emphasis of future work.

In conclusion, R-LA may be a novel dithiol compound that could be used pharmacologically to treat diseases linked to a dysfunctional ER, including the normal aging process. Given that redox regulation of gene expression is an important physiological mediator of genomic stress responses, our data suggest that by acutely modulating the ER thiol redox status, genomic stress response genes can be robustly upregulated and likely confer protection. In this sense, because of its extremely short half-life in cells and tissues, R-LA may be a superior compound to treat diseases of the ER as a weak ER stressing hormetic agent to prophylactically protect against toxicological insult.

The Aging Endoplasmic Reticulum

Chapter 6

General Discussion and Conclusions

6.1. General Discussion and Conclusions

The elderly are currently the fastest growing demographic in the United States and because aging itself is associated with an increased risk for morbidity and mortality, the elderly are the most vulnerable age-group to all types of degenerative diseases. In terms of healthcare spending, this will place a tremendous burden on the economy. Therefore, *it is imperative that preventative approaches to geriatric medicine are employed to prevent, or delay, disease onset and ultimately prolonging human healthspan*. However, to achieve this goal, it is paramount that the underlying mechanisms of the aging process be better understood. Thus, it was the goal of this dissertation to provide an increased understanding of the underlying cellular and molecular events that may contribute to the detrimental indices associated with the aging process and to provide novel therapeutic target(s) to prevent morbidity and increase healthspan in the elderly.

This work describes detrimental indices that specifically affect the endoplasmic reticulum in the context of aging. Together, the novel findings of this dissertation work include: 1) hepatocytes isolated from young and old rats placed in primary culture is an appropriate model for studying stress response mechanisms originating from the ER (Chapter 2); 2) the thiol redox status of the ER is significantly higher than previously reported (Chapter 3); 3) there is an age-related *increase* in the GSH:GSSG redox status, alterations in ER protein redox status, and no induction of ER stress response pathways basally with age (Chapter 4); and 4) the dietary compound *R*-alpha-lipoic acid (R-LA) reverses the detrimental indices of the aging process described in the previous chapters (Chapter 5). Together, these findings can be summarized into three general aging deficits: 1) no chronic induction of ER stress signaling; 2) alterations in ER thiol redox; and 3) the ability of R-LA to restore the negative consequences of each.

Loss of ER stress signaling and remediation by R-LA

To combat protein accumulation and other stressors, the cell and ER possess macromolecular complexes including chaperones and oxidoreductases, to minimize aggregation (45). Hence, in response to challenges to the proteome, such as oxidative or toxicological insults, the cell utilizes stress sensing mechanisms and inducible pathways to adapt to the stress. These include ER stress response pathways that function to counter the accumulation of unfolded and misfolded proteins. However, as we have shown (Chapter 4), there is an age-related increase in the ER thiol redox status and no chronic induction of ER stress signaling pathways. Therefore, treatments aimed at restoring redox status, protein homeostasis, and stress signaling pathways during the normal aging process could prove to beneficially influence healthspan.

A strategy currently employed to combat cellular stress is to pharmacologically induce endogenous cellular chaperones and antioxidant enzymes. One example of a compound used successfully is *trans*-4,5-dihydroxy-1,2-dithiane (DTTox) (127, 128, 146). *In vitro* and *in vivo* studies have established that DTTox enters the cell and is reduced by cellular oxidoreductases, induces ER stress response pathways, and confers resistance to xenobiotic challenge (127, 128, 146). This work established that the ER stress response gene, *grp78/BiP*, was essential for this protective effect.

Herein we show that R-LA may be working through a similar mechanism as DTTox (Chapter 5). Supplementation of R-LA to young and old rats similarly induced ER stress gene expression and preferentially increased *grp78/BiP* protein levels compared to *gadd153/CHOP*. These results show that R-LA is able to preferentially upregulate pro-survival ER stress response genes (*i.e.*, *grp78/BiP*) and may be an effective strategy to upregulate protective ER proteins. However, the mechanism for this preferential induction of the pro-survival arm of the ER stress response over the pro-death arm (*i.e.*, *gadd153/CHOP*) is entirely unknown. One possibility is that a “redox switch” governs ER stress response induction. For example, following R-LA supplementation (gavage; 120 mg/kg), *gadd153/CHOP* induction was observed early in the timecourse when the redox state was increasingly reduced. Conversely,

grp78/BiP expression (and protein levels) increased following maximal oxidation of the ER. Thus, a more reducing ER may favor induction of pro-death pathways while oxidation favors pro-survival pathways. However, the exact nature of the redox sensing mechanism(s) is entirely unknown.

In this regard, it is notable that a progressive age-associated decline in stress response mechanisms has been described in many animal species, which leads to heightened risk for both morbidity and mortality (6, 14, 82, 83). We recently showed the increased vulnerability that aged rats display to oxidative, xenobiotic, and toxicological stresses is due to a basal loss of stress response mechanism(s) brought about by a decline in Nrf2-mediated gene expression (19), a transcription factor that binds and regulates the expression of Phase II detoxification genes (19). As Nrf2 not only governs expression of GSH synthesis genes, but also nearly 100 other Phase II detoxification and antioxidant genes (147-159), the age-associated loss of Nrf2-driven gene expression may represent a significant underlying factor leading to heightened risk for a variety of insults in the elderly.

Nrf2 is known to be upregulated and essential for cellular survival following chemical induction of the ER stress response (73, 74). Furthermore, we also found that R-LA potently increases hepatic nuclear Nrf2 levels in a time-dependent manner (19). Thus, R-LA induction of Nrf2-mediated Phase II gene expression through modulating ER stress signaling mechanisms would be a novel mechanism and should be the focus of further studies to examine these potential therapeutic affects.

It is important to note, however, that two other Nrf2-dependent genes failed to be upregulated in hepatocytes derived from either young or old rats, namely GCLM and GST2A, thus calling into question the precise role of Nrf2 in the ER stress response. One potential explanation of these results is the independent findings of two separate research groups. In each instance, it was found that Nrf1, a transcription factor closely related to Nrf2 in structure and function, is anchored via its N-terminal domain to the membrane of the ER (160, 161). Nrf1 and Nrf2 have significant overlap in the genes they regulate (160, 161). Furthermore, Wang and Chan went on to show

that after treating cells with the ER stress inducing compound tunicamycin, Nrf1 translocated to the nucleus. Thus, Nrf1 may be a confounding affector in interpreting our results and may account for the heterogeneity of Phase II genes upregulated following treatments with R-LA. However, further studies will be necessary to delineate the differences in Nrf1- versus Nrf2-dependent gene transcription in the ER stress response and their precise roles in upregulation pro-survival Phase II detoxification genes.

Alterations in ER thiol redox and remediation by R-LA

Perhaps the most provocative finding of this research is the *reductive shift* that occurs in the aging ER (Chapter 4). This result is surprising because aging is generally considered to be the consequence of progressive and accumulated oxidative damage (9). Indeed, significant oxidative stress, as measured by a number of indices including the GSH:GSSG ratio, have been noted on a whole cell basis as well as in specific sub-cellular organelles such as the nucleus and mitochondria (19, 23, 162, 163). Thus, in the context of an age-related oxidative stress, the reductive shift in the ER seems counterintuitive. It is important to note that oxidative modifications have been noted in resident ER proteins; however, whether oxidative damage occurs directly in the ER, extra-luminally, or from oxidants that have diffused from other cellular locales is entirely unknown. Thus, the mechanism of oxidative damage in the ER warrants further study.

The reason for a higher ER thiol redox state in aging is entirely unknown. Furthermore, speculation on the causes of such a reductive shift is difficult because there is a significant lack of research surrounding the precise interactions of redox-active molecules within the ER, particularly with regard to what is ultimately providing oxidizing power to the ER. Additionally, transport characteristics of redox active compounds into, and out of, the ER are almost entirely unknown. Thus, without a fundamental understanding of these basic mechanisms, it is difficult to interpret our results. Such gaps in our understanding of ER redox mechanisms can be illustrated by

considering the role(s) of glutathione in ER function. There are currently conflicting reports surrounding whether reduced (GSH) or oxidized (GSSG) glutathione is the particular species of glutathione transported into the ER (41, 42, 88). For example, if GSSG is the transported species, one interpretation as to the mechanism of the reductive shift in the ER would be a decreased utilization of GSSG if it were providing the oxidizing equivalents to the ER. However, a consensus is slowly building in the literature that GSH is the actively transported species (41, 65, 88, 164). If GSH is the species transported, in light of our results showing increased levels of non-protein bound GSH and an increase in the GSH:GSSG ratio (Chapter 4), one interpretation would be the oxidizing machinery of the ER is compromised with age. Regardless, it is clear, that redox balance is disrupted in the aging ER.

In support of this latter scenario, previous reports showed a reversal of the ER redox status after *in vitro* additions of oxidized glutathione or dehydroascorbic acid to isolated rat liver microsomes (62, 63). Thus, the oxidative machinery of the ER is suspect and before precise mechanistic conclusions can be drawn, and the results of the current work put into the overall context of the aging ER, a greater understanding of ER processes must be ascertained. To date, it is known that the small molecular redox systems of both ascorbate/dehydroascorbate and GSH/GSSG are present in millimolar concentrations in the ER (41, 64, 65, 165). Interestingly, severe imbalances of both redox couples have been well characterized in aging (15, 20, 21, 23, 140). Although the amounts of dehydroascorbate and GSSG increase relative to their reduced counterparts (an oxidative shift) during aging, the absolute concentration of both total glutathione and ascorbate decrease on a whole tissue basis.

Dehydroascorbate has recently been proposed to be the terminal oxidizing compound of the ER (65, 124, 165). Dehydroascorbate transport into the ER occurs in a GLUT transporter-dependent mechanism where it is likely reduced and recycled back to the cytosol (165). Furthermore, as mentioned above, ascorbate levels are known to decline in the aging rat liver despite the fact rats have the ability to synthesize vitamin C. Thus, a decline in total ascorbate levels, and presumably the

absolute concentration of dehydroascorbate, may contribute significantly to this reductive shift by the decreased availability of this potential ER oxidant with age.

Severe aberrations in GSH metabolism have also been noted during aging. We have previously shown that both total glutathione (GSH + 2GSSG) and the GSH:GSSG ratio significantly decline with age (Chapter 4) (15, 19, 23, 101). More work from our laboratory has revealed that this age-related loss was the result of decreased expression of GSH synthesizing machinery as the result of aberrant Nrf2 signaling—also implicating a loss of ER stress response as a underlying factor in altered ER redox.

GSH is made exclusively in the cytoplasm and transported to various cellular locales. Thus, it is interesting to speculate that the adverse synthetic capacity of the liver as a whole, may contribute to the redox imbalance in the ER. However, the GSH status in the ER shows the exact opposite trends as the liver as a whole (Chapters 4 and 5). That is, there is a significant *increase* in total GSH (GSH + 2GSSG) *and* the GSH:GSSG ratio. Several explanation may account for this apparent paradox.

First, if GSH is the species transported intraluminally, then perhaps it is GSSG that is exported out of the ER. The liver is known to rapidly transport GSSG extracellularly under times of oxidative stress. Our data in Chapters 3 and 5 provides evidence of a GSSG efflux mechanism from the ER. The increase in total ER GSH (GSH + 2GSSG) is the result of increased levels of GSH and *not* GSSG (Chapters 4 and 5). However, as the ER becomes oxidized, either through *ex vivo* oxidation (Chapter 3) or via R-LA administration (Chapter 5), GSH levels decrease and GSSG levels rise. However, GSSG levels only increase to a specific concentration and plateau thereafter, while total GSH levels (GSH + 2GSSG) decline as a result. Thus, as more and more GSH is presumably converted to GSSG, concentrations of GSSG would increase towards the K_m of this theoretical GSSG exporter and the net effect would be a loss of total GSH (GSH + 2GSSG). Therefore, one possibility for the increase in total ER glutathione with age is that GSH is transported intraluminally and it is GSSG that is transported extraluminally. However, because of defects in the ER

oxidative machinery, GSH remains reduced in the ER and, in-effect, becomes “trapped”, having the net effect of increasing GSH, total GSH (GSH + 2GSSG), and the GSH:GSSG ratio. However, until transport characteristics of GSH and the precise interplay of redox active ER compounds are more fully characterized, the mechanisms for aberrant GSH status in the ER will only be conjecture. Nonetheless, it is intriguing to speculate that pharmacological compounds capable of oxidizing the ER, such as R-LA, would prove beneficial to maintain, or even improve, ER redox homeostasis.

A closer examination of the data reveals a striking nuance of the increased ER thiol redox ratio. In our initial studies assessing the involvement of *ex vivo* oxidation on the assessment of ER GSH, 9-11 mo old rats were used (Chapter 3). However, for our aging studies 3-5 mo and 24-26 mo old rats were employed (Chapters 4 and 5). When the data from these experiments are examined, there appears to be an “aging continuum” in the GSH:GSSG redox ratio; that is, the thiol redox ratio of the ER becomes increasingly more reduced with age from young to middle-aged to old rats. We found that in young rats (3-4 mo), the GSH:GSSG ratio was 3.8:1, in 9-11 mo old rats the GSH:GSSG ratio was 5.5:1, and in aged rats 24-26 mo old, the GSH:GSSG became almost 7:1 (Chapters 3-5). This data also has an interesting, albeit obscure precedent. Nardai *et al.* examined the thiol redox ratio in their chemically induced model of diabetes at various timepoints following initiation (63). Interestingly, they found that the reductive shift in the total thiol content developed early in their experimental model and was sustained throughout. However, the influence of this reductive shift on ER enzymatic activity was not noted until later timepoints. Thus, it is intriguing to suggest changes in the ER redox status may be an early event in the aging process and that ER redox state may be a predictor of longevity and additionally, could provide an early marker of diseases associated with ER dysfunction. However, in reality, implementation of clinical diagnostics of ER redox status, or markers thereof, will likely prove to be complex and require substantial research efforts.

The question also arises, is this reductive shift we have observed in this work “adaptive” or “causative”? As with many indices described during the aging process, it is difficult, if not impossible, to tease out “cause-or-effect”. That is to say, if an indice is noted to be changing in the context of aging, is that indice the cause of the decline or the result of other cellular deficits? Moreover, one must also consider that the redox changes noted in the aging ER are an adaptive response. For example, because proteins are known to accumulate with age, a reductive shift in the ER may be a compensatory mechanism to preferentially favor unfolding over folding activity. However, this would be predicted to severely impact nascent peptide formation. Thus, while potentially adaptive, the reductive shift noted in the ER could induce an irreversible chain of events that lead inevitably to compromised cellular function with age. As proteins accumulate and aggregate with age they become “stuck” in irreversible, misfolded intermediates. No amount of ATP or reducing power will unfold these protein aggregates. In fact, not even lysosomes can detoxify these aggregates.

Optimal protein folding *in vitro* has been shown to occur at a GSH:GSSG ratio of approximately 2:1 (42, 58, 67). Under increasingly more reductive conditions, protein folding kinetics and fidelity decrease, compromising nascent protein synthesis and would ultimately lead to *more* misfolded and aggregated proteins. This cycle would likely continue to perpetuate and should induce an ER stress response. However, as we showed in Chapter 4, there is no ER stress response basally with age and thus, if the cell cannot adequately respond, apoptotic and/or necrotic pathways would prevail and ultimately culminate in cell death. If this scenario were to occur in post-mitotic tissues such as the brain and heart, removal of these cells could have dire consequences to overall organ function, especially over time. However, following cell death, the cellular debris is phagocytosed by neighboring cells and these protein aggregates that originally caused cell death now become trapped in the phagolysosome of the healthy cell and would ultimately compromising the catabolic activity of that cell. This propagation may be one mechanism to explain why proteins continuously

and additively accumulate and cells become increasingly vulnerable to stresses with age.

Therefore, regardless whether or not the redox shift of the aging ER is causative or adaptive, perhaps a strategy to promote a more oxidizing ER environment may prove beneficial to ensure the fidelity of nascent peptides and break this vicious downward spiral. That is, re-oxidize the ER to minimize the accumulation of novel misfolded proteins and protein aggregate formation. While this approach would not fix the existing problem of protein aggregation, it would interrupt this cycle of continued protein accumulation, potentially delaying the detrimental effects. Thus, R-LA may be an effect therapeutic to re-equilibrate the redox status of the ER and slow the progression of age-related protein aggregation, prolong overall cellular homeostasis, and increase healthspan.

In conclusion, this dissertation has fulfilled the goals of identifying underlying cellular and molecular mechanisms that change with age. Given that redox regulation of gene expression is an important physiological mediator of genomic stress responses, our data suggests that by acutely modulating the ER thiol redox status, genomic stress response genes can be robustly upregulated and in terms of the ER and the age-related deficiencies described herein, completely reverse these phenotypes. Thus, R-LA would appear to have the multifunctional role of re-oxidizing the ER *and* inducing ER stress response pathways. In this sense, because of its extremely short half-life in cells and tissues, R-LA may be a superior hormetic agent to prophylactically protect cells against toxicological insults and could further be utilized to treat diseases of the ER and delay cellular aging. Thus, this dissertation has fulfilled its second goal to provide potential therapeutic target(s) to combat detrimental indices of aging. To this end, nutritional interventions with the dietary compound, *R*-alpha-lipoic acid, may provide an efficacious and cost-effect means to improve overall healthspan in the elderly.

REFERENCES

1. Bureau USC. 2004.
2. Centers for Medicare & Medicaid Services Beneficiary Survey DoHaHS. 2004.
3. Cohen JE. Human population: the next half century. *Science* 302: 1172-1175; 2003.
4. Lubitz J, Cai L, Kramarow E, Lentzner H. Health, life expectancy, and health care spending among the elderly. *N Engl J Med* 349: 1048-1055; 2003.
5. Ames BN, Shigenaga MK, Hagen TM. Oxidants, antioxidants, and the degenerative diseases of aging. *Proc Natl Acad Sci U S A* 90: 7915-7922; 1993.
6. Harman D, Aging and disease: extending functional life span, in *Ann NY Acad Sci*. 1996. p. 321-336.
7. Knight JA. The biochemistry of aging. *Adv Clin Chem* 35: 1-62; 2000.
8. Finkel T, Holbrook NJ. Oxidants, oxidative stress and the biology of ageing. *Nature* 408: 239-247; 2000.
9. Harman D. Aging: a theory based on free radical and radiation chemistry. *J Gerontol* 11: 298-300; 1956.
10. Sohal RS, Weindruch R. Oxidative stress, caloric restriction, and aging. *Science* 273: 59-63; 1996.
11. Sohal RS, Dubey A. Mitochondrial oxidative damage, hydrogen peroxide release, and aging. *Free Radic Biol Med* 16: 621-626; 1994.
12. Sohal RS. Hydrogen peroxide production by mitochondria may be a biomarker of aging. *Mech Ageing Dev* 60: 189-198; 1991.
13. Sohal RS, Sohal BH. Hydrogen peroxide release by mitochondria increases during aging. *Mech Ageing Dev* 57: 187-202; 1991.
14. Beckman KB, Ames BN. The free radical theory of aging matures. *Physiol Rev* 78: 547-581; 1998.
15. Hagen TM, Yowe DL, Bartholomew JC, Wehr CM, Do KL, Park JY, Ames BN. Mitochondrial decay in hepatocytes from old rats: membrane potential declines, heterogeneity and oxidants increase. *Proc Natl Acad Sci U S A* 94: 3064-3069; 1997.
16. Navarro A, Sanchez Del Pino MJ, Gomez C, Peralta JL, Boveris A. Behavioral dysfunction, brain oxidative stress, and impaired mitochondrial electron transfer in aging mice. *Am J Physiol Regul Integr Comp Physiol* 282: R985-992; 2002.
17. Robinson KM, Janes MS, Pehar M, Monette JS, Ross MF, Hagen TM, Murphy MP, Beckman JS. Selective fluorescent imaging of superoxide in vivo using ethidium-based probes. *Proc Natl Acad Sci U S A* 103: 15038-15043; 2006.
18. Sohal RS, Ku HH, Agarwal S, Forster MJ, Lal H. Oxidative damage, mitochondrial oxidant generation and antioxidant defenses during aging and in

- response to food restriction in the mouse. *Mech Ageing Dev* 74: 121-133; 1994.
19. Suh JH, Shenvi SV, Dixon BM, Liu H, Jaiswal AK, Liu RM, Hagen TM. Decline in transcriptional activity of Nrf2 causes age-related loss of glutathione synthesis, which is reversible with lipoic acid. *Proc Natl Acad Sci U S A* 101: 3381-3386; 2004.
 20. Dixon BM, Shenvi SV, Hagen T, Dietary antioxidants and cardiovascular disease, in *Advances in Cell Aging and Gerontology: Mechanisms of Cardiovascular Aging*, Hagen T, Editor. 2002, Elsevier: Amsterdam. p. 349-376.
 21. Michels AJ, Joisher N, Hagen TM. Age-related decline of sodium-dependent ascorbic acid transport in isolated rat hepatocytes. *Arch Biochem Biophys* 410: 112-120; 2003.
 22. Ames BN, Shigenaga MK, Hagen TM. Mitochondrial decay in aging. *Biochim Biophys Acta* 1271: 165-170; 1995.
 23. Hagen TM. Oxidative stress, redox imbalance, and the aging process. *Antioxid Redox Signal* 5: 503-506; 2003.
 24. Shenvi SV, Dixon BM, Shay KP, Hagen TM, A Rat Primary Hepatocyte Culture Model For Aging Studies, in *Current Protocols in Toxicology*. 2008.
 25. Hagen TM, Vinarsky V, Wehr CM, Ames BN. (R)-alpha-lipoic acid reverses the age-associated increase in susceptibility of hepatocytes to tert-butylhydroperoxide both in vitro and in vivo. *Antioxid Redox Signal* 2: 473-483; 2000.
 26. Hipkiss AR. Accumulation of altered proteins and ageing: causes and effects. *Exp Gerontol* 41: 464-473; 2006.
 27. Levine RL, Garland D, Oliver CN, Amici A, Climent I, Lenz AG, Ahn BW, Shaltiel S, Stadtman ER. Determination of carbonyl content in oxidatively modified proteins. *Methods Enzymol* 186: 464-478; 1990.
 28. Levine RL, Stadtman ER. Oxidative modification of proteins during aging. *Exp Gerontol* 36: 1495-1502; 2001.
 29. Smith CD, Carney JM, Starke-Reed PE, Oliver CN, Stadtman ER, Floyd RA, Markesbery WR. Excess brain protein oxidation and enzyme dysfunction in normal aging and in Alzheimer disease. *Proc Natl Acad Sci U S A* 88: 10540-10543; 1991.
 30. Stadtman ER. Importance of individuality in oxidative stress and aging. *Free Radic Biol Med* 33: 597-604; 2002.
 31. Stadtman ER, Moskovitz J, Levine RL. Oxidation of methionine residues of proteins: biological consequences. *Antioxid Redox Signal* 5: 577-582; 2003.
 32. Uchida K, Stadtman ER. Modification of histidine residues in proteins by reaction with 4-hydroxynonenal. *Proc Natl Acad Sci U S A* 89: 4544-4548; 1992.

33. Yoritaka A, Hattori N, Uchida K, Tanaka M, Stadtman ER, Mizuno Y. Immunohistochemical detection of 4-hydroxynonenal protein adducts in Parkinson disease. *Proc Natl Acad Sci U S A* 93: 2696-2701.; 1996.
34. Moreau R, Heath SH, Doneanu CE, Lindsay JG, Hagen TM. Age-related increase in 4-hydroxynonenal adduction to rat heart alpha-ketoglutarate dehydrogenase does not cause loss of its catalytic activity. *Antioxid Redox Signal* 5: 517-527; 2003.
35. Moreau R, Nguyen BT, Doneanu CE, Hagen TM. Reversal by aminoguanidine of the age-related increase in glycoxidation and lipoxidation in the cardiovascular system of Fischer 344 rats. *Biochem Pharmacol* 69: 29-40; 2005.
36. Cuervo AM, Bergamini E, Brunk UT, Droge W, Ffrench M, Terman A. Autophagy and aging: the importance of maintaining "clean" cells. *Autophagy* 1: 131-140; 2005.
37. Terman A. Catabolic insufficiency and aging. *Ann N Y Acad Sci* 1067: 27-36; 2006.
38. Terman A, Gustafsson B, Brunk UT. Autophagy, organelles and ageing. *J Pathol* 211: 134-143; 2007.
39. Carrard G, Dieu M, Raes M, Toussaint O, Friguet B. Impact of ageing on proteasome structure and function in human lymphocytes. *Int J Biochem Cell Biol* 35: 728-739; 2003.
40. Terman A, Dalen H, Eaton JW, Neuzil J, Brunk UT. Mitochondrial recycling and aging of cardiac myocytes: the role of autophagocytosis. *Exp Gerontol* 38: 863-876; 2003.
41. Bass R, Ruddock LW, Klappa P, Freedman RB. A major fraction of endoplasmic reticulum-located glutathione is present as mixed disulfides with protein. *J Biol Chem* 279: 5257-5262; 2004.
42. Hwang C, Sinskey AJ, Lodish HF. Oxidized redox state of glutathione in the endoplasmic reticulum. *Science* 257: 1496-1502; 1992.
43. Schafer FQ, Buettner GR. Redox environment of the cell as viewed through the redox state of the glutathione disulfide/glutathione couple. *Free Radic Biol Med* 30: 1191-1212; 2001.
44. Nuss JE, Choksi KB, DeFord JH, Papaconstantinou J. Decreased enzyme activities of chaperones PDI and BiP in aged mouse livers. *Biochem Biophys Res Commun* 365: 355-361; 2008.
45. Balch WE, Morimoto RI, Dillin A, Kelly JW. Adapting proteostasis for disease intervention. *Science* 319: 916-919; 2008.
46. Wiseman RL, Powers ET, Buxbaum JN, Kelly JW, Balch WE. An adaptable standard for protein export from the endoplasmic reticulum. *Cell* 131: 809-821; 2007.
47. Chaudhuri TK, Paul S. Protein-misfolding diseases and chaperone-based therapeutic approaches. *Febs J* 273: 1331-1349; 2006.
48. Yoshida H. ER stress and diseases. *Febs J* 274: 630-658; 2007.

49. Bates G. Huntingtin aggregation and toxicity in Huntington's disease. *Lancet* 361: 1642-1644; 2003.
50. Chen S, Ferrone FA, Wetzel R. Huntington's disease age-of-onset linked to polyglutamine aggregation nucleation. *Proc Natl Acad Sci U S A* 99: 11884-11889; 2002.
51. Askanas V, Engel WK. Sporadic inclusion-body myositis: a proposed key pathogenetic role of the abnormalities of the ubiquitin-proteasome system, and protein misfolding and aggregation. *Acta Myol* 24: 17-24; 2005.
52. Paz Gavilan M, Vela J, Castano A, Ramos B, del Rio JC, Vitorica J, Ruano D. Cellular environment facilitates protein accumulation in aged rat hippocampus. *Neurobiol Aging* 27: 973-982; 2006.
53. Csala M, Banhegyi G, Benedetti A. Endoplasmic reticulum: a metabolic compartment. *FEBS Lett* 580: 2160-2165; 2006.
54. Ellgaard L. Catalysis of disulphide bond formation in the endoplasmic reticulum. *Biochem Soc Trans* 32: 663-667; 2004.
55. Koivu J, Myllyla R. Interchain disulfide bond formation in types I and II procollagen. Evidence for a protein disulfide isomerase catalyzing bond formation. *J Biol Chem* 262: 6159-6164; 1987.
56. Lyles MM, Gilbert HF. Catalysis of the oxidative folding of ribonuclease A by protein disulfide isomerase: pre-steady-state kinetics and the utilization of the oxidizing equivalents of the isomerase. *Biochemistry* 30: 619-625; 1991.
57. Petersen JG, Dorrington KJ. An in vitro system for studying the kinetics of interchain disulfide bond formation in immunoglobulin G. *J Biol Chem* 249: 5633-5641; 1974.
58. Saxena VP, Wetlaufer DB. Formation of three-dimensional structure in proteins. I. Rapid nonenzymic reactivation of reduced lysozyme. *Biochemistry* 9: 5015-5023; 1970.
59. Wetlaufer DB, Branca PA, Chen GX. The oxidative folding of proteins by disulfide plus thiol does not correlate with redox potential. *Protein Eng* 1: 141-146; 1987.
60. Mezghrani A, Fassio A, Benham A, Simmen T, Braakman I, Sitia R. Manipulation of oxidative protein folding and PDI redox state in mammalian cells. *Embo J* 20: 6288-6296; 2001.
61. Molteni SN, Fassio A, Ciriolo MR, Filomeni G, Pasqualetto E, Fagioli C, Sitia R. Glutathione limits Ero1-dependent oxidation in the endoplasmic reticulum. *J Biol Chem* 279: 32667-32673; 2004.
62. Nardai G, Korcsmaros T, Papp E, Csermely P. Reduction of the endoplasmic reticulum accompanies the oxidative damage of diabetes mellitus. *Biofactors* 17: 259-267; 2003.
63. Nardai G, Stadler K, Papp E, Korcsmaros T, Jakus J, Csermely P. Diabetic changes in the redox status of the microsomal protein folding machinery. *Biochem Biophys Res Commun* 334: 787-795; 2005.

64. Dixon BM, Heath SH, Kim R, Suh JH, Hagen TM. Assessment of Endoplasmic Reticulum Glutathione Redox Status is Confounded by Extensive Ex Vivo Oxidation. *Antioxid Redox Signal* 10: 963-972; 2008.
65. Banhegyi G, Benedetti A, Csala M, Mandl J. Stress on redox. *FEBS Lett* 2007.
66. Benham AM. Oxidative protein folding: an update. *Antioxid Redox Signal* 7: 835-838; 2005.
67. Lyles MM, Gilbert HF. Catalysis of the oxidative folding of ribonuclease A by protein disulfide isomerase: dependence of the rate on the composition of the redox buffer. *Biochemistry* 30: 613-619; 1991.
68. Lundstrom-Ljung J, Holmgren A. Glutaredoxin accelerates glutathione-dependent folding of reduced ribonuclease A together with protein disulfide-isomerase. *J Biol Chem* 270: 7822-7828; 1995.
69. Nakamura T, Lipton SA. Emerging roles of s-nitrosylation in protein misfolding and neurodegenerative diseases. *Antioxid Redox Signal* 10: 87-102; 2008.
70. Schroder M, Kaufman RJ. ER stress and the unfolded protein response. *Mutat Res* 569: 29-63; 2005.
71. Marciniak SJ, Ron D. Endoplasmic reticulum stress signaling in disease. *Physiol Rev* 86: 1133-1149; 2006.
72. Papp E, Szaraz P, Korcsmaros T, Csermely P. Changes of endoplasmic reticulum chaperone complexes, redox state, and impaired protein disulfide reductase activity in misfolding alpha1-antitrypsin transgenic mice. *Faseb J* 20: 1018-1020; 2006.
73. Cullinan SB, Zhang D, Hannink M, Arvisais E, Kaufman RJ, Diehl JA. Nrf2 is a direct PERK substrate and effector of PERK-dependent cell survival. *Mol Cell Biol* 23: 7198-7209; 2003.
74. Cullinan SB, Diehl JA. PERK-dependent activation of Nrf2 contributes to redox homeostasis and cell survival following endoplasmic reticulum stress. *J Biol Chem* 279: 20108-20117; 2004.
75. Marciniak SJ, Yun CY, Oyadomari S, Novoa I, Zhang Y, Jungreis R, Nagata K, Harding HP, Ron D. CHOP induces death by promoting protein synthesis and oxidation in the stressed endoplasmic reticulum. *Genes Dev* 18: 3066-3077; 2004.
76. Oyadomari S, Mori M. Roles of CHOP/GADD153 in endoplasmic reticulum stress. *Cell Death Differ* 11: 381-389; 2004.
77. Zhang K, Kaufman RJ. Signaling the unfolded protein response from the endoplasmic reticulum. *J Biol Chem* 279: 25935-25938; 2004.
78. Erickson RR, Dunning LM, Holtzman JL. The effect of aging on the chaperone concentrations in the hepatic, endoplasmic reticulum of male rats: the possible role of protein misfolding due to the loss of chaperones in the decline in physiological function seen with age. *J Gerontol A Biol Sci Med Sci* 61: 435-443; 2006.

79. Li J, Holbrook NJ. Elevated gadd153/chop expression and enhanced c-Jun N-terminal protein kinase activation sensitizes aged cells to ER stress. *Exp Gerontol* 39: 735-744; 2004.
80. Stevenson DJ, Morgan C, McLellan LI, Helen Grant M. Reduced glutathione levels and expression of the enzymes of glutathione synthesis in cryopreserved hepatocyte monolayer cultures. *Toxicol In Vitro* 21: 527-532; 2007.
81. Moldeus P, Hogberg J, Orrenius S. Isolation and use of liver cells. *Methods Enzymol* 52: 60-71; 1978.
82. Humphries KM, Szweda PA, Szweda LI. Aging: a shift from redox regulation to oxidative damage. *Free Radic Res* 40: 1239-1243; 2006.
83. Balaban RS, Nemoto S, Finkel T. Mitochondria, oxidants, and aging. *Cell* 120: 483-495; 2005.
84. Liu Y, Guyton KZ, Gorospe M, Xu Q, Kokkonen GC, Mock YD, Roth GS, Holbrook NJ. Age-related decline in mitogen-activated protein kinase activity in epidermal growth factor-stimulated rat hepatocytes. *J Biol Chem* 271: 3604-3607; 1996.
85. Kitano S, Fawcett TW, Yo Y, Roth GS. Molecular mechanisms of impaired stimulation of DNA synthesis in cultured hepatocytes of aged rats. *Am J Physiol* 275: C146-154; 1998.
86. Lambert AJ, Merry BJ. Use of primary cultures of rat hepatocytes for the study of ageing and caloric restriction. *Exp Gerontol* 35: 583-594; 2000.
87. Gorchach A, Klappa P, Kietzmann T. The endoplasmic reticulum: folding, calcium homeostasis, signaling, and redox control. *Antioxid Redox Signal* 8: 1391-1418; 2006.
88. Csala M, Fulceri R, Mandl J, Benedetti A, Banhegyi G. Glutathione transport in the endo/sarcoplasmic reticulum. *Biofactors* 17: 27-35; 2003.
89. Liu G, Pessah IN. Molecular interaction between ryanodine receptor and glycoprotein triadin involves redox cycling of functionally important hyperreactive sulfhydryls. *J Biol Chem* 269: 33028-33034; 1994.
90. Gladyshev VN, Liu A, Novoselov SV, Krysan K, Sun QA, Kryukov VM, Kryukov GV, Lou MF. Identification and characterization of a new mammalian glutaredoxin (thioltransferase), Grx2. *J Biol Chem* 276: 30374-30380; 2001.
91. Xia R, Stangler T, Abramson JJ. Skeletal muscle ryanodine receptor is a redox sensor with a well defined redox potential that is sensitive to channel modulators. *J Biol Chem* 275: 36556-36561; 2000.
92. Zable AC, Favero TG, Abramson JJ. Glutathione modulates ryanodine receptor from skeletal muscle sarcoplasmic reticulum. Evidence for redox regulation of the Ca²⁺ release mechanism. *J Biol Chem* 272: 7069-7077; 1997.
93. Chakravarthi S, Jessop CE, Bulleid NJ. The role of glutathione in disulphide bond formation and endoplasmic-reticulum-generated oxidative stress. *EMBO Rep* 7: 271-275; 2006.

94. Chakravarthi S, Bulleid NJ. Glutathione is required to regulate the formation of native disulfide bonds within proteins entering the secretory pathway. *J Biol Chem* 279: 39872-39879; 2004.
95. Smith AR, Visioli F, Hagen TM. Vitamin C matters: increased oxidative stress in cultured human aortic endothelial cells without supplemental ascorbic acid. *Faseb J* 16: 1102-1104; 2002.
96. Hagen T, Zhang CY, Sliker LJ, Chung WK, Leibel RL, Lowell BB. Assessment of uncoupling activity of the human uncoupling protein 3 short form and three mutants of the uncoupling protein gene using a yeast heterologous expression system. *FEBS Lett* 454: 201-206; 1999.
97. Hagen TM, Ingersoll RT, Lykkesfeldt J, Liu J, Wehr CM, Vinarsky V, Bartholomew JC, Ames AB. (R)-alpha-lipoic acid-supplemented old rats have improved mitochondrial function, decreased oxidative damage, and increased metabolic rate. *Faseb J* 13: 411-418; 1999.
98. Hagen TM, Ingersoll RT, Wehr CM, Lykkesfeldt J, Vinarsky V, Bartholomew JC, Song MH, Ames BN. Acetyl-L-carnitine fed to old rats partially restores mitochondrial function and ambulatory activity. *Proc Natl Acad Sci U S A* 95: 9562-9566; 1998.
99. Hagen TM, Wehr CM, Ames BN. Mitochondrial decay in aging. Reversal through supplementation of acetyl-L-carnitine and N-tert-butyl-alpha-phenyl-nitrone. *Ann N Y Acad Sci* 854: 214-223; 1998.
100. Fariss MW, Reed DJ. High-performance liquid chromatography of thiols and disulfides: dinitrophenol derivatives. *Methods Enzymol* 143: 101-109; 1987.
101. Suh JH, Heath SH, Hagen TM. Two subpopulations of mitochondria in the aging rat heart display heterogenous levels of oxidative stress. *Free Radic Biol Med* 35: 1064-1072; 2003.
102. Jones DP, Carlson JL, Samiec PS, Sternberg P, Jr., Mody VC, Jr., Reed RL, Brown LA. Glutathione measurement in human plasma. Evaluation of sample collection, storage and derivatization conditions for analysis of dansyl derivatives by HPLC. *Clin Chim Acta* 275: 175-184; 1998.
103. Krueger SK, Yueh MF, Martin SR, Pereira CB, Williams DE. Characterization of expressed full-length and truncated FMO2 from rhesus monkey. *Drug Metab Dispos* 29: 693-700; 2001.
104. Burns JA, Butler JC, Moran J, Whitesides GM. Selective reduction of disulfides by tris(2-carboxyethyl)phosphine. *J Org Chem* 56: 2648-2650; 1991.
105. Holmgren A. Thioredoxin catalyzes the reduction of insulin disulfides by dithiothreitol and dihydrolipoamide. *J Biol Chem* 254: 9627-9632; 1979.
106. Hirs CH, Reduction and S-Carboxymethylation of Proteins, in *Methods in Enzymology*, Hirs CH, Editor. 1967, Academic Press: New York. p. 199-203.
107. Jocelyn PC, Biochemistry of SH Group. 1972, Academic Press. p. 94.
108. Duggan PF, Martonosi A. Sarcoplasmic Reticulum: The permeability of sarcoplasmic reticulum membranes. *Journal of General Physiology* 56: 147-167; 1970.

109. Share L, Hansrote RW. Permeability of Rat Liver Microsomes to Sucrose and Carboxypolyglucose in vitro. *J Biophysic and Biochem Cytol* 7: 239-242; 1960.
110. Ebadi M, Govitrapong P, Sharma S, Muralikrishnan D, Shavali S, Pellett L, Schafer R, Albano C, Eken J. Ubiquinone (coenzyme q10) and mitochondria in oxidative stress of parkinson's disease. *Biol Signals Recept* 10: 224-253; 2001.
111. Carelli S, Ceriotti A, Cabibbo A, Fassina G, Ruvo M, Sitia R. Cysteine and glutathione secretion in response to protein disulfide bond formation in the ER. *Science* 277: 1681-1684; 1997.
112. Narayan M, Welker E, Wedemeyer WJ, Scheraga HA. Oxidative folding of proteins. *Acc Chem Res* 33: 805-812; 2000.
113. Schwaller M, Wilkinson B, Gilbert HF. Reduction-reoxidation cycles contribute to catalysis of disulfide isomerization by protein-disulfide isomerase. *J Biol Chem* 278: 7154-7159; 2003.
114. Temussi PA, Masino L, Pastore A. From Alzheimer to Huntington: why is a structural understanding so difficult? *Embo J* 22: 355-361; 2003.
115. Tu BP, Ho-Schleyer SC, Travers KJ, Weissman JS. Biochemical basis of oxidative protein folding in the endoplasmic reticulum. *Science* 290: 1571-1574; 2000.
116. Tu BP, Weissman JS. Oxidative protein folding in eukaryotes: mechanisms and consequences. *J Cell Biol* 164: 341-346; 2004.
117. Raturi A, Mutus B. Characterization of redox state and reductase activity of protein disulfide isomerase under different redox environments using a sensitive fluorescent assay. *Free Radic Biol Med* 43: 62-70; 2007.
118. Hagen TM, Liu J, Lykkesfeldt J, Wehr CM, Ingersoll RT, Vinarsky V, Bartholomew JC, Ames BN. Feeding acetyl-L-carnitine and lipoic acid to old rats significantly improves metabolic function while decreasing oxidative stress. *Proc Natl Acad Sci U S A* 99: 1870-1875; 2002.
119. Hagen TM, Moreau R, Suh JH, Visioli F. Mitochondrial decay in the aging rat heart: evidence for improvement by dietary supplementation with acetyl-L-carnitine and/or lipoic acid. *Ann N Y Acad Sci* 959: 491-507; 2002.
120. Shigenaga MK, Hagen TM, Ames BN. Oxidative damage and mitochondrial decay in aging. *Proc Natl Acad Sci U S A* 91: 10771-10778; 1994.
121. Hussain S, Slikker W, Jr., Ali SF. Age-related changes in antioxidant enzymes, superoxide dismutase, catalase, glutathione peroxidase and glutathione in different regions of mouse brain. *Int J Dev Neurosci* 13: 811-817; 1995.
122. Liu Y, Gorospe M, Kokkonen GC, Boluyt MO, Younes A, Mock YD, Wang X, Roth GS, Holbrook NJ. Impairments in both p70 S6 kinase and extracellular signal-regulated kinase signaling pathways contribute to the decline in proliferative capacity of aged hepatocytes. *Exp Cell Res* 240: 40-48; 1998.
123. Csermely P, Penzes I, Toth S. Chronic overcrowding decreases cytoplasmic free calcium levels in T lymphocytes of aged CBA/CA mice. *Experientia* 51: 976-979; 1995.

124. Nardai G, Braun L, Csala M, Mile V, Csermely P, Benedetti A, Mandl J, Banhegyi G. Protein-disulfide isomerase- and protein thiol-dependent dehydroascorbate reduction and ascorbate accumulation in the lumen of the endoplasmic reticulum. *J Biol Chem* 276: 8825-8828; 2001.
125. Szanto I, Gergely P, Marcsek Z, Banyasz T, Somogyi J, Csermely P. Changes of the 78 kDa glucose-regulated protein (grp78) in livers of diabetic rats. *Acta Physiol Hung* 83: 333-342; 1995.
126. Yamagishi N, Nakayama K, Wakatsuki T, Hatayama T. Characteristic changes of stress protein expression in streptozotocin-induced diabetic rats. *Life Sci* 69: 2603-2609; 2001.
127. Asmellash S, Stevens JL, Ichimura T. Modulating the endoplasmic reticulum stress response with trans-4,5-dihydroxy-1,2-dithiane prevents chemically induced renal injury in vivo. *Toxicol Sci* 88: 576-584; 2005.
128. Halleck MM, Liu H, North J, Stevens JL. Reduction of trans-4,5-dihydroxy-1,2-dithiane by cellular oxidoreductases activates gadd153/chop and grp78 transcription and induces cellular tolerance in kidney epithelial cells. *J Biol Chem* 272: 21760-21766; 1997.
129. Brunk U, Terman A. Lipofuscin: mechanisms of age-related accumulation and influence on cell function(1)(2). *Free Radic Biol Med* 33: 611; 2002.
130. Brunk UT, Jones CB, Sohal RS. A novel hypothesis of lipofuscinogenesis and cellular aging based on interactions between oxidative stress and autophagocytosis. *Mutat Res* 275: 395-403; 1992.
131. Ikeyama S, Kokkonen G, Shack S, Wang XT, Holbrook NJ. Loss in oxidative stress tolerance with aging linked to reduced extracellular signal-regulated kinase and Akt kinase activities. *Faseb J* 16: 114-116; 2002.
132. Suh JH, Shigeno ET, Morrow JD, Cox B, Rocha AE, Frei B, Hagen TM. Oxidative stress in the aging rat heart is reversed by dietary supplementation with (R)-(α)-lipoic acid. *Faseb J* 15: 700-706; 2001.
133. Suh JH, Wang H, Liu RM, Liu J, Hagen TM. (R)- α -lipoic acid reverses the age-related loss in GSH redox status in post-mitotic tissues: evidence for increased cysteine requirement for GSH synthesis. *Arch Biochem Biophys* 423: 126-135; 2004.
134. Kim MS, Park JY, Namkoong C, Jang PG, Ryu JW, Song HS, Yun JY, Namgoong IS, Ha J, Park IS, Lee IK, Viollet B, Youn JH, Lee HK, Lee KU. Anti-obesity effects of α -lipoic acid mediated by suppression of hypothalamic AMP-activated protein kinase. *Nat Med* 10: 727-733; 2004.
135. Sen CK, Roy S, Khanna S, Packer L. Determination of oxidized and reduced lipoic acid using high-performance liquid chromatography and coulometric detection. *Methods Enzymol* 299: 239-246; 1999.
136. Bustamante J, Lodge JK, Marcocci L, Tritschler HJ, Packer L, Rihn BH. α -lipoic acid in liver metabolism and disease. *Free Radic Biol Med* 24: 1023-1039; 1998.

137. Packer L, Kraemer K, Rimbach G. Molecular aspects of lipoic acid in the prevention of diabetes complications. *Nutrition* 17: 888-895; 2001.
138. Smith AR, Shenvi SV, Widlansky M, Suh JH, Hagen TM. Lipoic acid as a potential therapy for chronic diseases associated with oxidative stress. *Curr Med Chem* 11: 1135-1146; 2004.
139. Suh JH, Moreau R, Heath SH, Hagen TM. Dietary supplementation with (R)-alpha-lipoic acid reverses the age-related accumulation of iron and depletion of antioxidants in the rat cerebral cortex. *Redox Rep* 10: 52-60; 2005.
140. Lykkesfeldt J, Hagen TM, Vinarsky V, Ames BN. Age-associated decline in ascorbic acid concentration, recycling, and biosynthesis in rat hepatocytes--reversal with (R)-alpha-lipoic acid supplementation. *Faseb J* 12: 1183-1189; 1998.
141. Liu H, Lightfoot R, Stevens JL. Activation of heat shock factor by alkylating agents is triggered by glutathione depletion and oxidation of protein thiols. *J Biol Chem* 271: 4805-4812; 1996.
142. Freeman ML, Borrelli MJ, Syed K, Senisterra G, Stafford DM, Lepock JR. Characterization of a signal generated by oxidation of protein thiols that activates the heat shock transcription factor. *J Cell Physiol* 164: 356-366; 1995.
143. Kim YK, Lee AS. Transcriptional activation of the glucose-regulated protein genes and their heterologous fusion genes by beta-mercaptoethanol. *Mol Cell Biol* 7: 2974-2976; 1987.
144. Piccirella S, Czegle I, Lizak B, Margittai E, Senesi S, Papp E, Csala M, Fulceri R, Csermely P, Mandl J, Benedetti A, Banhegyi G. Uncoupled redox systems in the lumen of the endoplasmic reticulum. Pyridine nucleotides stay reduced in an oxidative environment. *J Biol Chem* 281: 4671-4677; 2006.
145. Packer L, Witt EH, Tritschler HJ. alpha-Lipoic acid as a biological antioxidant. *Free Radic Biol Med* 19: 227-250; 1995.
146. Hung CC, Ichimura T, Stevens JL, Bonventre JV. Protection of renal epithelial cells against oxidative injury by endoplasmic reticulum stress preconditioning is mediated by ERK1/2 activation. *J Biol Chem* 278: 29317-29326; 2003.
147. Leonard MO, Kieran NE, Howell K, Burne MJ, Varadarajan R, Dhakshinamoorthy S, Porter AG, O'Farrelly C, Rabb H, Taylor CT. Reoxygenation-specific activation of the antioxidant transcription factor Nrf2 mediates cytoprotective gene expression in ischemia-reperfusion injury. *Faseb J* 20: 2624-2626; 2006.
148. Hu R, Xu C, Shen G, Jain MR, Khor TO, Gopalkrishnan A, Lin W, Reddy B, Chan JY, Kong AN. Identification of Nrf2-regulated genes induced by chemopreventive isothiocyanate PEITC by oligonucleotide microarray. *Life Sci* 79: 1944-1955; 2006.
149. Hu R, Xu C, Shen G, Jain MR, Khor TO, Gopalkrishnan A, Lin W, Reddy B, Chan JY, Kong AN. Gene expression profiles induced by cancer

- chemopreventive isothiocyanate sulforaphane in the liver of C57BL/6J mice and C57BL/6J/Nrf2 (-/-) mice. *Cancer Lett* 243: 170-192; 2006.
150. Shen G, Xu C, Hu R, Jain MR, Nair S, Lin W, Yang CS, Chan JY, Kong AN. Comparison of (-)-epigallocatechin-3-gallate elicited liver and small intestine gene expression profiles between C57BL/6J mice and C57BL/6J/Nrf2 (-/-) mice. *Pharm Res* 22: 1805-1820; 2005.
 151. Gebel S, Gerstmayer B, Bosio A, Hausmann HJ, Van Miert E, Muller T. Gene expression profiling in respiratory tissues from rats exposed to mainstream cigarette smoke. *Carcinogenesis* 25: 169-178; 2004.
 152. Lee JM, Calkins MJ, Chan K, Kan YW, Johnson JA. Identification of the NF-E2-related factor-2-dependent genes conferring protection against oxidative stress in primary cortical astrocytes using oligonucleotide microarray analysis. *J Biol Chem* 278: 12029-12038; 2003.
 153. Kwak MK, Wakabayashi N, Itoh K, Motohashi H, Yamamoto M, Kensler TW. Modulation of gene expression by cancer chemopreventive dithiolethiones through the Keap1-Nrf2 pathway. Identification of novel gene clusters for cell survival. *J Biol Chem* 278: 8135-8145; 2003.
 154. Thimmulappa RK, Mai KH, Srisuma S, Kensler TW, Yamamoto M, Biswal S. Identification of Nrf2-regulated genes induced by the chemopreventive agent sulforaphane by oligonucleotide microarray. *Cancer Res* 62: 5196-5203; 2002.
 155. Fukushima T, Kikkawa R, Hamada Y, Horii I. Genomic cluster and network analysis for predictive screening for hepatotoxicity. *J Toxicol Sci* 31: 419-432; 2006.
 156. Nair S, Xu C, Shen G, Hebbar V, Gopalakrishnan A, Hu R, Jain MR, Liew C, Chan JY, Kong AN. Toxicogenomics of endoplasmic reticulum stress inducer tunicamycin in the small intestine and liver of Nrf2 knockout and C57BL/6J mice. *Toxicol Lett* 168: 21-39; 2007.
 157. Purdom-Dickinson SE, Lin Y, Dedek M, Morrissy S, Johnson J, Chen QM. Induction of antioxidant and detoxification response by oxidants in cardiomyocytes: evidence from gene expression profiling and activation of Nrf2 transcription factor. *J Mol Cell Cardiol* 42: 159-176; 2007.
 158. Nair S, Xu C, Shen G, Hebbar V, Gopalakrishnan A, Hu R, Jain MR, Lin W, Keum YS, Liew C, Chan JY, Kong AN. Pharmacogenomics of phenolic antioxidant butylated hydroxyanisole (BHA) in the small intestine and liver of Nrf2 knockout and C57BL/6J mice. *Pharm Res* 23: 2621-2637; 2006.
 159. Wang X, Tomso DJ, Chorley BN, Cho HY, Cheung VG, Kleeberger SR, Bell DA. Identification of polymorphic antioxidant response elements (AREs) in the human genome. *Hum Mol Genet* 2007.
 160. Wang W, Chan JY. Nrf1 is targeted to the endoplasmic reticulum membrane by an N-terminal transmembrane domain. Inhibition of nuclear translocation and transacting function. *J Biol Chem* 281: 19676-19687; 2006.
 161. Zhang Y, Crouch DH, Yamamoto M, Hayes JD. Negative regulation of the Nrf1 transcription factor by its N-terminal domain is independent of Keap1:

- Nrf1, but not Nrf2, is targeted to the endoplasmic reticulum. *Biochem J* 399: 373-385; 2006.
162. Giblin FJ. Glutathione: a vital lens antioxidant. *J Ocul Pharmacol Ther* 16: 121-135; 2000.
163. Truscott RJ. Age-related nuclear cataract-oxidation is the key. *Exp Eye Res* 80: 709-725; 2005.
164. Banhegyi G, Lusini L, Puskas F, Rossi R, Fulceri R, Braun L, Mile V, di Simplicio P, Mandl J, Benedetti A. Preferential transport of glutathione versus glutathione disulfide in rat liver microsomal vesicles. *J Biol Chem* 274: 12213-12216; 1999.
165. Banhegyi G, Marcolongo P, Puskas F, Fulceri R, Mandl J, Benedetti A. Dehydroascorbate and ascorbate transport in rat liver microsomal vesicles. *J Biol Chem* 273: 2758-2762; 1998.